Rock glaciers and natural dams in Central Asia

Swenja Rosenwinkel

Univ.-Diss.

zur Erlangung des akademischen Grades
"doctor rerum naturalium"
(Dr. rer. nat.)
in der Wissenschaftsdisziplin "Geomorphologie"

eingereicht an der
Mathematisch-Naturwissenschaftlichen Fakultät
Institut für Erd- und Umweltwissenschaften
der Universität Potsdam

Ort und Tag der Disputation:	Potsdam, den 16. Februar 2018
Hauptbetreuer:	Oliver Korup
weitere Gutachter/innen:	Angela Landgraf
	Tobias Bolch

Published online at the
Institutional Repository of the University of Potsdam:
URN urn:nbn:de:kobv:517-opus4-410386
http://nbn-resolving.de/urn:nbn:de:kobv:517-opus4-410386

Declaration of Authorship

I hereby confirm, that I have authored this thesis entitled "Rock glaciers and natural dams in Central Asia" independently and without use of others than the indicated sources. This work was accomplished during the PhD candidature at the University of Potsdam. Where I referred to ideas from published work or quoted other authors, the sources are always given. Other sources of help are acknowledged. Where this work was completed in co-authorship with others, I clearly pointed out my contributions.

Berlin, May 4th, 2018

Swenja Rosenwinkel

Foreword

High mountain regions have impressed me throughout my life. The beautiful landscape and environment is home to diverse animal and plant species. Only few human populations are adapted to live in these often rough and unpredictable regions, but many are living close to them and profit from the abundance of water. Water abundance is of special concern in Central Asia as regions and countries without direct water accessibility depend on resources of the upstream countries. Conflicts about water already arose and might increase political destabilization of those regions. Water storages as glaciers, rock glaciers, dammed lakes, and their changes need to be better understood. Therefore I am glad to have had the opportunity to conduct research on rock glaciers and natural dams in Central Asia, because rock glaciers might play a crucial role in a changing climate. The influence of rock glaciers is twofold. They store important water resources, both internally and by damming lakes. But they pose also a hazard in case of dam building, that might become unstable and release the lake waters in outburst floods. In this thesis I am able to combine research questions of originally two proposals aiming to evaluate the situation of natural dams in Central Asia and the earthquake history of the region. These subjects are strongly entangled in the seismically active areas of Central Asia. Rock glaciers are not well studied not only in terms of their response to climate change, but also in their advance mechanisms. Earthquakes resulting in mass wasting processes are suggested to contribute to the rock glacier mass and thus to an acceleration of their gravitational movement. In several field trips to Kyrgyzstan and Kazakhstan we visited rock-glacier dams, which motivated me to analyse

how they form and deform. Outburst floods through the breaking of such natural dams threaten the live and livestock of people living downstream. To understand recent and predict future changes in landscapes, researchers always have to seek for evidences from historic events; especially extreme events are of great interest, as long-term monitoring may hide information about outliers. Issyk Kul, the second largest mountain lake in the world, is a mystery in its geological formation and history. Alternating damming and dam breaking events might have influenced the lake and its environment. In this regard, we tested several theories connected to megafloods in the Pleistocene history of the lake, again raising questions about the role of natural dams and their possible role on influencing large tracts of river systems in the Central Asian landscape. The nomadic living families we passed by during our field trips were generous, friendly people, who were born into very hard living circumstances, but whose lives so close to and in harmony with their environment impressed me. The pristine landscape attracts visitors as they search for relaxation and activity. I hope they are aware of the impact they can have and take care of the landscape and species within, which are very sensitive to environmental changes and need to be protected.

Acknowledgements

First of all I'd like to thank my supervisors Oliver Korup and Angela Landgraf for their support and motivating words whenever necessary. Their guidance with helpful suggestions and discussions was indispensable for the success of this thesis. I'd like to thank Oliver Korup for his his valuable inputs and his ability to resolve and explain scientific problems easily. My gratitude goes to to Angela Landgraf, who was my teacher in the field. Her scientific curiosity and interest in people made our fieldtrips great experiences.

I'd like to thank Atyrgul Dzhumabaeva who kindly provided our group not only with detailed scientific knowledge about Kyrgyzstan, but also shared stories and knowledge about country and people, and introduced us to Kyrgyz food specialities. Kanatbek Abdrakhmatov and Atyrgul Dzumabaeva is thanked for their support in organizing the fieldwork and providing the fieldwork infrastructure.

I'd like to thank Silke Merchel and the DREAMS team, who taught me very precise labwork and analysed my cosmo samples.

Many Bachelor-, Master, and PhD- students helped me with field-, and labwork. Thank you: Friedrich Vollkmer, Mansoor Ahmadi, Martin Zeckra, Steffi Tofelde David Käter, Philine Thöle, Lilian Pollozek, Martin Lang, Eric Rhoden, Julia Artel, Marieke Voigt, Henrieke Wilborn, Doreen Kauschus, and Loredana Sorg. Cornelia Wilske is thanked for her great company and support in lab and life in Dresden. Annina Sorg is thanked for her help with lichenometric measurements and guiding us to the beautiful Ordzhonikidze rock glacier.

I'd like to thank my various office mates and Potsdam University col-

leagues, with whom I spent the last six years in four different offices, and who made the work on the thesis more enjoyable. Especially the company of Amelie Stolle, Nele Meyer, Jan Blöthe, Henry Munack, and Agostiny Lontsi combined helpful discussions with laughs and coffee breaks.

My gratitude goes to Latex spezis Jenn Meyer and Ayliz Erginos, who helped me compiling this work, and Eric Mazelis and my father for proof reading.

And of course I thank friends and family, who have accompanied me the last years, for being there and sharing interesting and beautiful times.

Abstract

The formation and breaching of natural dammed lakes have formed the landscapes, especially in seismically active high-mountain regions. Dammed lakes pose both, potential water resources, and hazard in case of dam breaching. Central Asia has mostly arid and semi-arid climates. Rock glaciers already store more water than ice-glaciers in some semi-arid regions of the world, but their distribution and advance mechanisms are still under debate in recent research. Their impact on the water availability in Central Asia will likely increase as temperatures rise and glaciers diminish.

This thesis provides insight to the relative age distribution of selected Kyrgyz and Kazakh rock glaciers and their single lobes derived from lichenometric dating. The size of roughly 8000 different lichen specimens was used to approximate an exposure age of the underlying debris surface. We showed that rock-glacier movement differs significantly on small scales. This has several implications for climatic inferences from rock glaciers. First, reactivation of their lobes does not necessarily point to climatic changes, or at least at out-of-equilibrium conditions. Second, the elevations of rock-glacier toes can no longer be considered as general indicators of the limit of sporadic mountain permafrost as they have been used traditionally.

In the mountainous and seismically active region of Central Asia, natural dams, besides rock glaciers, also play a key role in controlling water and sediment influx into river valleys. However, rock glaciers advancing into valleys seem to be capable of influencing the stream network, to dam rivers, or to impound lakes. This influence has not previously been addressed. We quantitatively explored these controls using a new inventory of 1300 Central

Asian rock glaciers. Elevation, potential incoming solar radiation, and the size of rock glaciers and their feeder basins played key roles in predicting dam appearance. Bayesian techniques were used to credibly distinguish between lichen sizes on rock glaciers and their lobes, and to find those parameters of a rock-glacier system that are most credibly expressing the potential to build natural dams.

To place these studies in the region's history of natural dams, a combination of dating of former lake levels and outburst flood modelling addresses the history and possible outburst flood hypotheses of the second largest mountain lake of the world, Issyk Kul in Kyrgyzstan. Megafloods from breached earthen or glacial dams were found to be a likely explanation for some of the lake's highly fluctuating water levels. However, our detailed analysis of candidate lake sediments and outburst-flood deposits also showed that more localised dam breaks to the west of Issyk Kul could have left similar geomorphic and sedimentary evidence in this Central Asian mountain landscape. We thus caution against readily invoking megafloods as the main cause of lake-level drops of Issyk Kul. In summary, this thesis addresses some new pathways for studying rock glaciers and natural dams with several practical implications for studies on mountain permafrost and natural hazards.

Zusammenfassung

Die Entstehung und das Ausbrechen natürlicher Stauseen prägen die Landschaft, insbesondere in seinsmisch aktiven Hochgebirgsregionen. Stauseen bergen zugleich Potential für Wasserressourcen, aber Gefahr durch Überflutungen. Mit steigenden Temperaturen und voranschreitender Gletscherschmelze wird der Bedarf an alternativen Wasserressourcen steigen. Zentralasien unterliegt größtenteils ariden und semiariden Klimabedingungen. In manchen semiariden Gebieten der Welt speichern Blockgletscher heute schon mehr Wasser als Eisgletscher. Ihr Anteil an der Wasserverfügbarkeit in Zentralasien wird in Zukunft vermutlich steigen.

Die Verteilung und die Mechanismen, die das Auftreten und das Vorrücken der Blockgletscher beeinflussen, sind allerdings noch nicht gut erforscht. In der vorliegenden Arbeit wurden Blockgletscher in Kirgistan und Kasachstan ausgewählt, um die Altersverteilung ihrer Loben relativ mit Lichenometrie zu bestimmen. Dafür wurden etwa 8000 Flechtendurchmesser gemessen, die, bei bekannter Wachstumsrate, Aussagen über das Expositionsalter des unterliegenden Gesteins zulassen und somit über die Zeit, seitdem keine Bewegungen mehr stattgefunden haben, die eine andere Seite des Gesteins exponiert hätten. Es zeigte sich, dass die Blockgletscherbewegungen auf kleinräumiger Skala sehr unterschiedlich sind und nicht allein von großräumigen topoklimatischen Gegebenheiten abhängen. Diese Erkenntnis bedeutet eine Einschränkung des in der Literatur häufig gezogenen Rückschlusses von Blockgletscherbewegungen auf klimatische Veränderungen oder der Nutzung von Blockgletscherhöhen als Indikator für die untere Grenze des Permafrostbereiches.

Natürliche Staudämme spielen eine Schlüsselrolle dabei den Wasser- und Sedimenteintrag in die Flüsse zu kontrollieren. Blockgletscher können ebenfalls so weit in das Tal vorrücken, dass sie Flussläufe beeinflussen und Seen aufstauen. Diesem Phenomen wurde in dieser Arbeit erstmals nachgegangen und mit einem neu erstellten Inventar von 1300 Blockgletschern die möglichen Kontrollfaktoren, die zu der Bildung eines Blockglestcherdamms führen, ausgewertet. Die Blockgletscherhöhe, die potentielle Sonneneinstrahlung, sowie die Größe der Blockgletscher und ihrer Einzugsgebiete spielen dabei eine große Rolle für die Vorhersage des Auftretens von Blockgletscherdämmen. Für die beiden eben genannten Studien wurde ein Bayesisches Verfahren gewählt, um die mit Hilfe der Größenunterschiede der Flechtendurchmesser auf den einzelnen Blockgletschern und ihren Loben gewonnenen relativen Gesteinsexpositonsaltersunterschiede zu identifizieren. Desweiteren wurde die Methode genutzt, um die Parameter ausfindig zu machen, die am wahrscheinlichsten dazu führen, dass Blockgletscher Dämme bilden.

Mit einer Kombination aus Datierungen vergangener Seespiegelstände und Flutmodellierungen möglicher Seeausbrüche des Issyk Kul in Kirgistan, des zweitgrößten Bergsees der Welt, geht diese Arbeit der Plausibilität der Zusammenhänge zwischen Seespiegelschwankungen und –ausbrüchen nach, die sich im Quartär zugetragen haben. Dabei wurde ein zeitlicher Zusammenhang zwischen Seespiegelsenkung und Flutablagerungen bestätigt. Die Modellierungen deuten auf große Seeausbrüche hin, zeigen allerdings auch die Möglichkeit auf, dass ein kleinerer aufgestauter See westlich des Issyk Kul auch ähnliche Spuren im Sedimentarchiv hinterlassen haben könnte. Somit sind die Seespiegelabfälle nicht eindeutig katastrophalen Seeausbrüchen zuzuordnen.

Zusammenfassend zeigt diese Arbeit neue Wege Blockgletscher und natürliche Staudämme zu analysieren und die Ergebnisse liefern praktische Hinweise für die Permafrost- und Naturgefahrenforschung.

Contents

List of Figures x

List of Tables xi

0 Introduction 1

0.1 Motivation . . . 1
0.2 Scientific rational . . . 7
0.2.1 Lichenometry . . . 7
0.2.2 Rock glaciers . . . 8
0.2.3 Natural dams . . . 12
0.3 Study area . . . 13
0.4 Thesis structure and objectives . . . 16
0.5 Chapter outline and author contributions . . . 20

1 Limits to Lichenometry 23

1.1 Introduction . . . 24
1.2 Study area . . . 27
1.3 Methods . . . 30
1.4 Results . . . 33
1.5 Discussion . . . 38
1.5.1 Environmental controls on lichen growth . . . 38
1.5.2 Uncertainties of lichen-growth models . . . 40
1.5.3 Implications for the dynamics of rock glaciers . . . 41
1.6 Conclusions . . . 43

2 Rock-glacier dams **45**
2.1 Introduction . . . 46
2.2 Study area . . . 49
2.3 Methods . . . 51
2.4 Results . . . 56
2.5 Discussion . . . 67
2.6 Conclusions . . . 71

3 Late Pleistocene outburst floods **75**
3.1 Introduction . . . 76
3.2 Study area . . . 79
3.3 Methods . . . 80
3.3.1 Exposure dating with ^{10}Be and ^{26}Al . . . 80
3.3.2 Radiocarbon dating . . . 84
3.3.3 Infrared stimulated luminescence . . . 84
3.3.4 Lake levels and chronology . . . 84
3.3.5 Palaeoflood modelling . . . 85
3.3.6 Channel steepness . . . 87
3.4 Results . . . 87
3.4.1 Boulder provenance . . . 87
3.4.2 Palaeoflood modelling . . . 88
3.4.3 Cosmogenic exposure ages . . . 91
3.4.4 Radiocarbon, IRSL, and pIR ages . . . 97
3.5 Discussion . . . 98
3.6 Conclusions . . . 102

4 Discussion **105**
4.1 Rock-glacier activity . . . 105
4.2 Rock glaciers as natural dams . . . 110
4.3 Natural dams in Central Asia . . . 113
4.4 Future challenges . . . 114

5 Conclusions **117**

A *Supplementary material*
Limits to lichenometry 119

B *Supplementary material*
Late Pleistocene outburst floods from Issyk Kul, Kyrgyzstan? 129

References 147

List of Figures

1 Landslide threatening railroad 2
2 Rock-glacier lake 6
3 Rock glaciers in the alpine landscape continuum 9
4 Rock glacier morphology 10
5 Rock-glacier activity 11
6 Discharges of outburst and meteorological floods of the world . 12
7 Major river catchment areas of high mountains in Asia 15
8 Sketch of research covered by this thesis. 17

1.1 Study area and rock glaciers 28
1.2 Lichen-growth model 33
1.3 Lichen-age calibration 34
1.4 Distribution of lichen diameters on individual rock glacier lobes 35
1.5 Posterior probability density of the contrast of the largest lichen diameters 36
1.6 Box-and-whisker plots of calibrated lichen ages of individual rock glacier lobes 37
1.7 Species-dependent separability of rock-glacier lobes on the basis of the ten largest lichen diameters 38
1.8 Comparison of median ages for rock glacier lobes and estimated probability densities for the lichen ages 41

2.1 Examples rock glaciers damming or obstructing rivers in High Asia 48
2.2 Regional map of High Asian rock-glacier inventory 49

2.3 Hierarchical model of Bayesian robust multiple logistic regression for predicting the probability that a given rock glacier from our sample with characteristics disrupts a mountain-river channel 54
2.4 Probability density estimates of rock-glacier area, mean annual temperature, annual temperature range, and mean annual precipitation 56
2.5 Rock-glacier toe elevations are correlated with mean annual temperature and maximum potential incoming solar radiation 58
2.6 Distribution of study-area elevation and rock glacier-toe elevations 59
2.7 Rock glacier impact on river systems in High Asia 61
2.8 Posterior distributions of Bayesian robust logistic regression intercept and weights of topographic and climatic predictors . 62
2.9 Results of Bayesian robust logistic regression with credible decision boundaries sampled from the posterior distribution . . . 63
2.10 Posterior distributions of logistic regression intercepts and weights for predictors shown in Figure 2.9 64
2.11 Posterior distributions of logistic regression intercept and weights of the first eight principal components (PCs) 66
2.12 Median predictive posterior probabilities of a rock glacier disrupting a mountain river for predictors 67
2.13 Rock-glacier dam height and dam width versus upstream catchment area and relief 72

3.1 Study area and shorelines 77
3.2 Longitudinal profile of Chu River and its tributaries 81
3.3 Lake highstands and modeled peak discharges for estimated outburst-flood volumes 82
3.4 Boulder analyses 89
3.5 Modelled outburst flood scenarios 90
3.6 Probability densities of calibrated radiocarbon ages, TCN and pIR ages with respect to their sampling elevations 91

3.7 Peak discharge and flood volume of large Quaternary floods of different dam breach types 102

4.1 Distribution for lichen colonisation time 106
4.2 Elevation distribution of lichen species 107
4.3 Lichen measurements on dated gravestones for growth-curve calibration in northern Kyrgyzstan. 108
4.4 Some rock glaciers lie low 111

List of Tables

1.1 Selected characteristics of the six large and low-lying rock glaciers 30

2.1 Variables (for rock glaciers and their catchment areas) used as predictors in Bayesian logistic regression. 53
2.2 Parameters in Bayesian robust multiple logistic regression. . . 55
2.3 Reported estimates of spatial densities of rock glaciers in mountain belts throughout the world. 57
2.4 Rock glaciers and their geomorphic impact on rivers in three High Asian mountain belts. 60
2.5 Interpretation of the first eight principal components 5 of 59 topographic and climatic candidate predictors; last column indicates whether these principal components have credible non-zero weights in their posterior distributions derived from Bayesian robust logistic regression (Figure 2.10) 65

3.1 TCN sampling locations and results for exposure ages. 83
3.2 Assumptions for shoreline and lake-highstand deposit comparison. 85
3.3 Radiocarbon sampling locations and dating results. 93
3.4 IRSL/ pIR sampling locations and dating results 97

Chapter 0

Introduction

0.1 Motivation

Natural dams form by various processes, and the most hazardous ones result from river blockage by landslides, moraines or glaciers (Costa and Schuster, 1988). The geologically rapid formation of natural lakes has been documented at least some two centuries ago by Davis (1882), who stated:

"Glacial lakes are now of little importance; a few occur in the higher mountain chains, but they are trifling in size, and rank with many other species only as curiosities unless they become of disastrous importance in the valleys below, from floods that follow a giving way of their barriers".

This warning has been taken serious and many researchers contributed to further knowledge about the formation and failure of natural dams. Amongst the types of natural dams, Costa and Schuster (1988) declared landslide dams, glacier-ice dams, and late-Neoglacial moraine dams to have the highest risk to life and property of humans, although other landforms such as lava flows, sand dunes, or sediment tails can also block rivers. Some natural dams have a reputation for being short-lived, and thus giving rise to geomorphic instability. For example, while most landslide dams fail shortly after their formation (50% within the first 10 days for those that did reportedly fail), most of the dams that failed did so by overtopping. Still, some natural dams persist over 10^{2-3} years (Clague and Evans, 1994) despite strong rainstorms

or severe earthquake shaking in places. Landslide and glacier dams abound in many mountains throughout the world. Yet one of the regions that remain somewhat under-reported in terms of such natural dams are the mountains of Central Asia, which makes these ranges ideal candidates to learn more, and to test existing hypotheses and models, about the formation and failure of natural dams. About 1500 to 2000 mountain lakes of all types have been discovered in the Kyrgyz Tien Shan, and some 20% of their dams may eventually become unstable (Yerokhin, 2002). Moraine-glacial, supraglacial, and landslide (including rockfalls and debris flows) dams are thought to make up for the majority of thus hazardous dams (Yerokhin, 2002). Earthquakes, excessive rainfall, and snowmelt are also the main trigger for dam-forming landslides (Costa and Schuster, 1988). Seismically active regions are especially prone to landslides (Havenith et al., 2003), posing a risk to live, livestock, and infrastructure (Figure 1).

Figure 1: Landslide threatening the main and only railroad between Bishkek and Balykchi (NW Issyk Kul).

Strong earthquakes are abundant in the Tien Shan, and largely result

from far-field effects of the ongoing Himalayan orogeny. Over 100 existing landslide dams have been mapped in Central Asia so far; the largest is Usoi dam in Tajikistan (the landslide deposit involves an estimated rock and debris volume of 2.2 km^2), which formed in 1911, and has been impounding the world's deepest natural water reservoir since (Strom, 2010).

Natural dams have been studied around the world to assess their formation triggers (Korup, 2005) and failure mechanisms (Clague and Evans, 1994), to learn more about what controls their stability and longevity (Hermanns et al., 2004), to anticipate their impact on human water resources (Costa and Schuster, 1988; Hewitt et al., 2008), and to quantify their potential to failing and producing outburst floods (Delaney and Evans, 2011). Despite these and many other case studies, it is perhaps surprising to see that rock glaciers seem to have escaped the many case and few systematic regional studies on natural dams. Rock glaciers are mixtures of ice and rock originating in permafrost areas. These masses slowly deform under the influence of gravity and have a special role in higher altitudes, especially in semi-arid regions. They can be important water resources capable of storing more water than ice glaciers in the driest parts of mountainous regions such as the Andes (Azócar and Brenning, 2010). Similar situations have been reported from other mountain ranges, as the Himalayas and Karakorum (Jones et al., 2018; Owen and England, 1998), or the Sierra Nevada in the USA (Millar and Westfall, 2008). This importance is likely to increase with regard to warming temperatures and shrinking glaciers, as predicted for Central Asia (Unger-Shayesteh et al., 2013). Most current research about rock glaciers addresses their response to changing climate variables (Millar and Westfall, 2008; Sorg et al., 2015), their internal structure and ice content (Monnier and Kinnard, 2015), or even more theoretical foundations such as the search for a general and appropriate definition (Berthling, 2011; Giardino et al., 2011).

The Tien Shan mountains of Central Asia are a fascinating place to study rock glaciers because these mountains have larger and more spatially clustered rock glaciers than, for example, the Swiss Alps or parts of the Himalayas (Bolch and Gorbunov, 2014). Furthermore large, low-lying rock glaciers advance at velocities of as high as 5–10 m yr^{-1} in the Tien Shan (Gorbunov

et al., 1992), thus outpacing the advance rates of rock glaciers in other regions, such as the Swiss Alps, by one ore even two orders of magnitude (Delaloye et al., 2010). The Bérard rock glacier in the French Alps was one of the exceptions with comparably high deformation rates that occurred after its sudden collapse in 2006, which was likely a response to long-term (atmospheric warming) and short-term (heavy rain falls) climatic changes (Bodin et al., 2016b). Warm permafrost conditions, interaction with polythermal glaciers, intensive weathering, or debris input by rock avalanches may play further key roles in forming and deforming the large rock glaciers in the Tien Shan (Bolch and Gorbunov, 2014). The assumption that rock glaciers develop and exist only at temperatures within the permafrost belt, i.e. near the 0°C-isotherm, has been useful for taking these landforms as proxies for modelling past and future distributions of sporadic permafrost at the mountain-belt scale (Janke, 2005). However, the occurrences of some rock glaciers at or below the lower limit of the local permafrost boundaries contributes to our motivation to question this general assumption and to test various climatic and morphological parameters on their likely contribution to rock-glacier locations and their river-damming potential. The first two core chapters combine these important aspects of rock glaciers as an understudied, if not previously unrecognised, landform or at least landform proxy of disturbance in high mountain regions. Few recent hypotheses are available to explain the differing rates of rock-glacier activity, and most explanatory attempts involve either atmospheric warming or site-specific geomorphic changes. In their dendrogeomorphical work Sorg et al. (2015) emphasise the contrasting response of rock glaciers to atmospheric warming. While the activity of four Tien Shan rock-glacier increases synchronously with rising summer air temperatures, a multi-decadal observation of these rock glaciers seems to reflect more site-specific effects. These effects include topography, debris supply, and the ground ice content, which may yet trigger feedbacks of the rock-glacier's response to air temperature (Sorg et al., 2015). Debris supply need not be limited to climatic constraints, however. For example, mass wasting through strong ground shaking is well documented in the Tien Shan (Strom, 2010), though rarely mentioned in connection with acting as

a sediment source or replenishment for active rock glaciers. Hence the influence of earthquakes on rock-glacier activity remains speculative (Bolch and Gorbunov, 2014). To work out the connection between rock-glacier advance and its trigger mechanisms, I present in my core chapter 1 lichenometry as a dating tool to compare 1) small-scale movement differences of individual rock-glacier lobes, and 2) local age-differences of strategically selected rock glaciers in the northern Tien Shan. By using lichens to date rock-glacier lobes, one could hope for better constraints about their maximum, if not formation, age. Dating might also help to pinpoint discrete episodes of large debris input, for example by earthquake-induced rock falls that could rejuvenate individual parts of rock glaciers, and possibly steering them out of equilibrated permafrost conditions by prompting higher movement rates. Other dating methods that afford similar, if not better, (near-)annual precision such as dendrochronology depend on the occurrence of trees. However, trees are not ubiquitous in the mountain areas we studied, so that lichens offer a broader look at the behaviour of different parts of the rock glaciers. Lichens growing on the surfaces of rock glaciers moreover offer a fast and cheap dating method. Whether lichenometry is also objective and reproducible enough in this context, remains partly unresolved so that we explored ways to better capture the temporal resolution and reliability of this method. Our strategy was to take advantage of the high deformation rates of rock glaciers in the Tien Shan, and to make use of these dynamics as a methodological and conceptual challenge to this late Quaternary dating method, which, although widely used, has been criticised heavily recently (Osborn et al., 2015).

While lichenometry may or may not be a practical method for dating rock-glacier lobes, we know even less about the potential processes at work that enable fast advancing lobes to interfere with river channels. It appears that rock glaciers that have advanced into major river valleys can influence the river network and eventually act as natural dams, particularly at high elevations (Figure 2). This induces an unquantified amount of hazard and risk in case of sudden dam breaching and spontaneous flooding of downstream regions. Outburst floods or debris flows that resulted from the failure of natural dams have reshaped large tracts of river systems and caused severe

Figure 2: View from rock-glacier toe to impounded lake at Djassik Kul in northern Kyrgyzstan.

damage in many populated mountain areas. Increasing rock-glacier activity and advances towards river valleys has been reported recently in the Tien Shan (Sorg et al., 2015). However, the possible impacts that such geomorphic coupling might have on the water and sediment flux are not mentioned in current rock-glacier research. The second core chapter deals with ways of predicting from a set of candidate variables those conditions under which such dams build, and broadens the view by also including rock glaciers from other mountain ranges of Central Asia, thus covering a broad range of environmental conditions. While most of the rock-glacier literature focuses on one particular region, we present a here new dataset of nearly subcontinental scope, and use this new inventory to assess and compare the conditions that may be conducive for geomorphic impacts of rock glaciers on mountain rivers.

The final part of this thesis addresses ways of integrating natural dams, be they formed by landslides, glaciers, rock glaciers, or other processes, and

the longer-term evolution of Central Asian mountain valleys. High mountain lakes and the hazard they pose in case of water masses being released, have been studied around the world. Yet only few data, let alone quantitative hazard or risk assessments, are available for hazardous lakes in the Kyrgyz Tien Shan (Janský et al., 2006). Most work has been mainly concentrated on recently formed lakes and their potential risks (Delaney and Evans, 2011; Janský et al., 2010). Outburst flood dynamics and their potential flood power can be estimated by studying geomorphic and sedimentary proxies of large Quaternary lakes and their downstream courses (Carling et al., 2002). Fewer studies have considered the potential of catastrophic outburst episodes from lakes that still exist today. One example is Issyk Kul in Kyrgyzstan: the lake lies in an tectonically active deforming basin (Korjenkov et al., 2007; Zubovich et al., 2010), and has garnered much scientific interest as a large sedimentary and palaeo-environmental archive. Large sediment deposits surrounding the lake record numerous fluctuations of its water surface by up to 400 m during the last 10 kyr (Trofimov, 1978; Burgette et al., 2017; De Batist et al., 2002). These lake-level changes indicate that the lake basin alternated between closed and open states with a westward drainage through the Boam gorge. One theory holds that repeated damming and dam breaching could have caused these oscillating lake-level stands; candidates for such ephemeral dams could be either landslides or glaciers (Grosswald et al., 1994). In a combination of field observations, absolute dating, and palaeoflood modelling, the third core chapter of this thesis tests the notion of possible outburst floods that might have occurred during the Quaternary history of the lake. Palaeoflood studies like these are important to understand the type and longevity geomorphic consequence of natural dam failures, especially in an earthquake-prone area such as Central Asia.

0.2 Scientific rational

0.2.1 Lichenometry

Lichens are symbiotic communities between algae and fungi. Their radial growth has been widely used to determine the age of abandoned rock surfaces, which lichens colonize shortly after their exposure. Dating landforms has become more precise due to the development of modern dating techniques such as in situ cosmogenic nuclide dating. Lichenometry as a traditional and low-cost dating method is still used today thanks to the extreme environments in which lichens can survive. Lichens have been demonstrated their capability of survival in extra-terrestrial environments and showed no changes in the photosynthetic activity when attached at the outer shell of an Earth orbiting satellite (Sancho et al., 2008). The method is also easy to apply and mostly straightforward to calibrate with independently dated rock surfaces. While the measuring itself only involves an accurate capture of the maximum thallus diameter, there are several drawbacks of the method including the determination of the species in the field, lack of available growth curves, and differing colonisation times (Osborn et al., 2015). Many studies in palaeoseismology, the discipline of reconstructing prehistoric or pre-instrumental earthquakes, have made use of lichens as they colonise fresh rock surface, which have been exposed either through fault rupture or freshly emplaced or overturned via seismically triggered rockfalls. Even chronologies of past earthquake series have been independently corroborated by dating lichens on rockfall desposits (Bull et al., 1998). Glaciology makes wide use of lichens by determining glacial retreat from the age succession of the ice-free surfaces (Sancho et al., 2011), or seeking age information for the glacial chronology from moraines (Kirkbride and Dugmore, 2001); however, the method has seen little application to rock glaciers (Konrad and Clark, 1998).

A number of theoretical models of lichen growth curves exist; some of them involve several phases, including a colonisation phase or lag time, great growth, and deceasing growth (Bull et al., 1998). This simplistic view has been disputed by Loso and Doak (2006), who presented the typical sigmoidal

growth curve as "function of the interaction of mortality and sampling efficiency, rather than real lichen growth rates or patterns". In any case, the method of lichenometry hinges primarily on the choice of growth curve and its calibration with dated rock surfaces, such as those of gravestones, stone buildings, or dated debris. If unstable or highly dynamic, episodic re-exposure of fresh rock surfaces may locally disrupt lichen growth, thus producing potentially noisy diameter distributions. Rapidly shifting rock glaciers are emblematic of such conditions, such that we intended to push lichenometric dating to its potential limits to see how much we can learn from this method when applied to highly dynamic permafrost landforms.

0.2.2 Rock glaciers

Rock glaciers are common features in many alpine environments. They have been studied for more than one hundred years (Cross et al., 1905). A growing number of scientific articles has appeared since then, and improved the knowledge of these "perennially frozen debris masses which creep down mountain slopes in some ways similar to the behaviour of lava streams" (Haeberli, 1985). A number of explorative methods, including borehole measurements, spring temperature determination, geophysical soundings (Haeberli et al., 1998), and detailed temporal observations (Bodin et al., 2016a) have added the information about these permafrost bodies. Large inventories of rock glaciers are now available for parts of mountain ranges, e.g., the European Alps (Scotti et al., 2013), the Andes (Brenning, 2005), and also the Tien Shan (Bolch and Gorbunov, 2014). Such databases are indispensible for offering statistically robust insights to better define and distinguish between rock glaciers in terms of their origin, formative processes, current and past activity, and geomorphic consequences. The definition of rock glaciers remains debated, depending on whether one prefers using genetic or morphologic criteria. Berthling (2011) identified two major points of view on this, 1) the 'permafrost creep school' arguing that rock glaciers are permafrost-related landforms (Haeberli, 1985; Wahrhaftig and Cox, 1959), and 2) the 'continuum school' arguing that rock glaciers represent a continuum of a mixture

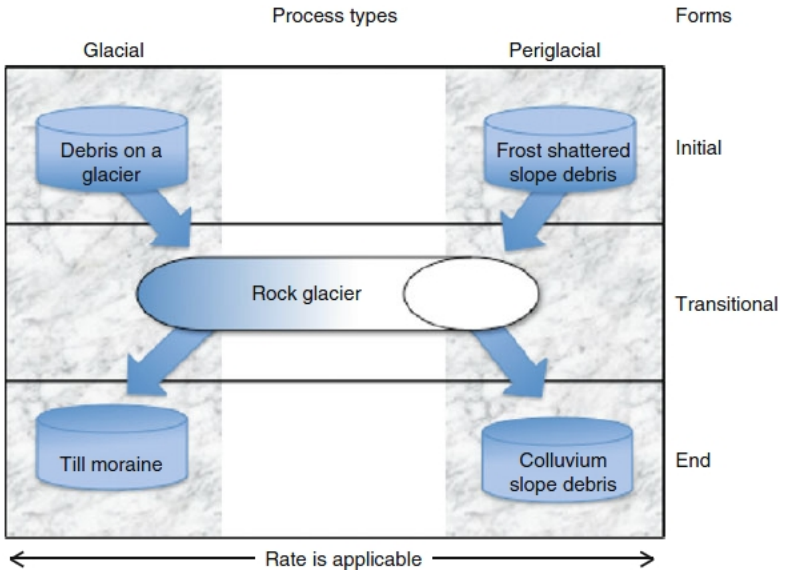

Figure 3: Rock glaciers in the alpine landscape continuum (from Giardino et al. (2011) after Giardino and Vitek (1988).

of ice and debris of varying origin (Potter, 1972). The latter view can be expanded to include deposits from catastrophic rockfalls and rock avalanches, if these deposits either entail or accumulate enough pore-space ice to facilitate creeping after their emplacement (Whalley and Azizi, 2003). Berthling (2011) proposed a new genetic definition for rock glaciers as "cryo-conditioned landforms" with permafrost as a genetic condition for the creeping process, but with ice and debris of both glacial and periglacial origin of the rock-glacier material. Giardino and Vitek (1988) pointed out that a rock glacier's appearance is a transitional state between its origin in either debris-covered glaciers or talus and slope debris, and its subsequent transformation into a sedimentary deposit (Figure 3). Rock-glacier geometry is described as either tongue or lobate shaped, mostly with lengths of 200–800 m and a thickness of 20–100 m (Barsch, 1992). Their tongue-like shape with horizontal lobes crossing the rock glacier is accompanied by transverse ridges and furrows, which reflect differential deformation during down-slope flow (e.g. Haeberli et al. (2006), Figure 4).

From the perspective of process activity, rock glaciers can be divided into intact and relict forms. Intact rock glaciers are either actively moving

Figure 4: Rock glacier morphology shown for rock glacier Ordzhonikidze in Kazakhstan.

downslope by deformation of internal permafrost and ice, or inactive, still containing permafrost, though having stagnated their motion (Barsch, 1996; Haeberli, 1985). Through permafrost degradation, relict rock glaciers lack both movement and significant ice content (Haeberli (1985), Figure 5). Analysis of time series of remote sensing data helps to detect whether and how rock glaciers are active. In the field, steepness of the front slope, vegetation cover, and the state of surface erosion largely contribute to such assessment (Roer and Nyenhuis, 2007). Rock glaciers are used to approximately infer, among other landforms and temperature measurements, not only the lower limits of sporadic mountain permafrost (Cremonese et al., 2011; Lilleøren and Etzelmüller, 2011), but also more widely for modelling past and future permafrost distributions (Janke, 2005).

In general, mountain landscapes are stages for large turnovers and storage of energy and mass, mostly in the form of solid rock, sediment, or water. Research on these processes is important to understand changes of temperature increase or glacial retreat (Gärtner-Roer, 2012), but also critical for changes

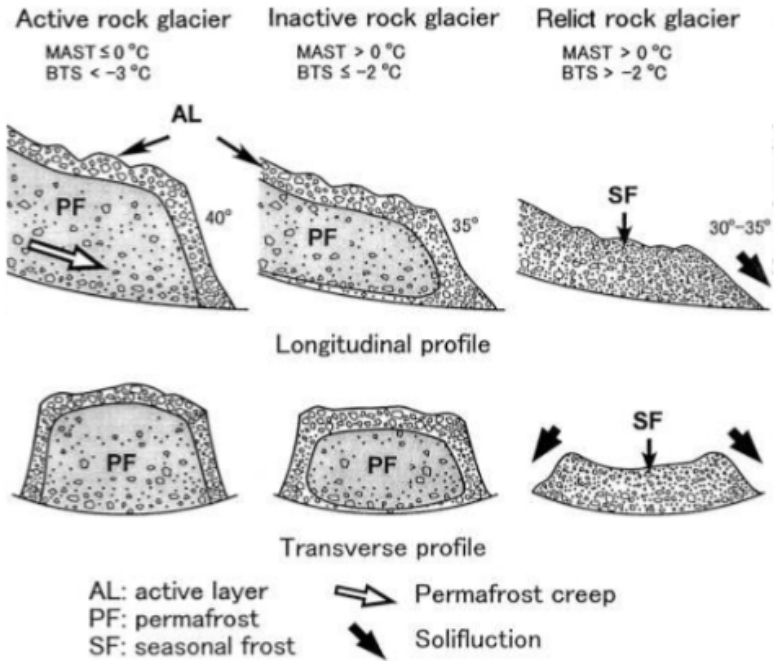

Figure 5: Schematic drawing of rock glaciers of different activity status (Ikeda and Matsuoka, 2002).

in perennially frozen ground. Rock glaciers contribute differently to sediment transport and retention depending on their mass (high mass = more material) and their dynamics (high velocity rates = lower retention time of the sediment) (Gärtner-Roer, 2012). Therefore, early studies realised and documented that rock-glaciers can function as impressive archives of mass wasting from nearby rock walls. Benchmark studies demonstrated how, for example, a rock-glacier's debris volume can be used to estimate the rates of rock-wall retreat in high mountains, largely driven by physical weathering (Barsch, 1977; Schrott, 1996).

0.2.3 Natural dams

Natural dammed lakes and artificially planned water reservoirs, including those formed via controlled explosions to trigger rockslide dams, are a globally ubiquitous means to warrant water availability and energy supply from hydropower. Hydropower plants are widely used in mountainous areas re-

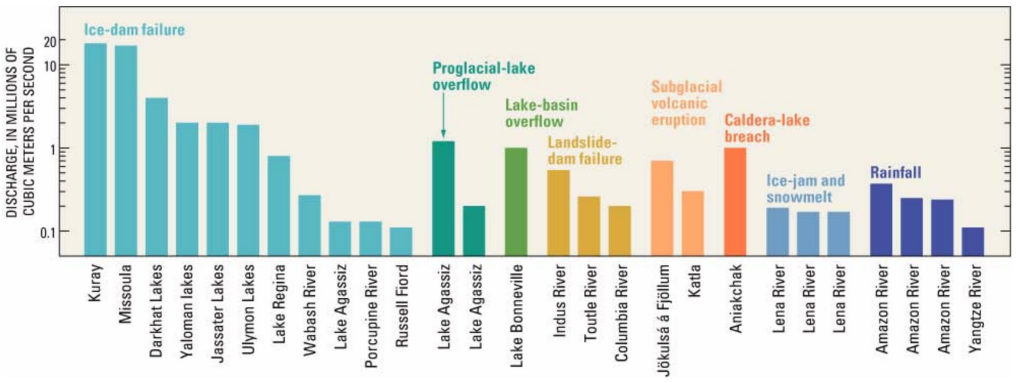

Figure 6: Discharges of outburst and meteorological floods of the world (from O'Connor and Costa (2004)).

garding the abundance of water. In seismic active areas they bear a large hazard potential, as they release large floods when they breach. Much attention has been drawn to the Himalayas in this context, where heavy monsoonal rainfall, floods, glacial lake outburst floods, and landslides threaten these plants (Sundriyal et al., 2015). But natural dams and their lakes often provide similar, if not greater, volumes of water, and hence higher flood impacts upon failure. Yet the state of natural dams in Central Asian mountain ranges in particular is only partly documented. Strom (2010) counted more than 100 large-scale landslide-impounded lakes, which still exist today. The largest is Lake Sarez in Tajikistan, dammed by the Usoi rockslide, which has been triggered by the Pamir earthquake in 1911. This natural dam is the highest in the world and impounds 16 km^3 of water (Ischuk, 2011). Earthquakes are one of the major dam failure triggers world-wide, as ground shaking might destabilize the dam or further rockslides lead to overtopping and fast erosion of the dam. However, several cases of long-lived landslide dams in seismically active regions caution against generalising this observation. Strom and Korup (2006) analysed several large rockslides in the Tien Shan and found evidences for co-seismic triggering as their proximity to active faults and spatial clustering. But they also found other factors such as the sporadic occurrence of permafrost, which could have compromised slope stability. In the context of atmospheric warming this phenomenon seems likely to increase in the Tien Shan. In this context, lake outbursts may be an underestimated

hazard, as catastrophic outburst floods from the sudden breaching of natural dams can be several magnitudes higher compared to river discharges (Figure 6 and references therein), carry much higher amounts of sediments, and thus produce higher impact forces. Various prehistoric and recent examples of floods from dam breaching underline the importance of studying hazard identification and mitigation (Delaney and Evans, 2011). For example, the 2010 Attabad landslide blocked the Hunza valley in northern Pakistan and killed 20 people. Hundreds of houses were destroyed by the landslide or by the extension of the forming lake. To mitigate a catastrophic outburst, a spillway was constructed, which currently seems to successfully drain the lake while avoiding its overtopping (Hayat et al., 2010).

0.3 Study area

The geographic focus of this thesis is on the northern Tien Shan mountains, where I also conducted most of my fieldwork. The high abundance of rock glaciers and examples of recent and historic natural dams, including rock-glacier dams made this area attractive to study these phenomena. Described as part of the Central Asian water towers, the Tien Shan mountains play a crucial role for the future water supply in a changing climate. I chose three mountain belts with largely differing environmental boundary conditions, namely the Tien Shan, the Altai, and the Himalayan Karakorum. The study areas are described in detail in Chapters 1–3, so that I only offer a broad overview here: the study areas cover an area of more than one million km^2 (roughly from 33° to 48°N and from 72° to 88°E). They encompass climate zones from temperate in the Himalayan regions to dry continental in the Tien Shan and Altai (climate-zone.com, 2017). The highest peaks are Pik Pobedy at 7,439 m asl in the Kyrgyz Tien Shan, and K2 at 8,611 m asl in the Pakistan Karakoram Himalaya. The high topography of these ranges is a product of the ongoing Indian-Eurasian collision (Molnar and Tapponnier, 1975; Tapponnier and Molnar, 1979). All ranges are actively uplifting and prone to large earthquakes, though of different mechanisms that reflect the

different tectonic settings. The northward propagation of deformation related to the building of the Himalayas has caused some rejuvenation of older intracontinental mountain ranges, and the migration of neotectonic activity along thrust belts and strike-slip faults that had developed during pre-Cenozoic phases of mountain building (Avouac and Tapponnier, 1993). The Cenozoic tectonic history of Central Asia is described in detail by Buslov (2004). The ongoing seismic activity is documented by some of the largest documented intracontinental earthquakes, which struck the Central Asian mountain belts during the 19th and 20th century (Kalmetieva et al., 2009).

The high mountains (Himalayas, Hindu Kush, Pamir Alai, and Tien Shan) have the highest concentrations of glaciers worldwide, and 800 million people depend on their meltwater (Pritchard, 2017). Fluctuations in precipitation and periodic water shortness assigns glaciers a critical role in storing the water dearly needed in the regions (Figure 7). Water stress threatens the political stability, economic independence, and sustainable development of these regions (Malone, 2010).

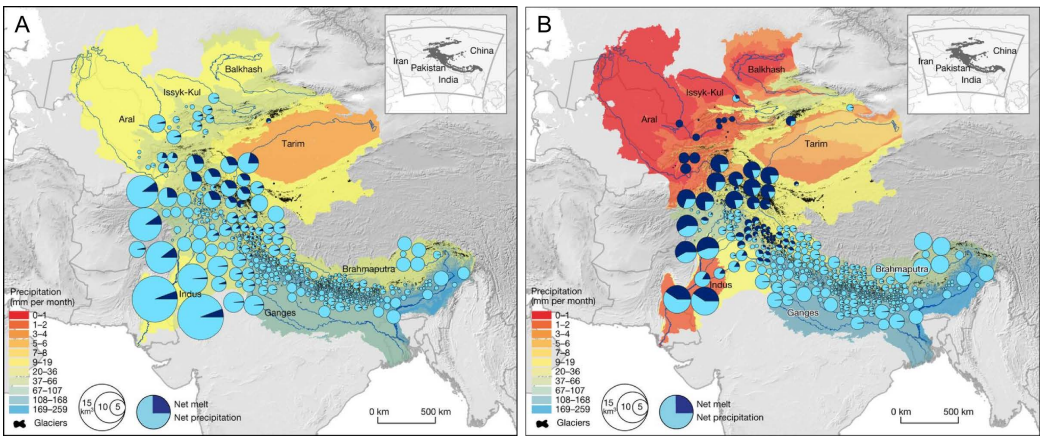

Figure 7: Major river catchment areas of high mountains in Asia (Aral, Issyk Kul, Balkhash, Tarim, Indus, Ganges, and Brahmaputra). Monthly precipitation and discharge values (circles separated into melt and precipitation proportions) shown for mean annual (A) and dry year (B) values (after Pritchard (2017)).

The Quaternary glacial histories might also affect the contemporary distribution of natural dams and rock glaciers in these mountain ranges, as many rock glaciers occur above the limits of Pleistocene glaciations (Lehmkuhl

et al., 2003), whereas many larger rockslide-dam deposits in the Himalayas seem to have originated from elevations below those of glacial trim lines. Glaciers in the Tien Shan advanced to their maximum during marine oxygen isotope stages (MIS) 5 and 4 in the north and east, and during MIS 3 in the south and west, respectively. During MIS 2 glaciers in the Tien Shan advanced hardly beyond the limit of modern glaciers (Koppes et al., 2008). Evidence of two major glacial stages (MIS 2 and 4) during the Pleistocene also occurs in Western Mongolia, while another glacial advance (MIS 3) occurred in Central Mongolia (Lehmkuhl et al., 2016). More recently, glaciers shrunk by about 19% in the Mongolian Altai since the 1950s, and this trend is predicted to continue in the 21st century (Shahgedanova et al., 2010). In the Kyrgyz Tien Shan, glaciers lost about 32% of their area in past decades, depending mostly on location and elevation (Bolch, 2007). Glacial loss has also been observed in the Hindu Kush Himalaya region, but the loss is increasing in most of Central Asia (Bolch et al., 2012). Detailed measurements record accelerated rock-glacier advances of up to several meters per year during the past decades in the Tien Shan, though whether this is solely in response to atmospheric warming requires more research (Bolch and Marchenko, 2006; Gorbunov et al., 1992). These studies of temperature increase, glacier shrinkage (Takeuchi et al., 2014; Sorg et al., 2012), and precipitation increase (Aizen et al., 1996) in Central Asia and the Tien Shan mountains are alarming. The Central Asian mountains follow a trend of global glacier shrinkage since the beginning of the Holocene (Solomina et al., 2016). Further information about climate (change) are given in Aizen et al. (1996, 1995). As a rule of thumb, permafrost occurs between 3500 and 5500 m asl in the Hindu Kush Himalayas (Schmid et al., 2015), between 2700 and 3500 m asl in the northern Tien Shan (Gorbunov, 1996), and between 600 and 3200 m asl in the Mongolian Altai (Sharkhuu, 2003). Permafrost in Mongolia occurs at temperatures close to 0°C and is thus likely unstable (Sharkhuu, 2003); rock glaciers lie between 2300 and 3400 m asl (Lehmkuhl et al., 2003). Active rock glaciers in the northern Tien Shan cover up to 5% of the area above 3000 m asl (state of 1999) (Bolch and Marchenko, 2006). They reach down below the 0°C isotherm, and some larger ones have advanced below the

permafrost limit (Bolch and Gorbunov, 2014).

0.4 Thesis structure and objectives

Natural dams are a double-sided coin in semi-arid and arid mountainous regions. On the one hand, these dams offer potentially important water and energy resources. On the other hand, the sudden failure of natural dams impounding larger water masses may release destructive outburst floods. In this context, rock glaciers may become more important as water resources in the future, although how important remains to be established more robustly. Similarly the role of rock glaciers as potential dam builders also needs more systematic study. Following from the introductory comments and motivation, this thesis addresses these two issues from three major angles in studies that make up the core chapters (Figure 8). Each of these chapters has been published or submitted to peer reviewed journals. The aims of the three core chapters are

1. To test how well lichenometry works as a technique for dating rock-glacier lobes in the northern Tien Shan. This low-cost method may allow distinguishing between generations of rock glaciers or rock-glacier lobes and thus provide insight into their mobility and longevity. This study focuses on rock glaciers at the local scale.

2. To pinpoint those controls that separate those rock glaciers that impact mountain rivers from those that do not, in different mountain ranges in Central Asia. This study focuses on rock glaciers at the large regional scale.

3. To reconstruct in detail whether there is a possibility of causally linking between episodic outburst floods from lake Issyk Kul and correlate lake-level changes. This study focuses on natural dams and the regional Quaternary history of outburst floods.

The three studies cover and question rock-glacier dynamics at differing spatial scales. While age dating is essential foremost on a local scale, it is useful

to zoom out to compare rock glaciers from different Central Asian mountain belts when dealing with the question if their ability to dam lakes is predictable on the basis of multiple climatic and geomorphic parameters. The broader regional context of the dam breach history of the lake Issyk Kul deals with the natural dams' contribution to form the surrounding landscape during the Quaternary.

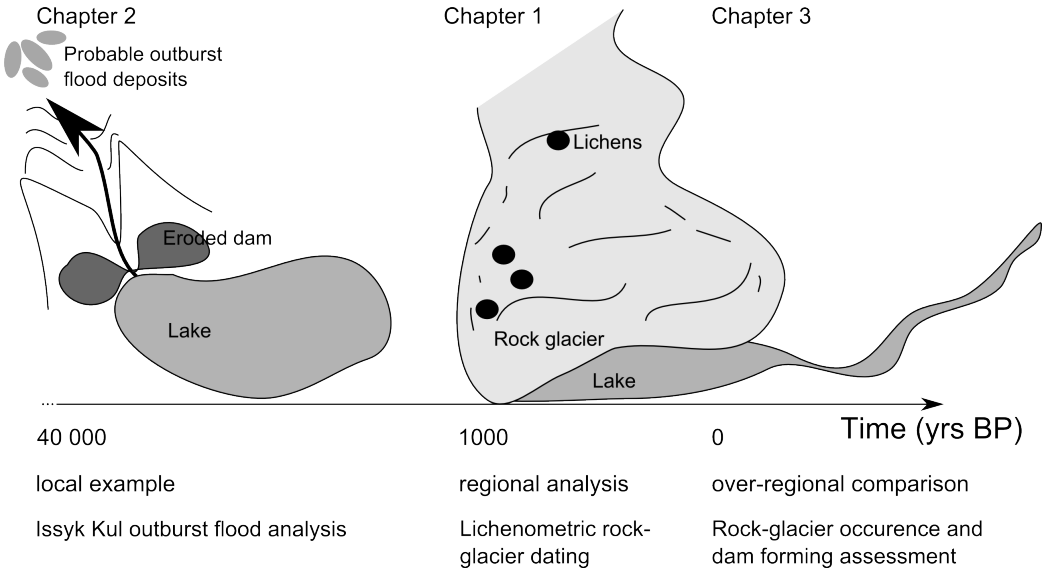

Figure 8: Sketch of research covered by this thesis.

The first core chapter aims to resolve age relationships of different rock-glacier lobes and different rock glaciers of the northern Tien Shan. Dating rock glaciers has been difficult partly because they are highly dynamic landforms. Dendrochronology has been successfully used to date the last rock-glacier activities by analysing tree-ring damages (Sorg et al., 2015), but can only give information for those parts, which are below the tree line. Thus the method is limited to low-lying and stable, if not inactive, lobes that offer surfaces stable enough for trees to grow on. Using cosmogenic nuclide dating may not be recommendable as the blocks on active rock glaciers might be moving too much. I have chosen lichenometry to date the surface of rock glaciers, which uses the diameter of lichens growing radially on the rock surfaces. Lichenometry is an easy and low cost method. The ability to measure large quantities of lichen diameters lowers the bias resulting from

rocks that might have moved independently of any climatic or seismic driver. Lichenometry has been criticised recently, because lichen growth depends highly on the micro-environment and the subjective sampling and measurement method (Osborn et al., 2015). To check for the validity of dates of several strategically selected rock-glacier lobes, the first core chapter of my thesis concentrates on a methodological question:

> **Q1:** *Is the resolution from lichenometric dating high enough to distinguish between ages of rock glaciers and their lobes with confidence?*

Lichens have large lifespans and can grow for several thousand years in extreme cases. One specimen of Rhizocarpon geographicum on East Baffin Island has been estimated to be 9500 years old (Miller and Andrews, 1972). With question Q1 I'm testing 1) whether the resolution of the method is high enough to separate ages between different rock-glacier lobes, and 2) whether these date estimates are congruent between those different lobes of the different rock glaciers and fit into the regional glacial or earthquake history.

The second core chapter concentrates on those rock-glaciers which influence the river stream or impound a lake by blocking the stream. Rock-glacier research has largely focussed on permafrost, hydrology and environmental change (Schmid et al., 2015; Thies et al., 2013). The geomorphic influence and impact of rock glaciers on the stream network still awaits detailed research. Changes in rock-glacier advance rates through increasing air temperatures and retreating permafrost might lead to an increasing connectivity to the river network, and thus pave the way for more disturbances of water and sediment flux in the river system. The spatial pattern of rock-glacier occurrence depends not solely on geomorphometric and climatic conditions, but possibly also earthquakes and site-specific patterns of permafrost (Bolch and Gorbunov, 2014). Chapter 2 aims at a regional analysis to identify significant parameters that influence rock-glacier occurrence and characteristics, and addresses the following question:

> **Q2:** *Which parameters are more likely to lead to the ability of rock glaciers to dam rivers?*

River damming and lake outbursts are common in high mountains, especially where seismic activity is high. To better understand the possible consequences of major lake outbursts around Issyk Kul, in my third core chapter I present one prominent example of where purported lake outbursts in prehistoric times caused major lake-level changes. The lake Issyk Kul shows evidence of pronounced lake level changes that may have resulted from multiple damming and outburst events. Lake highstands are marked by shorelines at up to 40 m above the present day lake level dated back to the early Late Pleistocene. Low levels down to 110 m below today's lake level are marked by submerged channels (De Batist et al., 2002) dated to Late Pleistocene (Bondarev and Sevastianov, 1991; Markov, 1971) and Middle Holocene (Trofimov, 1978) times. Aarchaeological remnants dated to 2,500 years ago at 20 m below the recent water level (Lukashov and Lukashov, 2012; Romanovsky, 2002) also indicate lower prehistoric lake levels. The highest-lying of these documented shorelines suggests that the lake that had expanded at its western edge well into the Boam Gorge, through which the Chu River slices before entering the foreland of the northern Tien Shan. Lake sediments in the gorge record former lake highstands, and their geometric assemblages suggests that a natural dam must have been existed there previously to retain the corresponding volumes of water. Downstream of the gorge numerous up to 4-m large boulders, partly rounded, pose possible evidence of a catastrophic lake outburst. We synthesise all previous and new field evidence and reconstruct that an outburst flood from a large lake, probably lake Issyk Kul, carried these large boulders to their current position. To reconstruct the past conditions of a possible lake, we need to ask:

> **Q3:** *Do ages of deposited rocks indicate one or more flood events, and are these connected to lake level drops?*

To answer this question, we determined exposition ages using the concentration of the cosmogenic nuclide ^{10}Be, a beryllium isotope, which accumulates with time due to the interaction of cosmic rays with the oxygen atoms of the surface rock. We also used ^{10}Be to determine the surface ages of river terraces. Sediments of lake highstands were dated using ^{14}C isotope in shells,

molluscs, and charcoal, and the sediment burial age was determined using IRSL (infrared stimulated luminescence). A connection between lake level changes and lake outbursts resulting from tectonic or climatic changes has been discussed in other studies (De Batist et al., 2002; Grosswald et al., 1994). In my third core chapter we examine different indices that document lake-level fluctuations and outburst floods and piece them together.

0.5 Chapter outline and author contributions

The three chapters presented in the following were published or submitted in international peer-reviewed journals. The work in the three studies was done collaboratively. Here I shortly outline these core chapters of my thesis, and acknowledge all co-authors' and my own contributions to each of the studies.

Chapter 1 – Limits to Lichenometry

This study points out the difficulties that arise from lichenometry and the benefits from the Bayesian statistic approach we chose to capture these uncertainties objectively. We credibly show within the limits of resolution the differences and similarities between rock glacier lobes due to their different lichen diameters and associated inferred ages. Climate, earthquakes, and the (limited) resolution of lichen growth rates are discussed to explain those differences.

Rosenwinkel, S., Korup, O., Landgraf, A., Dzhumabaeva, A. (2015): "Limits to lichenometry", *Quaternary Science Reviews*, 129, 229–238

All co-authors collected the field data, and contributed to discussions. S.R. and O.K. analysed the data, designed the artwork, and wrote the article.

Chapter 2 – Rock glacier dams in High Asia

For this study we compiled a new dataset of over 1300 rock glaciers, and used a Bayesian logistic regression to identify predictors for the conditions under which rock glaciers may dam rivers or interact with them.

Blöthe, J.-H., Rosenwinkel, S., Höser, T., Korup, O. (2018):

"Rock glacier dams in High Asia", in Review process at *Earth Surface Processes and Landforms*

All co-authors collected the data, contributed to discussions, interpretations, art work, and writing. Bayesian analysis was conducted by O.K. and S.R. The second revisions were carried out thoroughly by J.B. including further mapping and recalculations. Therefore J.B. and S.R. changed first-authorship for the second review process in January, 2018 to appreciate the work of J.B.

Chapter 3 – Late Pleistocene outburst floods from Issyk Kul, Kyrgyzstan?

Palaeo-lake sediment deposits and large megaclasts which were observed in the field point to a linkage between alternating lake-damming or highstands and outburst-flood scenarios. We combined age constraints of lake and delta deposits and palaeo-outburst flood modelling to assess this linkage, and to discuss its implications for the longer-term evolution of mountain valleys to the west of the lake.

Rosenwinkel, S., Landgraf, A., Schwanghart, W., Volkmer, F., Dzhumabaeva, A., Merchel, S., Rugel, G., Preusser, F., Korup, O. (2017): "Late Pleistocene outburst floods from Issyk Kul, Kyrgyzstan?", *Earth Surface Processes and Landforms*, 42, 10, 1535-1548

S.R., A.L., F.V., A.D., and O.K. conducted fieldwork and collected the data. S.R. prepared rock samples and performed laboratory treatment for cosmogenic nuclide analysis. The AMS measurements for ^{10}Be were performed at HZDR by A.M. and G.R, and discussed with them. The OSL samples were analysed and interpreted by F.P.. W.S. and F.V. performed the paleoflood modelling. F.V. included the results in a Bachelor thesis. The results of the combined methods were discussed and written by S.R., A.L., W.S., and O.K. The artwork was designed by the latter and F.V. Chemistry methodology was carefully improved by S.M. and F.P.

Furthermore I helped with the fieldwork and contributed to the field discussions of the following publication, which is published in Bulletin of the

Seismological Society of America:

Patyniak, M., Landgraf, A., Dzhumabaeva, A., Abdrakhmatov, K. E., Rosenwinkel, S., Korup, O., Preusser, F., Fohlmeister, J., Arrowsmith, R. J., Strecker, M. R. (2017): "Paleoseismic record of three Holocene earthquakes rupturing the Issyk-Ata fault near Bishkek, North Kyrgyzstan", *BSSA*, 107(6), 2721-2737

Chapter 1

Limits to Lichenometry

Abstract

Lichenometry is a straightforward and inexpensive method for dating Holocene rock surfaces. The rationale is that the diameter of the largest lichen scales with the age of the originally fresh rock surface that it colonised. The success of the method depends on finding the largest lichen diameters, a suitable lichen-growth model, and a robust calibration curve. Recent critique of the method motivates us to revisit the accuracy and uncertainties of lichenometry. Specifically, we test how well lichenometry is capable of resolving the ages of different lobes of large active rock glaciers in the Kyrgyz Tien Shan. We use a bootstrapped quantile regression to calibrate local growth curves of *Xanthoria elegans*, *Aspicilia tianshanica*, and *Rhizocarpon geographicum*, and report a nonlinear decrease in dating accuracy with increasing lichen diameter. A Bayesian type of an analysis of variance demonstrates that our calibration allows discriminating credibly between rock-glacier lobes of different ages despite the uncertainties tied to sample size and correctly identifying the largest lichen thalli. Our results also show that calibration error grows with lichen size, so that the separability of rock-glacier lobes of different ages decreases, while the tendency to assign coeval ages increases. The abundant young (<200 yr) specimen of fast-growing *X. elegans* are in contrast with the fewer, slow-growing, but older (200–1,500 yr) *R. geographicum* and *A.*

tianshanica, and record either a regional reactivation of lobes in the past 200 years, or simply a censoring effect of lichen mortality during early phases of colonisation. The high variance of lichen sizes captures the activity of rock-glacier lobes, which is difficult to explain by regional climatic cooling or earthquake triggers alone. Therefore, we caution against inferring palaeo-climatic conditions from the topographic position of rock-glacier lobes. We conclude that lichenometry works better as a tool for establishing a relative, rather than an absolute, chronology of rock-glacier lobes in the northern Tien Shan.

1.1 Introduction

Lichenometry is an inexpensive and straightforward dating technique based on a systematic relationship between the lichen thallus size and the age of the rock surface the lichen grows on. If adequately calibrated, this relationship can be used to estimate the exposure age of an undated rock surface assuming it has remained stable and undamaged (Beschel, 1973). Lichenometry is a common tool for dating Holocene glacier advances, earthquakes, and floods using moraines (Solomina et al., 1994), rock-fall debris (Nikonov and Shebalina, 1979; Bull et al., 1998), and fluvial sediments (Foulds et al., 2014), respectively. The basic four variants of lichenometry involve measuring (i) the largest lichen(s) on a landform of interest; (ii) the largest lichen(s) within a specified unit area; (iii) different lichen-size distributions; and (iv) the relative fraction of a rock surface covered by lichens (Bradwell, 2009).

The growth curve is at the core of the lichenometry, and models the systematic change of thallus diameter with age. Directly measured growth rates are roughly between 0.02 and 1.5 mm yr^{-1} for *Rhizocarpon* subgenus (Matthews and Trenbirth, 2011), positively correlated with lichen diameter (Roof and Werner, 2011), and reproduced best by concave-upward to linear growth-rate models (e.g., Trenbirth and Matthews (2010)). Direct measurements cannot capture any long-term changes, and reveal only contemporary growth rates (Roof and Werner, 2011). This is why indirect measurements,

such as fitting a regression model to lichen diameters with known calendric dates, remain widely used for determining growth curves, at least for geomorphic purposes. These regression models show negative correlations between growth rate and lichen diameter. The convex upward shape of most associated growth curves may reflect phases of fast growth for smaller lichens followed by linear growth for larger lichens (Solomina et al., 1994; Bull et al., 1998). Part of this nonlinear growth possibly mirrors changes in environmental conditions during the long life spans of lichens: one specimen of R. geographicum on East Baffin Island has an estimated age of 9,500 years (Miller and Andrews, 1972). Loso and Doak (2006) argued that the convex-upward shape of lichen-growth curves is consistent with the linear growth observed in direct measurements, if accounting for lichen mortality and the decreasing probability of finding the largest lichen with increasing surface age. They suggested using indirect measurements together with estimates of the probability to find the largest lichen by including ecological parameters such as the rates of colonization, growth, and survival. Direct lichen measurements of *R. geographicum* in Wales (Armstrong, 1983) and Iceland (Bradwell and Armstrong, 2007) confirm that lichen size depends on growth rates as detected by indirect measurements. These studies show a parabolic relationship between growth rates and thallus diameter with increasing growth rates for small lichen thalli, constant rates for larger thalli, and decreasing rates for the largest lichen thalli. However, indirect measurements in recently deglaciated areas in southern South America returned linear growth curves for *R. geographicum* during the past 30 years, with rates as high as 0.63 mm yr^{-1} (Sancho et al., 2011).

Lichenometry has earned repeated critique because of inconsistent and partly irreproducible measurement and sampling strategies, data handling, treatment of errors, and several questionable assumptions regarding lichen growth (Osborn et al., 2015). Traditional approaches to lichenometry rely on sampling the largest lichen(s) on a rock surface or landform of interest (Solomina et al., 1994), assuming that the largest lichens are the first colonizers. Using only a few of the largest lichens to establish a growth curve via regression models can produce misleading results compromised by a small

sample size or several outliers (Calkin and Ellis, 1984), although the thresholds for these outliers are arbitrary (Loso and Doak, 2006). Averaging across the largest lichen diameters helps to decrease the error due to, for example, anomalously large lichens that could have survived the transport from older surfaces. Size-frequency distributions of many samples (n ∼1000) also help to identify anomalous large lichens, and can further aid dating purposes based on mean diameter-age correlations (Innes, 1983; Winchester and Harrison, 1994). Other researchers used digital image analysis to estimate the age of a rock surface from the degree of lichen coverage that is assumed to increase with time (McCarthy and Zaniewski, 2001).

In meeting these potential shortcomings, lichenometrists have suggested several statistical approaches to quantify the uncertainties tied to the method. Jomelli et al. (2007) compared the effects of different sampling strategies by applying them on dated tombstones, and found that methods measuring only the largest, the five or the ten largest lichen diameters were unable to reliably predict the tombstone dates. Instead they suggested to use a hierarchical Bayesian model based on a Generalized Extreme Value (GEV) distribution for analysing only the largest lichen measurements (Cooley et al., 2006). Cluster analysis is another statistical approach to distinguish between two lichen-size distributions and returns a goodness-of-fit parameter (termed Watson's U2) describing the proximity of the two distributions in parameter space (Watson, 1961). Watson's U2 can be used to distinguish significantly different lichen populations and their habitats, for example moraine surfaces, and mainly offers a relative rather than absolute dating tool (Orwin et al., 2008). Regardless of the level of success, the complexity and lacking user friendliness of these approaches have been recognised a major disadvantage when compared with the original simplicity of the method (Bradwell, 2009).

Here we contribute to this discussion on the accuracy, uncertainty, and choice of methodological complexity of lichenometry. We explore bootstrapped quantile regression as a robust technique for objectively fitting nonlinear growth curves to a number of the largest lichen diameters of known ages. This method allows quantifying the temporal resolution and precision of lichenometry as a function of thallus size. We then use a Bayesian ana-

logue to the classic analysis of variance or ANOVA (Kruschke, 2012) as a means to test whether lichenometry is capable of resolving the formation ages of large active rock-glacier lobes in the Kyrgyz Tien Shan. We test whether differences in lichen diameters and inferred ages on selected rock-glacier lobes reflect different phases of inception or mobility, and discuss some of the potential causes of multiple lobes on the rock glaciers. The actively deforming surfaces of creeping rock glaciers provide many fresh but partly unstable rock surfaces for lichen colonisation in a highly continental climate, and thus put lichenometry to a stringent test. Another motivation for focusing on rock glaciers is that they are popular indicators of mountain permafrost and past climatic cooling episodes; yet despite their increasingly acknowledged relevance worldwide (Haeberli et al., 2006), few rock glaciers have been dated. Moreover, rock glaciers store significant volumes of freshwater that, per unit area, is comparable to, or even higher, than in glaciers (Gorbunov et al., 1992), and may therefore play a seminal role in the hydrology of semiarid high-mountain ecosystems (Azócar and Brenning, 2010). Thus rock glaciers become increasingly important in the context of temperature increase and pronounced melting of glaciers during the last decades (Bolch and Marchenko, 2006), and especially so in the northern Tien Shan, which has a higher spatial density of rock glaciers than the Swiss Alps or parts of the Nepal Himalaya (Bolch and Gorbunov, 2014).

1.2 Study area

The high topography of the Tien Shan mountains is the result of the ongoing Indian-Eurasian collision (Molnar and Tapponnier, 1975; Tapponnier and Molnar, 1979). The Tien Shan still exhibits uplift and seismic activity. Our study area around Lake Issyk Kul in the northern Tien Shan was affected by a series of major earthquakes in the late 19^{th} and early 20^{th} centuries, among them some of the strongest intracontinental events such as the M_{lh} 8.1 Chon Kemin (1911), M_{lh} 6.9 Kemino-Chu (1938), M_{lh} 6.9 Belovodskoe (1885), M_{lh} 7.3 Verny (1887), M_{lh} 8.3 Chilik (1889), and M_{lh} 6.8 Sarykamysh

(1970) earthquakes (Kalmetieva et al., 2009) (Figure 1.1). In the northern Tien Shan, mean annual air temperature (MAAT) ranges from –4 °C at the Tuyuksu glacier station (3,434 m asl) (Figure 1) to ∼9 °C at the northern edge of the Zailisky Range (850 m asl) (Bolch, 2007). A temperature increase of ∼0.02 K yr^{-1} was recorded at different stations in northern Tien Shan since the 1950s (Aizen et al., 1997; Bolch, 2007). Compared to lowland areas, Aizen et al. (1997) detected a higher temperature increase at >2,000 m asl, whereas Bolch (2007) reported a less pronounced positive trend; Giese and Moßig (2004) even reconstructed a temperature decrease. The highest precipitation occurs in early summer with 1,000 mm on windward northern slopes, and 800 mm on leeward southern slopes; precipitation has been more variable since the 1950s, though without a clear trend (Aizen et al., 2007; Bolch, 2007). Summer precipitation is derived from North Atlantic, Mediterranean, and Black Sea cyclones and recycled moisture from the Aral-Caspian drainage basin (Aizen et al., 2006). During winter the Siberian high blocks the air masses and only small amounts of precipitation reach our study area; the average precipitation in January is ∼15 mm at ∼2500 m asl) (Aizen et al., 1996).

Permafrost in the northern Tien Shan occurs in a continuous (>3,500 m asl), discontinuous (3,200–3,500 m asl), and sporadic (2,700–3,200 m asl) belt (Gorbunov, 1996). Isolated patches of permafrost have been found at north-facing or shaded slopes, inside blocky debris or beneath moss cover below 2,700 m asl, and even as low as 1,800 m asl (Gorbunov et al., 1992). Rock glaciers form under these permafrost conditions as ice-rich debris creeps downslope. Of the more than 1,000 rock glaciers in the region (Gorbunov et al., 1992), the largest examples in the northern Tien Shan are 1–3 km long, and reach down to or below the zero-degree isotherm (Bolch and Gorbunov, 2014). Warm permafrost favours high frontal velocities of as much as 5–10 m yr^{-1} (Gorbunov et al., 1992), which outpace those of rock glaciers in other mountains such as the Swiss Alps by one to two orders of magnitude (Delaloye et al., 2010). Morphometric analyses indicate that the distribution and the extraordinary size of some rock glaciers cannot be fully explained by topographic characteristics of their source area: instead the

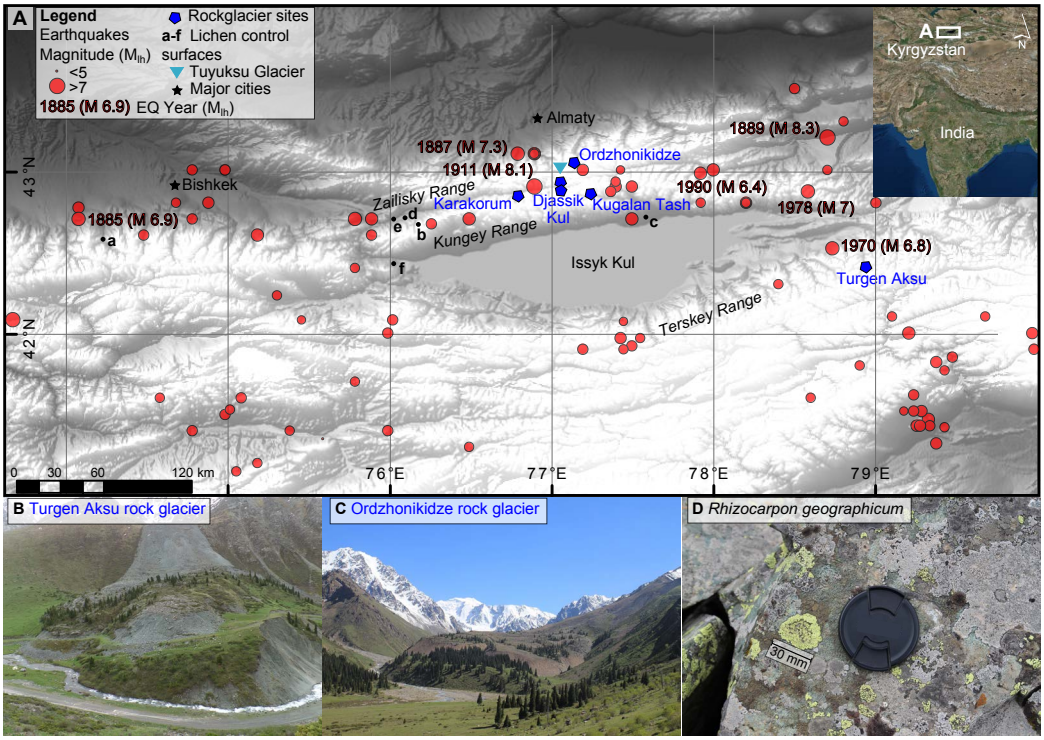

Figure 1.1: A. Shaded relief model (90-m SRTM) of northern Kyrgyzstan with rock-glacier sites and control surfaces for lichen measurements, i.e. the Belogorka, Kainde, and Ananevo rock falls (a–c); and dated tombstones (d–f). Red circles are locations of historic earthquakes (Kalmetieva et al., 2009) scaled to their local magnitude. B. Turgen Aksu rock glacier (photo by M. Zeckra). C. Ordzhonikidze rock glacier. C. Lichen species *Rhizocarpon geographicum*.

interaction with polythermal glaciers, intensive weathering, or debris input by rock avalanches may play a key role in forming these larger rock glaciers (Bolch and Gorbunov, 2014).

The Karakorum, Djassik Kul (North and South), Kugalan Tash, Turgen Aksu, and Ordzhonikidze are among the longest and lowest lying rock glaciers in the northern Tien Shan (Figure 1.1, Table 1.1). All of them descended into permafrost-free areas (Bolch and Gorbunov, 2014), and thus may offer insights into the timing or causes of such conspicuous long-reach advances. The dynamics of these rock glaciers differed in recent decades. For example, the Karakorum rock glacier on the northern slope of the Kungey Range was the fastest moving with velocities of 2–7 m yr^{-1} between 1969 and 1977 (Gorbunov et al., 1992), and accelerated since 2000 (Sorg et al., 2015).

In contrast, the Djassik Kul rock glaciers in the headwaters of the Chon Kemin River converged from opposite slopes, dammed an 800-m long and 200-m wide lake, and likely limit each other's movement. Photogrammetric and dendrogeomorphic measurements show that only the Kugalan Tash, Turgen Aksu, and Ordzhonikidze rock glaciers decelerated since the 1980s (Sorg et al., 2015). For these three rock glaciers, we report our lichenometric results in detail. The Kugalan Tash rock glacier partly blocks the Chon Aksu River, and has younger lobes overriding older ones, judging from different vegetation-stand heights and lobe-riser steepness. Ordzhonikidze rock glacier is in the Leviy Talgar valley, Zailisky Range, and fed by three glaciers. Turgen Aksu is named after a valley south of Issyk Kul, and is the shortest, but steepest of the three rock glaciers that we studied (Table 1.1). All sampled rock glaciers emerge from small cirque glaciers, contain granitic rocks and schists (Gorbunov et al., 1992), and feature steep ridges, furrows, and scarce vegetation with deformed trees on blocky surfaces. The toes of the rock glaciers are inclined at slopes of up to ∼38° (Sorg et al., 2015).

Table 1.1: Selected characteristics of the six large and low-lying rock glaciers that we sampled for lichenometry (Gorbunov et al., 1992; Bolch and Gorbunov, 2014; this study)

Name	Latitude [°N]	Longitude [°E]	Toe elevation [m asl]	Aspect	Max length [m]	Max width [m]	Mean slope [%]
Kugalan Tash	42.848	77.263	3024	SE	3700	540	15
Turgen Aksu	42.415	78.96	2943	N	970	450	22.6
Ordzhonikidze	43.072	77.166	2718	NE	3390	540	15.6
Karakorum	42.878	76.848	2671	N	4000	550	14.2
Djassik Kul North	42.908	77.105	3123	SSW	3150	500	19
Djassik Kul South	42.908	77.105	3123	N	4360	800	9.7

1.3 Methods

We measured lichen diameters on six active rock glaciers during three field seasons in the summers of 2012, 2013, and 2014. We targeted 37 distal lobes on these rock glaciers in order to put the lichenometric method to a

rigorous test. Our objective was to check how well the method is capable of resolving differential rock-glacier movement by inferring the ages of individual lobes. We used digital calipers to measure the diameter of a total of 8,565 lichens to the nearest mm. We chose the lichen species *Xanthoria elegans*, *Aspilicia tianshanica*, and *Rhizocarpon geographicum*, because these occurred on all studied rock glaciers as well as on most rock surfaces that we used for calibration. Field observation show that *X. elegans* grows preferentially at lower elevations, and is gradually replaced by *R. geographicum* at higher elevations; *R. geographicum* was very rare at the Kugalan Tash rock glacier.

Our data include 678, 160, and 380 thallus measurements of *X. elegans*; 159, 160, and 694 of *A. tianshanica*; and 14, 178, and 1279 of *R. geographicum* on the Kugalan Tash, Turgen Aksu, and Ordzhonikidze rock glaciers, respectively. We focused on circular lichens; sample measurements of the minimum and maximum diameter of some 80 lichens returned negligible differences. From the total number of measurements, we used the ten largest lichens on each rock-glacier lobe. To constrain lichen colonisation to the nearest calendar year, we also measured 88 largest lichens on nearby dated tombstones at 42°27'N/76°3'E, 42°44'N/76°9'E, and 42°44'N/76°3'E that were erected between 1959 and 1999. We further sampled 677 lichens on the deposits of three large rockslides (Belogorka at 42°38'N/74°16'E, Ananevo at 42°38'N/77°37'E, and Kainde at 42°43'N/76°12'E) that were triggered by the Belovodsk earthquake in 1885 (Havenith et al., 2003), and the Chon Kemin earthquake in 1911 (Bogdanovitch et al., 1914). We also included 260 lichen measurements from Northern Kyrgyzstan (81 for *X. elegans*, 70 for *A. tianshanica*, and 16 for *R. geographicum*) on moraines and debris-flow deposits; these measurements were calibrated by historical aerial photos (Koshoev, 1986; Pomortsev, 1980; Solomina, 1987), and ^{14}C ages of buried soils (Savoskul and Solomina, 1996), respectively.

To convert our lichen diameters to lichen ages we used the lichen growth model proposed by Bull et al. (1998):

$$D = D_0(1 - \exp(-K(\tau - \tau_0))) + C(\tau - \tau_0), \tag{1.1}$$

where D is the largest lichen diameter [mm], D_0 is the excess lichen size produced by great growth [mm], K is the non-linear component of the growth rate during the great growth phase [yr^{-1}], τ is the age of substrate exposure [yr], τ_0 is mean colonization time [yr], and C is the constant growth rate during the linear growth phase [mm yr^{-1}]. This four-parameter model assumes that lichen colonisation occurs several years after a fresh rock surface has formed. According to this model, lichen diameters begin to grow exponentially, followed by a linear growth phase, and deceleration of growth after some time. We applied this model to the largest of our lichen diameters that we separated by lichen species to obtain species-dependent growth rates and potentially different surface ages, respectively. Comparing the applicability of this growth model to several alternatives is beyond the scope of this study. Instead, we report on some of the limits to lichenometry using this particular model.

We used nonlinear quantile regression to objectively identify the largest lichen conditional on their age by fitting Equation 1 to the 0.95 quantile to lichen diameters for which we had absolute age control. Our choice of quantile model is arbitrary, and could equally well be the 0.99 or any other high-ranking quantile. We used simple bootstrapping to quantify the role of sample consistency for calibrating our growth model. We created 1,000 random subsets containing 75% of the dated lichens, and fitted Equation 1 to each of them. This resampling procedure simulates absent or uncertain observations, for example, scenarios in which largest lichens remained unfound or in which they were simply older, and passively rafted onto the rock glaciers from adjacent hillslopes. We computed the 95% bootstrap confidence intervals for the four model parameters and calculated the commensurate fitting error to the nearest mm of lichen diameter.

We then tested whether and how well our calibrated lichen diameters and their ages were able to distinguish between different rock-glacier lobes. To this end, we used a Bayesian implementation of an analysis of variance or ANOVA (Kruschke, 2012). This method allowed us to check for credible differences in the posterior distributions of the lichen diameters and ages across different lobes and rock glaciers. The method is based on the deviations (or

contrasts) of the measured diameters and ages from the common mean β_0, and checks whether these contrasts are credibly different from zero:

$$y_i = \beta_0 + \Sigma_j \beta_{[j]} x_{[j]}(i), \tag{1.2}$$

where y_i is the predicted contrast for the ith data point with a normal distribution specified by the right-hand side of Equation 2, containing the common mean β_0, and coefficients β_j across j groups, which in our case are the different rock-glacier lobes. The hierarchical setup of the model places a normal distribution on βj with zero mean and a standard deviation taken from a gamma hyperprior with a mode of 0.1 and a standard deviation of 10, i.e. $\Gamma(1.01005, 0.1005)$ (see Kruschke, 2012 for details). We chose the 95% highest density interval of the posterior distributions and checked whether these included zero contrasts, meaning that lichen diameters (or alternatively, their inferred ages) on the compared rock-glacier lobes were not credibly different. The computation involved a Markov Chain Monte Carlo sampling scheme that we implemented in the R programming language and the JAGS extension.

1.4 Results

Bootstrapped quantile regression offers two important insights into the use of lichen as timestamps for rock surfaces. First, among all lichen species sampled, X. elegans diameters between 30 and 50 mm have the narrowest 95% bootstrap confidence interval, and are most suitable for predicting rock-surface ages that are ∼20 to ∼40 yr old (Figure 1.2). We note that the generalisation error is likely to be higher when predicting ages for unobserved cases. Second, larger lichens achieve less temporal resolution across all species. Assuming the growth model (Equation 1) is applicable, the best age estimate we can expect for *X. elegans* with a diameter of 85 mm is 90-122 yr with 95% confidence. Increasing the lichen diameter only slightly to 90 mm substantially broadens the predicted age range to 98-144 yr. This increased uncertainty for larger lichen means that a measurement error of only 1 mm

translates to misestimates of 2-5 years for lichen diameters between 95 and 110 mm (Figure 1.3).

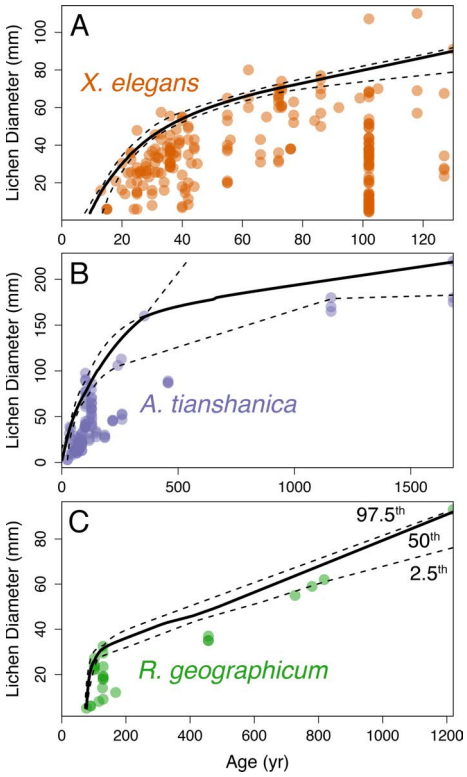

Figure 1.2: Results from fitting the lichen-growth model by Bull et al. (1998) to the 0.95-quantile conditional on rock-surface age for three lichen species using bootstrapped quantile regression. We fitted 1,000 models to randomly drawn subsets containing 75% of the measured data. Black and dashed lines are median and 95% bootstrap confidence intervals of these models, respectively.

The spatial distribution of lichen sizes on the rock-glacier lobes reveals some local, but no overarching or consistent linear, trend with mean elevation for any of the sampled species (thick grey lines in Figure 1.4B). For example, *X. elegans* appears to increase in size towards the toe only on Kugalan Tash rock glacier, where we measured most of the smallest, and least variable, lichen sizes. In contrast, the spread of lichen diameters on individual lobes is largest on the Ordzhonikidze rock glacier (Figure 1.4).

The results from a Bayesian ANOVA show that different rock-glacier lobes as well as different rock glaciers can be credibly separated using the largest lichen diameters and their predicted ages. Figure 1.5 shows the posterior probability densities of the difference in means of the ten largest lichen sizes on all lobes of the Kugalan Tash, Turgen Aksu, and Ordzhonikidze rock glaciers. Lichen diameters on Kugalan Tash and Turgen Aksu are 95%

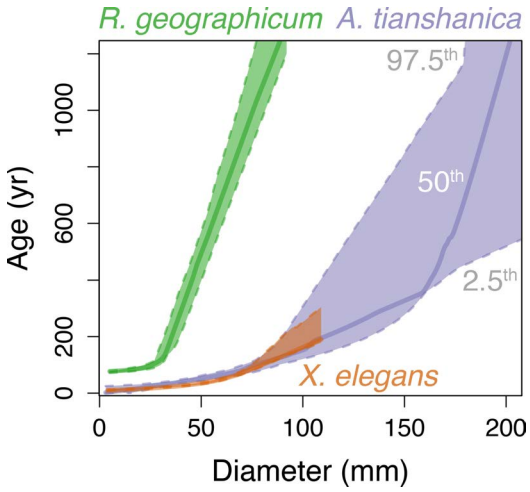

Figure 1.3: Calibrated age range for a given lichen diameter and species, estimated from bootstrapped quantile regression using the growth model by Bull et al. (1998). Shaded areas are the 95% bootstrap confidence intervals of the 0.95-quantile regression model; thick lines are median estimates. Note the similar calibration of *X. elegans* and *A. tianshanica* for lichen diameters <100 mm.

credibly different for all species, given that a zero contrast probability is not contained in the 95% highest density intervals (HDIs) of the posterior distributions. However, we cannot credibly distinguish between the Kugalan Tash and Ordzhonikidze rock glaciers if using *X. elegans*; the same goes for Turgen Aksu and Ordzhonikidze when using species *R. geographicum* (Figure 1.5). Of all six studied rock glaciers, we can credibly separate 7, 13, and 5 out of 15 possible rock-glacier pairs using diameters of *X. elegans*, *A. tianshanica*, and *R. geographicum*, respectively. In other words, *A. tianshanica* has the highest differences in measured diameters between the individual rock-glacier sites, regardless of lobe habitat (Table S1).

When using the calibrated age range (Figure 1.3) instead of measured lichen diameter, our Bayesian analysis shows that ten out of 15 rock glacier pairs have a 95% credible difference for *A. tianshanica*, whereas only a maximum of two rock-glacier pairs can be distinguished from each other using the predicted lichen ages of other species (Table S1). Thus the posterior probabilities of contrasts in predicted ages return fewer distinguishable lobe pairs than the posterior probabilities of contrasts in lichen diameters. The two lichen species growing on Kugalan Tash rock glacier have the youngest

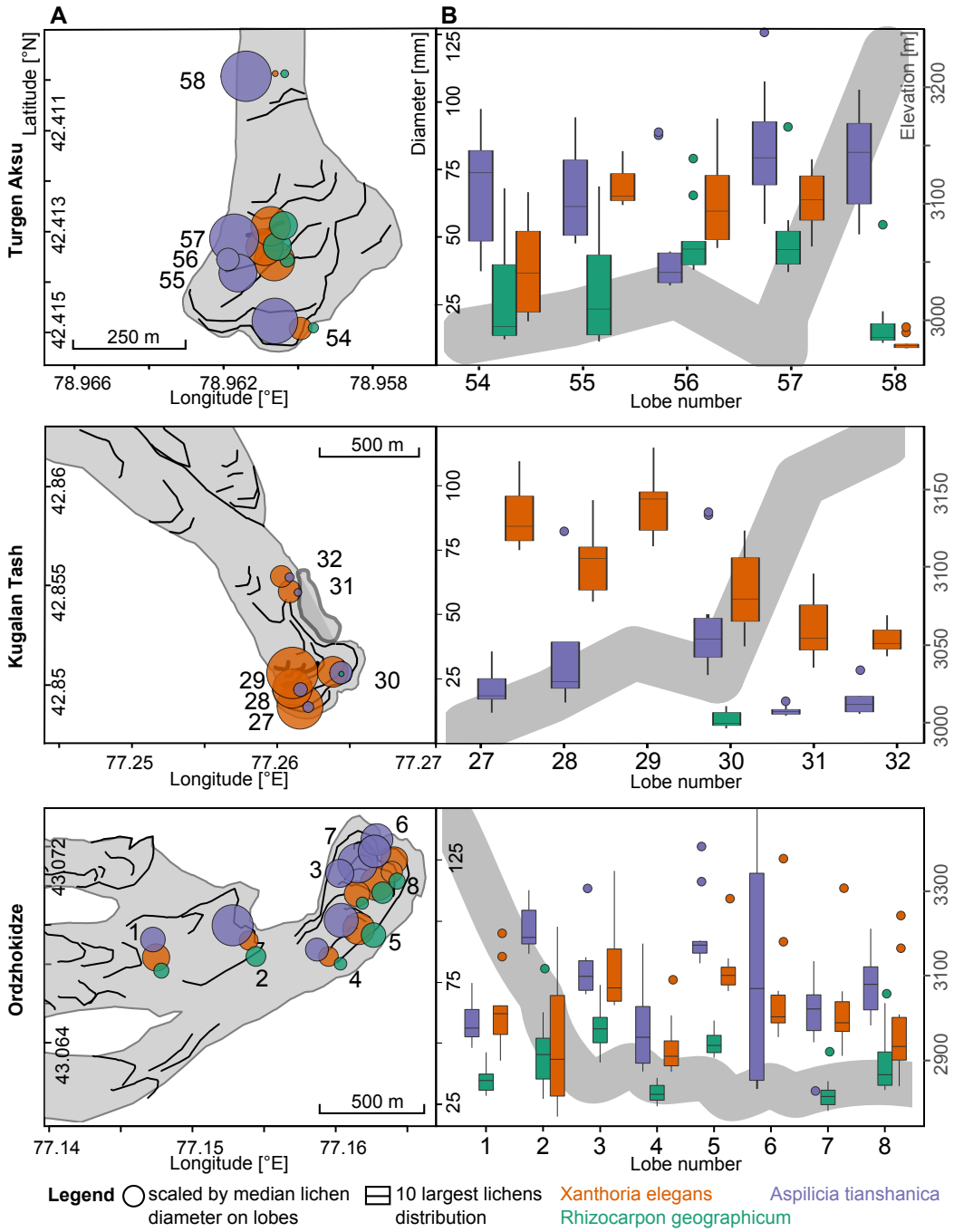

Figure 1.4: Distribution of lichen diameters on individual rock glacier lobes (# 54-58, 27-32, and 1-8 are for Turgen Aksu, Kugalan Tash, and Ordzhonikidze rock glaciers, respectively; approximate coordinates pooled for each lobe). A. Lichen diameter scaled by median size of the ten largest lichen diameters. B. Boxplot of the ten largest lichen with black horizontal as median and upper and lower box boundary as the 25th and 75th percentile. Grey shaded line is average elevation of the different lobes.

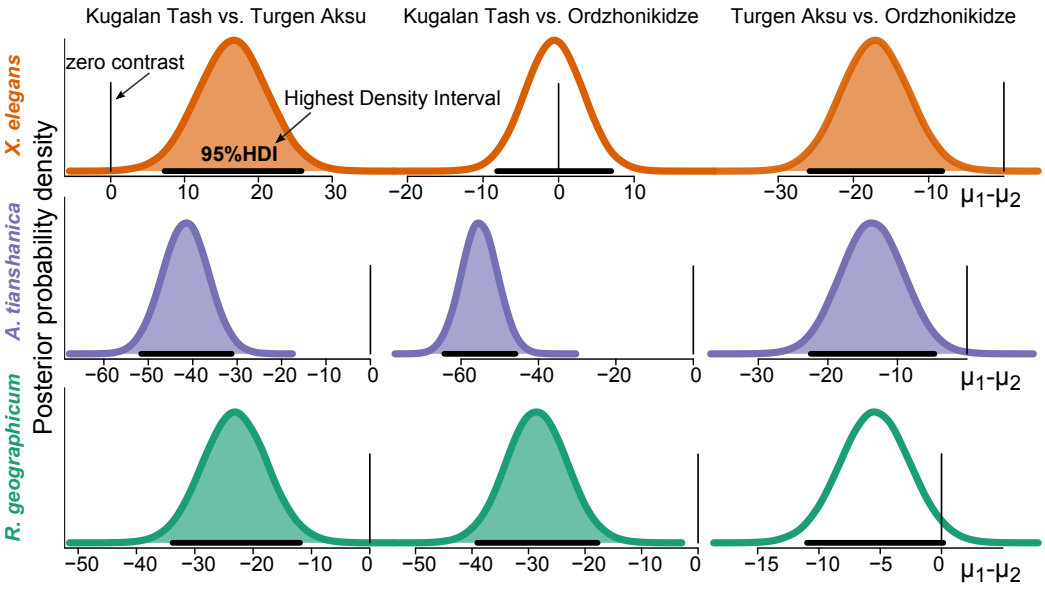

Figure 1.5: Posterior probability density of the contrast (difference of means ($\mu 1$˘$\mu 2$) [mm]), of the largest lichen diameters on Kugalan Tash, Turgen Aksu, and Ordzhonokidze rock glaciers. Shaded density curves indicate lichen diameters with 95% credible contrasts different from zero, i.e. their 95% highest density intervals (HDIs; black horizontal lines) do not include zero. Open density curves including zero contrast indicate that lichen diameters cannot be distinguished with sufficient credibility.

individuals of all sites (Figure 1.6), but also afford the highest separability of rock-glacier lobes (Figure 1.7). 86% of all pairwise comparisons between lobes return credible differences in lichen diameters for *X. elegans*, whereas this is the case for only 66% if we use the calibrated median age (Figure 1.7). Overall, calibrated ages offer a consistently lower distinction potential between any two rock-glacier lobes. The lowest contrasts in diameter and calibrated ages are at Ordzhonikidze rock glacier, where our calibrated median ages of *X. elegans* and *A. tianshanica* do not reveal any credible difference between individual lobes despite some large lichens growing on the debris. Instead, both the diameters and calibrated median ages of *R. geographicum*, which we estimate to be between 100-930 yr old, offer a distinction between 57% of all pairs of lobes (Figure 1.6,Figure 1.7, Table S4).

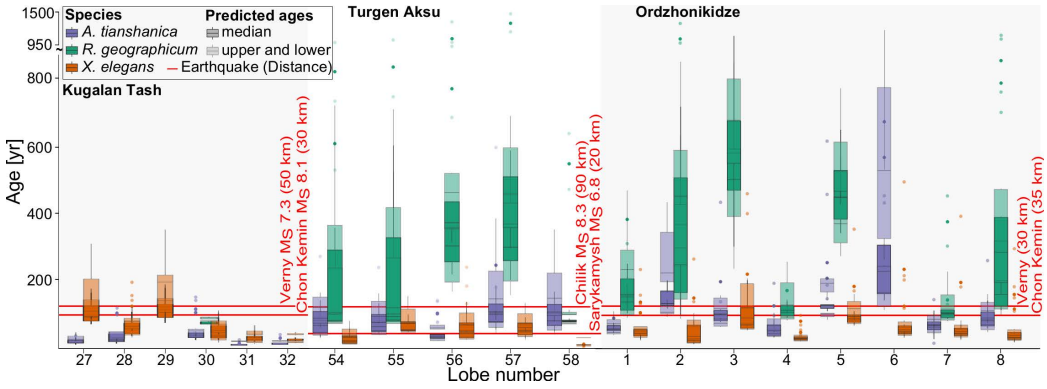

Figure 1.6: Box-and-whisker plots of calibrated lichen ages of individual rock glacier lobes at Kugalan Tash, Turgen Aksu, and Ordzhonikidze; 'median', 'upper', and 'lower' refers to the median, and the lower and upper bound of the 95% bootstrap interval of the calibrated ages, respectively (see Figure 1.3). Red horizontals mark two of the strongest earthquakes which happened during the last 130 yr in the vicinity (<100 km) of each rock glacier (epicentre–rock glacier distance is noted in brackets).

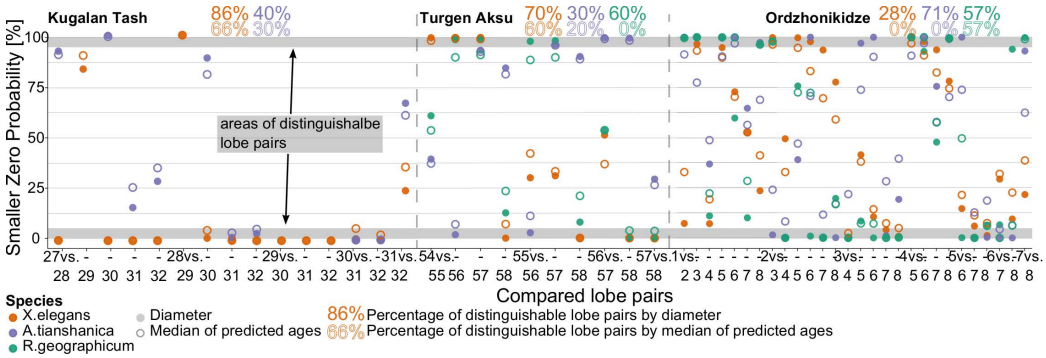

Figure 1.7: Species-dependent separability of rock-glacier lobes on the basis of the ten largest lichen diameters at Kugalan Tash, Turgen Aksu, and Ordzhonikidze, using a Bayesian implementation of ANOVA. Solid circles are lichen diameters; open circles are median calibrated ages. Upper and lower percentages are the fraction of diameters and calibrated median ages that are distinguishable with 95% credibility, respectively.

1.5 Discussion

Our results show that lichen diameters on several rock glaciers in the northern Kyrgyz Tien Shan have a sufficiently high variance to discriminate individual lobes; the same goes for calibrated ages, albeit at a much lower separability. In the following we discuss some of the environmental and methodological sources of this high variance. We then summarise how our findings address the limits to lichenometry, and the dynamics of large, low-lying rock-glacier

toes in the area.

1.5.1 Environmental controls on lichen growth

Previous work has stressed that lichen growth depends on many environmental factors including temperature, humidity, exposition to sunlight, snow cover, and air quality (McCarthy, 1999). Some of these controls are correlated and complicate the search for single predictors of lichen growth. Elevation and slope aspect in particular influence climatic variables such as temperature, humidity, and type of precipitation in mountains, and hence, ultimately lichen growth. Exceptions seem to confirm this rule. Nikonov and Shebalina (1979) showed in a study in the mountains of Tajikistan that aspect did not affect the growth of Lecidea muralis, whereas elevation did (1,600–2,000 m asl). Smirnova and Nikonov (1990) also found that lichen growth correlated with elevation in the southern Tien Shan and Pamirs (3,550–7,100 m asl). In contrast, Solomina et al. (1994) reported that growth of species *Caloplaca elegans*, *A. tianshanica*, and *R. geographicum* appeared to be independent of elevation in the northern Tien Shan (2,300–2,800 m asl). Bull (2014) observed a comparable robustness of lichen-growth characteristics with respect to elevation over a 900-km long mountainous region. Trenbirth and Matthews (2010) studied growth rates of *R. geographicum* over 25 years in Norway and found no dependence on altitude, aspect, or continentality. Our available lichen measurements span elevations between 1,550 and 2,120 m asl, and cover an E-W distance of ∼270 km. Any clear linear relationship between lichen size and elevation is elusive at our rock-glacier sites, except perhaps for *X. elegans* at Kugalan Tash, where the smallest lichen are on higher lobes (Figure 1.4B). We cannot exclude that other local environmental factors are responsible for the heterogeneous distribution of lichen diameters at our study sites. Some of the largest lichen may have benefited from local exposure or microclimatic variations in temperature and moisture. Local wind fields, patchy snow cover, and the rotation or toppling of rocks can also affect lichen sizes. Prolonged snow cover may kill lichens instead of decelerating their growth (Benedict, 1991). For example, Benedict (1990b) argued

from direct measurements in the Colorado Front Range that *R. geographicum* could not survive snow cover lasting more than about 40–43 weeks per year. The Northern Tien Shan has modest amounts of winter precipitation, and the duration of snow cover at altitudes between 2,000 and 3,000 m, where the toes of the studied rock glaciers are situated, is only between 14 and 25 weeks (Getker, 1988). We measured lichens below elevations of 3,500 m, and only above this elevations snow cover duration exceeds 40 weeks. Thus we neglect the effect of snow kill in our study. Rock fall from nearby hillslopes can transport old lichens onto younger rock-glacier lobes, and thus lead to overestimates of the lobe age. Cosmogenic ^{10}Be dating demonstrated that such contamination with older (or younger) rock debris from hillslopes is also a problem for dating valley-filling landslide deposits in the Kyrgyz Tien Shan (Sanhueza-Pino et al., 2011). Some lichens may not survive such impacts or at least lose their circular shape that we used as a selection criterion for measuring. In essence, more work is need to investigate how the combined influences of these and other environmental parameters can limit any reliable age estimates of rock-glacier surfaces.

1.5.2 Uncertainties of lichen-growth models

Generating regional lichen-growth curves is limited to the scarcity of dated, especially older, surfaces. This means that regression-based growth models hinging on only handful of older ages are prone to larger uncertainties. The mortality of lichens also increases with age, which lessens the probability of finding the largest lichen of the initial cohort. This effect may be responsible for the convex-upward shape of growth curves (Loso and Doak, 2006). Our use of quantile regression partly remediates these effects, as the method is robust to outliers and does not make any particular assumptions about error distributions. The additional bootstrap of the 0.95-quantile model simulates sample inconsistency and effects of overlooking the highest lichen diameter, and thus further raises the robustness of our method. Errors during the field measurements cannot be avoided, however; for example, species may be misidentified or single lichen insufficiently separated where they overlap

in growth position. However, these errors can easily be integrated into the bootstrapping scheme, and thus estimated. Other errors might arise from uncertainties tied to the exact age of the rock surfaces used for calibration. We used multiple rock surfaces for calibration together with bootstrapping to contain potential errors. The Ananevo and Kainde rockslides that we used as calibration sites were triggered by the 1911 Kemin earthquake (M_{lh} 8.1), and a coseismic origin of the Belogorka landslides has been inferred from the freshness of their deposits and their close proximity to the epicentre of the 1885 M_{lh} 6.9 Belovodsk earthquake (Abdrakhmatov and Strom, 2002). Using cemeteries for calibrating the lichen growth produces minimum ages, as the tombstones might have been erected later than the date they bear. Some tombstones may also have been intentionally cleared of lichens. At Turgen Aksu, we have independent validation of our lichenometric measurements from tree-ring data. This rock glacier sustains 77 spruces (*Picea shrenkiana*) and junipers (*Juniperus sp.*) that offer minimum ages of several rock-glacier lobes. Lichen ages from *X. elegans* and *A. tianshanica* on these lobes are several hundred years, and largely agree with the dendrochronological estimates (Sorg et al., 2015) (Figure 1.8). Yet both methods also demonstrate the scatter of inferred ages across the lower rock glacier.

1.5.3 Implications for the dynamics of rock glaciers

Most calibrated ages of *X. elegans* growing on lobes of the Kugalan Tash, Turgen Aksu, and Ordzhonikidze rock glaciers range from 50 to 200 yr, whereas older lichen are rare (Figure 1.6). Older lichens (up to ∼1,500 yr) are almost exclusively *R. geographicum*, regardless of lobe position or geographic location of the rock glacier. The narrow age range of the fast-growing *X. elegans* indicates the creation of fresh rock surfaces on nearly all lobes during the past 200 years. Widespread toppling of surface rocks during rock-glacier advances or widespread addition of fresh rocks could explain this recent colonisation. Climatic cooling is among the traditional explanations for the formation of new lobes on rock glaciers (Kellerer-Pirklbauer et al., 2008). The Little Ice Age that ended in the mid-19th century was the only major episode of re-

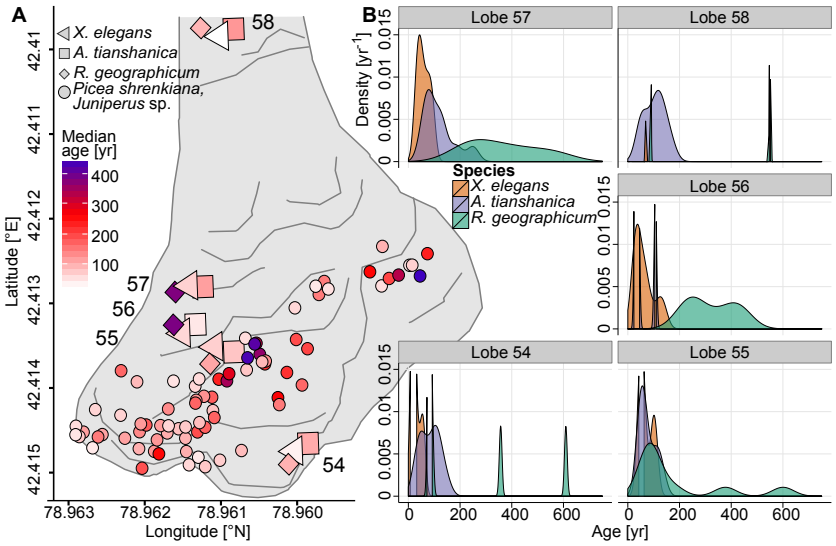

Figure 1.8: A. Comparison of median ages for rock glacier lobes (# 54–58) at Turgen Aksu predicted from diameters 10 largest lichens of *X. elegans*, *A. tianshanica*, and *R. geographicum* with estimated ages from tree rings (personal communication, Sorg, 2014). B. Estimated probability densities for the lichen ages stratified by species and lobe.

gional cooling in the northern Tien Shan in the past ∼200 yr, and could explain the abundance of young *X. elegans*, though hardly their differing size distributions, on adjacent lobes (Figure 1.6). Aizen et al. (2007) noted that the precipitation in the northern Tien Shan did not increase significantly during the past 100 yr, and stressed the trend of increasing temperatures instead. Several lobes would have formed during that warming period also, judging from the size of the largest specimen of *X. elegans*, so that a cooler climate cannot have been the sole reason for generating those lobes. All the rock glaciers that we studied have entered terrain largely devoid of permafrost (Bolch and Gorbunov, 2014); hence we infer that their toes including the lower lobes that we sampled may be out of equilibrium with the current regional climatic conditions.

Apart from climatic cooling, strong seismic ground shaking could have triggered a pulsed regional input of fresh rocks in the form of rock falls from adjacent hillslopes, and thus rejuvenated the lichen population by offering new bare rock surfaces for colonisation. The Kugalan Tash, Turgen Aksu, and Ordzhonokidze rock glaciers are 20–170 km from the epicentres of large

earthquakes that occurred in the past 130 yr (Figure 1.1). These earthquakes had macroseismic intensities of >8 even ∼100 km away from their epicentres (Mushketov, 1891; Abdrakhmatov et al., 2002; Bindi et al., 2014). However, recent M_{lh} 6–7 earthquakes (in 1970, 1978, and 1990) in the vicinity of Turgen Aksu rock glacier seem to have had little impact on the lower lobes, as numerous trees growing there predate these earthquakes (Sorg et al., 2015). Yet we cannot discard the scenario that the young and regionally consistent lichen ages of *X. elegans* and also mostly *A. tianshanica* reflect the creation of habitat from coseismic rock falls onto the rock glaciers.

However, we recall that the dating precision deteriorates with increasing lichen diameter, and decelerating growth, so the absence of lichen older than ∼200 yr may simply approach the method's temporal resolution limit. Alternatively, the rough stratification of lichen ages by species (Figure 1.6) may result from successive colonisation and mortality effects rather than climatic cooling or coseismic debris input. The result would be that early colonists are rarely found on older rock surfaces (Loso and Doak, 2006). In this case, multiple modes in lichen-size distributions may not reflect discrete events but rather a changing availability of inhabitable niches (McCarthy, 1999). We conclude that the difficulty of distinguishing between physical (climatic or seismic), biological (growth and mortality) or ecological (niches and habitats) controls of lichen diameters and inferred ages puts major limits to lichenometry of rock-glacier surfaces in the northern Tien Shan.

1.6 Conclusions

- The success and temporal resolution of lichenometry for differentiating ages of lobes of active rock glaciers in the Tien Shan depends on the type of species, assuming that the growth model by Bull et al. (1998) is valid. *X. elegans* offers the narrowest calibrated age range for a given diameter, but rarely occurs in sizes large enough to allow dating of rock surfaces that are >200 yr old.

- Despite the limitations of fast-growing lichen species such as *X. elegans*,

we can discern phases of mobility both on individual rock glaciers and between different rock glaciers. Deriving a single age for a given rock glacier from lichen diameters is clearly unrealistic, whereas lichenometry has a good potential for constraining the relative stratigraphy of rock-glacier lobes.

- Our statistical simulations show that —even when sufficiently calibrated— the largest lichen(s), which are routinely used for lichenometric dating, also have the largest prediction errors for rock-surface ages. This finding also holds for the slowest growing lichen species (*R. geographicum*), mainly because of its low data density.

- Rock-glacier lobes are more separable by lichen diameter than by predicted ages. The age calibration introduces broader error margins, and thus decreases the capability of distinguishing between lobes, so that there is a higher tendency to assign coeval ages to lichen dated rock glaciers.

- The abundance of young (<200 yr) fast-growing *X. elegans* contrasts with fewer occurrences of slow-growing and older (200–1,500 yr) *R. geographicum* and *A. tianshanica*, and likely reflects either the regional reactivation of lobes in the past 200 yr or simply censoring effects due to the mortality of early colonisers. Either way our data document highly localised dynamics of rock- glacier lobes that may be difficult to explain by regional climate cooling or episodic coseismic input of fresh rock material alone. We conclude that inferring climatic conditions from the topographic location of rock-glacier lobes may be problematic. Given these constraints, we favour the use of lichenometry for establishing a relative —rather than an absolute— chronology of rock-glacier lobes in the northern Tien Shan.

Acknowledgments

This work was funded by the German Ministry for Education and Research (BMBF) within the TIPTIMON project (contract no. 03G0809), and the Potsdam Research Cluster for Georisk Analysis (PROGRESS). We also thank the Volkswagen Foundation for funding our collaboration with A. Dzhumabaeva (contract no. 86 860). We used the free R software (https://cran.r-project.org/) environment, the JAGS module (http://mcmc-jags.sourceforge.net/), and modified code by J. Kruschke for computing all statistics. K. Abdrakhmatov kindly organised our field support. We thank A. Sorg for providing estimated tree ages from dendrochronological analysis, and L. Sorg, F. Volkmer, M. Ahmadi, and M. Zeckra for help with lichen measurements in the field. H. Sipman supported us with the identification of lichen species. L. Sancho, J. Carrión, and an anonymous reviewer commented helpfully on the manuscript.

Supplementary material

Supplementary material can be found in Appendix A.

Chapter 2

Rock-glacier dams in High Asia

Abstract

Rock glaciers in semiarid mountains store large amounts of ice and might therefore be important water reservoirs aside from glaciers, lakes, and rivers. Yet whether and how rock glaciers interact with watercourses in mountain valleys remains largely unresolved. We examine the potential for rock glaciers to block or disrupt river channels, using a new inventory of more than 2000 intact rock glaciers that we mapped from remotely sensed imagery in the Karakoram (KR), Tien Shan (TS), and Altai (ALT) mountains. We find that between 5% and 14% of rock glaciers partly buried, blocked, diverted or constricted at least 95 km of mountain rivers in the entire study area. Average rock glacier density is 2.6% (TS), 2.2% (KR), and 0.9% (ALT), and thus higher than glacier density in favourable conditions. We use a Bayesian robust logistic regression with multiple topographic and climatic predictors to discern those rock glaciers disrupting mountain rivers from those with no obvious impacts. We identify elevation and potential incoming solar radiation (PISR), together with the size of feeder basins, as dominant predictors, so that lower-lying and larger rock glaciers from larger basins are more likely to disrupt river channels. Given that elevation and PISR are key inputs for modelling the regional distribution of mountain permafrost from the positions of rock-glacier toes, we infer that river-blocking rock glaciers may

be diagnostic of non-equilibrated permafrost. Principal component analysis adds temperature evenness and wet-season precipitation to the controls that characterise rock glaciers impacting on rivers. Clarifying whether rapidly advancing rock glaciers can physically impound rivers, or fortify existing dams instead, deserves future field investigation. We conclude that rock-glacier dams are conspicuous features that may have a polygenetic history and encourage more research on the geomorphic coupling between permafrost lobes, river channels, and the sediment cascades of semiarid mountain belts.

2.1 Introduction

Rock glaciers are landforms diagnostic of permafrost, and have entered the discussion about dwindling water resources in high mountains (Huss et al., 2017), adding to estimates of how much freshwater is currently stored in glaciers and ice caps (Immerzeel et al., 2010). Regional estimates hold that rock glaciers may contain more water than glaciers in the driest parts of mountain belts such as the Andes (Arenson and Jakob, 2010; Azócar and Brenning, 2010), the Himalayas (Jones et al., 2018; Owen and England, 1998) or the southwestern United States (Millar and Westfall, 2008). In the semiarid Tien Shan mountains, rock glaciers become increasingly important as freshwater sources in times of atmospheric warming and shrinking glaciers (Bolch and Marchenko, 2006). The ongoing decline of glaciers in many of High Asia's mountain belts (Bolch et al., 2012; Bolch and Gorbunov, 2014) makes the role of ground ice contained in mountain permafrost a general issue of concern.

Despite realising that rock glaciers are useful tools for mapping the distribution of permafrost, the state of permafrost hydrology, local water availability and quality, and environmental change (Schmid et al., 2015; Thies et al., 2013), few scientists have explored whether and how rock glaciers influence mountain rivers by advancing onto valley floors, and physically disrupting water and sediment fluxes in channels. Having screened the literature and available rock-glacier inventories, we found hardly any mention of

rock glaciers disturbing rivers, let alone impounding lakes. Yet, rock glaciers seem capable of building dams or even impounding lakes in mountain rivers of High Asia (Figure 2.1), thus disrupting the downstream motion of sediment, covering large tracts of valley floor with ice-rich debris, and forming potential sources of catastrophic outburst floods. The pioneering work by Costa and Schuster (1988) on natural dams formed by landslides, glaciers, dunes or lava flows discloses little about rock glaciers as potential obstacles to river flow; neither do more recent reviews concerning the forms, dynamics, and distribution of rock glaciers in mountainous terrain (Jones et al., 2018; Janke, 2013; Scotti et al., 2013). However, recent studies reported increasing rock-glacier activity and advance rates into river valleys in response to atmospheric warming (Sorg et al., 2015), or even the sudden collapse of rock glaciers producing debris flows (Bodin et al., 2016b; Iribarren Anacona et al., 2015; Scotti et al., 2017). Clearly, the geomorphic impact of rock glaciers on rivers, and especially whether and how rock glaciers divert, disturb, or even completely block sediment and water fluxes, deserves detailed enquiry.

We start filling this knowledge gap by presenting a first regional reconnaissance of rock glaciers and their possible impact on rivers and valley floors in parts of three mountain belts of High Asia. Specifically, our aim is to investigate the impact of rock glaciers on mountain rivers in High Asia, and to identify and quantify the possible controls of rock-glacier lobes that impound lakes or valley fills. We briefly compare these rock-glacier dams with other natural dams, and test whether a set of topographic and climatic candidate metrics allows predicting the conditions under which rock-glacier lobes block, bury, or otherwise alter the geometry of river channels

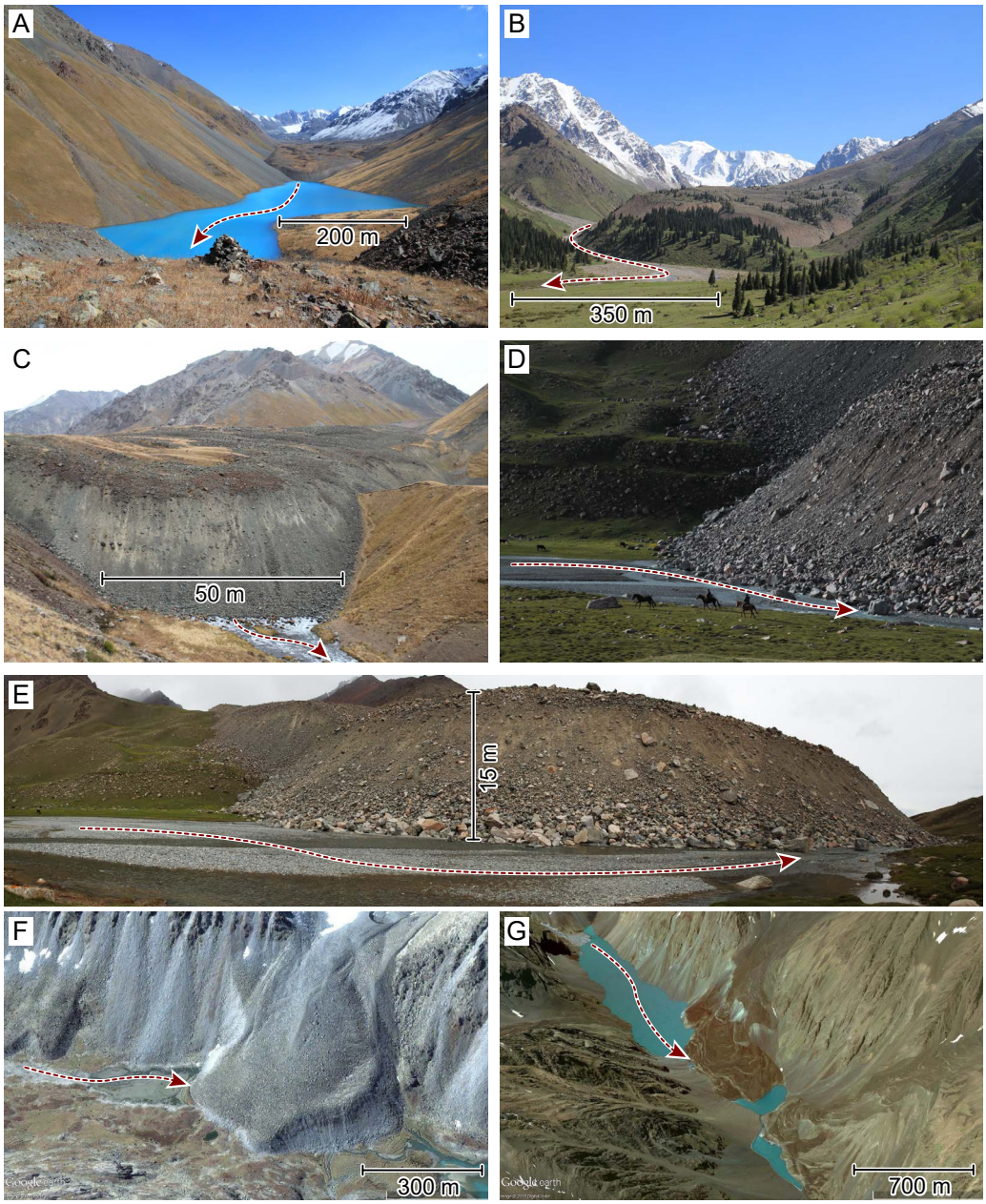

Figure 2.1: Examples of rock glaciers damming or obstructing rivers in High Asia (arrows point downstream). A. Rock-glacier dammed lake Djassik Kul, Chon Kemin valley, Kyrgyz Tien Shan. B. Ordzhonikidze rock glacier, Zailisky range, Kazakhstan, diverts the flow of a gravel-bed river. C. Rock-glacier dam outlet of A. D and E. Chon Aksu rock glacier, Kungey range, Krygyz Tien Shan, partly damming and diverting the river. F. Large rock-glacier lobe impounds a small lake, western Mongolian Altai. G. Large rock-glacier dam, Gilgit river basin, Karakoram; the large lake in the background is about 2.2 km long, and the dam 900 m wide. Images in F and G modified after Google EarthTM (2017).

2.2 Study area

To get an overview of the distribution of High Asian rock glaciers and how they interfere with the drainage network, we compiled an inventory of rock glaciers in three different mountain ranges, the Karakorum (KR), the northern Tien Shan (TS), and the Altai (ALT) (Figure 2.1, Figure 2.2). Despite sharing many similar climatic and topographic conditions, the three mountain belts span a range of varying environmental conditions. We intentionally kept this range broad as to rigorously test where and why rock glaciers interfere with river channels. Moreover, our mapping independently augments the geographic coverage of a recent inventory of about 700 rock glaciers in the Himalayan arc (Schmid et al., 2015).

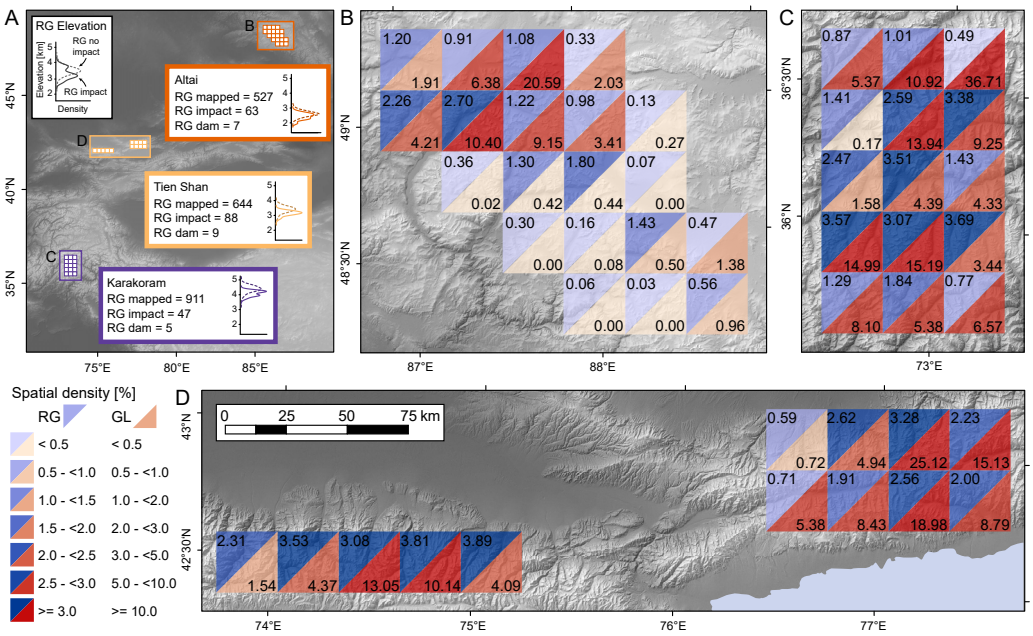

Figure 2.2: Regional maps of High Asian rock-glacier (RG) inventory. A. SRTM topography with 48 rectangular segments in which RG were mapped, colour-coded by mountain belt. Insets show probability density estimates for RG toe elevations with and without impact on rivers for the three regions. B, C, and D. Detailed maps of the three regions Altai (B), Karakoram (C), and Tien Shan (D) with squared grid cells of 25x25 km^2 each, colour coded by RG and glacier (GL) density in blue and red, respectively (numbers indicate exact fraction), both calculated as the fraction of total area of RG and GL per unit area above the lowest RG toe. GL data from RGI consortium (2017).

The high topography of High Asia's mountain ranges is the result of the ongoing collision of the Indian and Eurasian tectonic plates (Molnar and Tapponnier, 1975; Tapponnier and Molnar, 1979). The ranges are actively uplifting and prone to large earthquakes, but have formed in different tectonic settings. The northward propagation of deformation related to the building of the Himalayas has caused some rejuvenation of older intra-continental mountain ranges, and the migration of neotectonic activity along thrust belts and strike-slip faults that had developed during pre-Cenozoic phases of mountain building (Avouac and Tapponnier, 1993). Many of High Asia's topographic and climatic conditions conducive to permafrost, and hence also rock glaciers, were recently reviewed by (Gruber et al., 2017). All studied ranges lie leeward of the influence of the Indian monsoon, and receive low amounts precipitation, partly delivered by cyclones from the west-wind drift. Regionally, the mean annual temperature, and incoming solar radiation decrease northward and thus toward the continental interior. Mean annual precipitation similarly decreases northward from the Karakoram to the Tien Shan and the Altai, but also shows topographic effects. The KR has annual precipitation ranges from 200 mm in the valleys to 1500 mm above 5000 m asl (Wake, 1989), falling mainly as snow in winter and spring (Archer et al., 2010). In the TS, most precipitation falls in early summer, though in highly variable amounts with 1000 mm on windward northern slopes, and 800 mm on leeward southern slopes (Aizen et al., 2007). The ALT runs from southern Siberia through Mongolia and China, and has a low mean annual precipitation (470–540 mm) strongly influenced by cold arctic air masses (Panagiotopoulos et al., 2005). Most precipitation falls between April and September, often as snow (Shahgedanova et al., 2010).

These generally cool and dry high-altitude climates cater for intact rock glaciers in all three mountain regions (Owen and England, 1998). Rock glaciers tend to occupy the niches of clear ice glaciers under suitable conditions (Brenning and Trombotto Liaudat, 2006). Amongst these conditions, low solar radiation aids the growth of low-lying rock glaciers in arid mountains (Schrott, 1996; Brenning and Trombotto Liaudat, 2006). Patchy field observations of permafrost throughout High Asia make rock glaciers the

proxy of choice for modelling to first order the regional distribution of perennially frozen ground: judging from the elevations of rock glacier toes, the lower permafrost limit is at 3500 m asl in the greater Himalayan region and southern Tibetan Plateau (Schmid et al., 2015). Permafrost reaches down to 2700 m asl in the northern Tien Shan (Gorbunov, 1996), though some rock glaciers have advanced below the 0°C isotherm (Bolch and Gorbunov, 2014). There, warm permafrost favours rock glaciers advancing at 5–10 ma^{-1} (Gorbunov et al., 1992), one to two orders of magnitude faster than rock glaciers in the Swiss Alps (Delaloye et al., 2010). Permafrost in Mongolia may occur as low as 600 m asl, though mostly in a state of decay (Sharkhuu, 2003); most rock glaciers lie between 2300 and 3400 m asl (Lehmkuhl et al., 2003).

2.3 Methods

In total, we mapped 2082 intact rock glaciers, i.e. active and inactive forms (Barsch, 1996) with a minimum planform area of 0.025 km^2 in parts of the Karakoram (KR, 9,375 km^2), Tien Shan (TS, 8,125 km^2), and Altai (ALT, 12,500 km^2) mountains (Figure 2.2), largely relying on high-resolution satellite images draped over a digital globe (Google EarthTM). We preferred cloud- and snow-free imagery with ground resolutions of $<$2.5 m (e.g. GeoEye, QuickBird, WorldView, IKONOS, SPOT 5). We subdivided the study area into 48 squares of 625 km^2 each, and calculated rock-glacier density as the fraction of total rock glacier area per unit study area above the elevation of the lowest rock-glacier toe [%] (Gorbunov, 1983).

For identifying rock glaciers we used the diagnostic criteria outlined by Barsch (1996), including well-developed frontal ramps of debris lobes with distinct flow structures, transverse ridges and longitudinal furrows (Janke et al., 2015), and a distinctly wrinkled surface (Burger et al., 1999; Cremonese et al., 2011; Janke et al., 2015; Scotti et al., 2013). We mapped rock glaciers as polygons extending from the root zone to the base of their frontal slope (Barsch, 1996) We distinguished between talus-derived rock glaciers that de-

velop from frost-shattered rock fragments beneath steep and mostly ice-free headwalls, and moraine-derived rock glaciers, under which we subsume forms generating from laterofrontal moraines and transitional landforms where the lower parts of debris covered glaciers grade into rock glaciers, acknowledging rock glaciers as cryo-conditioned landforms (Berthling, 2011; Bolch and Gorbunov, 2014; Haeberli and Vonder Mühll, 1996).

For both the rock glaciers and their feeder basins, defined here as the upslope area contributing ice and sediment to the rock glacier, we computed various topographic, climatic, and geographic metrics from 30-m resolution digital elevation models (Shuttle Radar Topographic Mission, SRTM), and from the global WorldClim data (www.worldclim.org; Fick and Hijimans (2017)), respectively (Table 2.1). Main topographic metrics include elevation, local slope, feeder-basin area, and slope aspect, whereas the WorldClim data feature 19 different temperature and precipitation-related metrics and their diurnal, seasonal, and annual variability. Feeder basins were automatically extracted from digital topography, using all pixels contained in a rock-glacier polygon above the median elevation as pour points. Feeder basins that expand onto valley floors are prone to overestimation, so that we manually checked all basins for consistency. We mapped intact and former rock-glacier dams along with rock glaciers from high-resolution satellite images; intact dams are associated with lakes or backwater sediment wedges where channels disappear upstream and resurface below the dam, whereas former dams are incised or undercut by channels. We derived channel networks for our study areas from the digital elevation models, using a threshold of 10 km^2 for channel initiation. We classified rock glaciers as impacting river channels if the Euclidean distance between a rock glacier polygon and the river network was $<$90 m (i.e. three pixels). To estimate the regional geomorphic impact on the river system, we extracted the basin area above damming and impacting rock glaciers as a fraction of each 625-km^2 study square.

Logistic regression has been among the premier methods for predicting mountain permafrost from the pattern of active and inactive rock glaciers (Boeckli et al., 2012; Brenning and Trombotto Liaudat, 2006; Etzelmüller et al., 2006; Monnier and Kinnard, 2015). Despite some enquiry into choice

Table 2.1: Variables (for rock glaciers and their catchment areas) used as predictors in Bayesian logistic regression.

Variables	Unit
Latitude and Longitude	°
Elevation (min, max, mean, median)	m asl
Area	m^2
Slope (min, max, mean, median)	°
Relief (min, max, mean, median)	m
PISR (min, max, mean, median)	kWh m^{-2} a^{-1}
Slope aspect	°
Annual Mean Temperature (BIO1)	°C
Mean Diurnal Range (Mean of monthly (max temp - min temp)) (BIO2)	°C
Isothermality (BIO2/BIO7) (×100) (BIO3)	-
Temperature Seasonality (standard deviation ×100) (BIO4)	°C
Max Temperature of Warmest Month (BIO5)	°C
Min Temperature of Coldest Month (BIO6)	°C
Temperature Annual Range (BIO5-BIO6) (BIO7)	°C
Mean Temperature of Wettest Quarter (BIO8)	°C
Mean Temperature of Driest Quarter (BIO9)	°C
Mean Temperature of Warmest Quarter (BIO10)	°C
Mean Temperature of Coldest Quarter (BIO11)	°C
Annual Precipitation (BIO12)	mm
Precipitation of Wettest Month (BIO13)	mm
Precipitation of Driest Month (BIO14)	mm
Precipitation Seasonality (Coefficient of Variation) (BIO15)	-
Precipitation of Wettest Quarter (BIO16)	mm
Precipitation of Driest Quarter (BIO17)	mm
Precipitation of Warmest Quarter (BIO18)	mm
Precipitation of Coldest Quarter (BIO19)	mm

and performance of logistic regression and other classifiers for detecting rock glaciers from digital terrain data and satellite imagery (Brenning, 2009), few studies traced how correlated predictors or propagating uncertainties in the data affected the model outputs. We adopt a Bayesian robust logistic regression that caters for explicitly quantifying such uncertainties in deciding whether rock glaciers impact mountain rivers or not. Bayesian logistic regression has seen some applications in the environmental sciences, but is new in geomorphic and cryospheric research (Das et al., 2012). We defined two classes, i.e. class 1: rock glaciers that dam, bury, divert or otherwise visibly change the geometry of mountain-river channels; and class 0: rock glaciers that do not impact rivers, let alone impinge on channels. The Bayesian approach allows us to update our initial (or prior) belief about individual regression weights by learning their joint probability distribution from the data, offering a posterior predictive probability (distribution) that a rock glacier with a given combination of topographic and climatic characteristics

belongs to class 1.

We compiled 76 topographic and climatic candidate predictors for each rock glacier and its feeder basin, omitting 17 redundant parameters that were strongly correlated ($r > 0.99$). We then ran the logistic regression for two input variants. First, we selected at least two of these candidate predictors. Following the spirit of previous work, we chose elevation and potential incoming solar radiation, as these are key predictors for modelling the regional distribution of mountain permafrost (Brenning and Trombotto Liaudat, 2006). We also considered rock-glacier planform area, and the size of the feeder basin as possible predictors of whether rock glaciers impacted mountain rivers or not. Second, we ran a varimax-based principal component analysis to boil down the full candidate predictor set, thus eventually discarding linearly correlated variables, and instead taking into account as predictors only the scores of those principal components that explained most of the total variance.

Table 2.2: Parameters in Bayesian robust multiple logistic regression.

Symbol	Parameter	Range of values
y_i	Posterior probability of ith rock glacier disrupting a river	[0, 1]
β_0	Intercept of logistic regression model	~Normal $(M_0 T_0^- 1)$
β_j	Weight of jth predictor in logistic regression	~Student t $(\mu_\beta, \tau_\beta, df)$
μ_β	Prior mean of logistic regression weights, location parameter of t-distribution	~Normal $(M_\beta T_\beta^- 1)$
τ_β	Prior shape parameter of t-distributed prior on logistic regression weights	~Gamma $(S_\beta R_\beta)$
df	Degrees of freedom of t-distributed prior on logistic regression weights	$\sim 1 - G \ln(u)$
M_0	Prior mean of intercept of logistic regression	0
T_0	Prior precision (inverse of variance) of intercept of logistic regression	10^{-12}
M_β	Hyperprior mean of μ_β	0
T_β	Hyperprior precision of μ_β	0.1
S_β	Hyperprior shape parameter of τ_β	10^{-4}
G	Hyperprior (gain parameter) of df	1
u	Random uniform number	]0, 1[

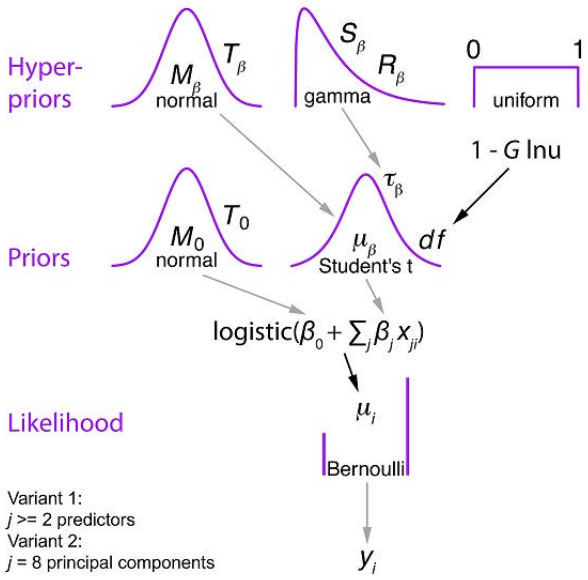

Figure 2.3: Hierarchical model of Bayesian robust multiple logistic regression for predicting the probability y_i that a given rock glacier from our sample ($i = 1, 2, \ldots, 1285$) with characteristics x_{ji} disrupts a mountain-river channel. We ran the model for two variants: out of a set of 69 candidate predictors we selected j >= 2 predictors, and also the first eight principal components ($j = 1, 2, \ldots, 8$) of the entire candidate set. The regression weights are labelled β_i. Grey arrows indicate probabilistic links, whereas black arrows are deterministic relationships between the model parameters (Table 2.1). For example, we believe that the intercept of the logistic regression β_0 is normal distributed with mean M_0 and precision (the inverse of the variance) T_0, whereas mi is equal to the logistic function at $(\beta_0 + S_j \beta_j x_{ji})$.

For both types of predictors, i.e. the principal components and the few selected original ones, we set up a hierarchical model that assumes that all regression coefficients (or weights) come from the same Student's- t-distribution (Figure 2.3, Table 2.2). This distribution of weights is more robust to outliers than a Gaussian, and admits only very high (absolute) regression weights, hence the name 'robust regression'. We believe that this prior is appropriate given the high collinearity between the candidate predictors. By setting the degrees of freedom df in a hyperprior, we impose short tails in the t-distributed regression weights, reflecting our belief that only few coefficients are credibly different from zero, and thus of relevance for the classification. This approach erases spurious regression weights that may arise from correlated predictors. Using a prior distribution of the regression weights also

enforces that their posterior estimates are informed by each other during the learning process. We thus randomly subsampled equal shares from these two classes, standardised the variables, and numerically approximated the joint posterior in four independent Markov Chain Monte Carlo (MCMC) chains of 50,000 simulations each using the JAGS language. Having checked that these chains converged successfully after 3,000 burn-in simulations each, we obtained samples of the multivariate posterior distributions. We report the performance of the model using the area-under-the-curve (AUC) value of the receiver-operating-characteristic (ROC) curve, which plots the true positive rate over the false positive rate. The Bayesian treatment allows reporting a distribution of AUC values that we sampled from the posterior probabilities. Finally, we used the medians of the MCMC samples for approximating the predictive posterior by marginalising over the posterior regression weights, thus obtaining the probability that a rock glacier not contained in our inventory disrupts a river channel, given the data at hand.

2.4 Results

The 2082 rock glaciers that we mapped from remote-sensing imagery in three High Asian mountain belts have individual areas of between 0.025 and 3.6 km^2 (Figure 2.4), and cover a total of about 452 km^2. The average spatial density of rock glaciers is 2.6%, 2.2%, and 0.9% in the TS, KR, and ALT, respectively, and thus roughly comparable to densities reported from other rock-glacier inventories around the world (Table 2.3), although local variations dominate the regional distribution (Figure 2.2).

The majority (90%) of rock-glacier lobes lies in areas with mean annual temperatures (MAT) of between –2.3 and –9.6°C, with pronounced and closely neighbouring peaks at around –5°C for the KR and TS, and a lower maximum around –9°C for the ALT. This narrow temperature band for KR and TS marks a distinct thermal niche that holds regardless of 7 degrees difference in latitude, a distinctly different mean annual precipitation, and more than 2500 vertical metres (Figure 2.4, Figure 2.5). Only 31 of all rock

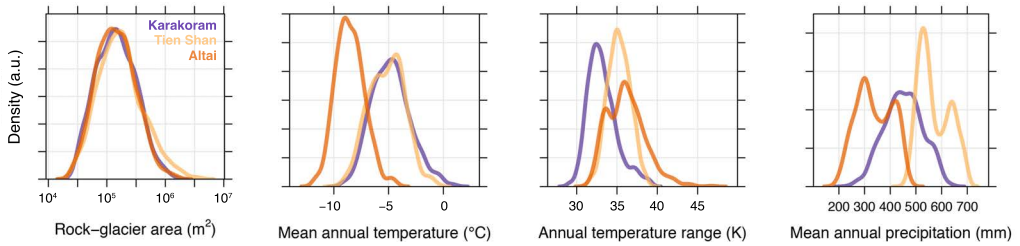

Figure 2.4: Probability density estimates of rock-glacier area (A), mean annual temperature (B), annual temperature range (C), and mean annual precipitation (D) at the mapped rock-glacier toes in three High Asian mountain belts.

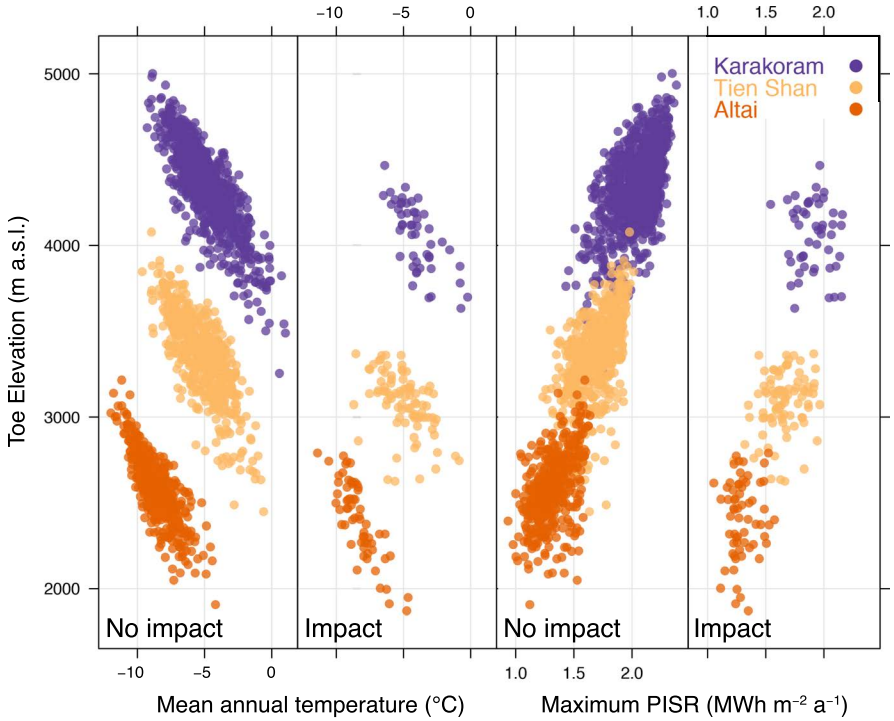

Figure 2.5: Rock-glacier toe elevations are correlated with mean annual temperature and maximum potential incoming solar radiation, regardless of whether they have a geomorphic impact on mountain rivers or not. These correlations can compromise empirical models for predicting impacts of rock glaciers or inferring from their distribution the pattern of mountain permafrost.

glaciers mapped (i.e. 1.5%)„ have advanced to positions where the estimated MAAT is above –1°C, 28 of which are in the KR, and three in the TS. The local annual temperature range at the mapped sites is between 29 and 47 K; with the highest range affecting the most poleward rock glaciers in the

Table 2.3: Reported estimates of spatial densities of rock glaciers in mountain belts throughout the world.

Region	Estimated rock-glacier density*	Reference
Northern Tien Shan	1.5%	(Bolch and Gorbunov, 2014)
Himalaya, Mt. Everest	0.15% to 0.33%	(Gorbunov, 1983) based on (Higuchi et al., 1978) and (Barsch, 1977)
Central Andes, Argentina and Chile (∼33°S)	5.0% to 6.7%	(Brenning, 2005)
Central Andes, Argentina and Chile	1.59%	(Angillieri, 2010)
Patagonian Andes, Argentina	1.4%	(Falaschi et al., 2015)
Arid Andes, Chile (27°-29°S)	0.8%	(Azócar and Brenning, 2010)
Semiarid Andes, Chile (29°-°32S)	1.6%	(Azócar and Brenning, 2010)
Zailyiskiy and Kungey Alatau (Kazakhstan/ Kyrgyzstan)	2.65	(Bolch and Marchenko, 2006)
Italian Alps	2.21%	(Scotti et al., 2013)
Nepalese Himalaya	3.4%	(Jones et al., 2018)
Karakoram	2.16%	This study
Tien Shan	2.59%	This study
Altai	0.86%	This study

*Estimated as either the fraction of total area of rock glaciers per unit area above the elevation of the lowest rock-glacier toe [%] (Gorbunov, 1983)

continental climate of the Altai. All mapped rock glaciers flow from feeder basins with areas between 0.02 and 20 km^2 that receive a mean annual precipitation (MAP) between 200 - 700 mm (Figure 2.4), the ALT being the driest region with average MAP of 350 mm, followed by the KR and TS with 480 mm and 580 mm, respectively. We observe that larger catchments generally give rise to larger rock glaciers and notice a strong correlation between elevation, MAAT, and maximum PISR, both within and across the different mountain belts (Figure 2.5). Solar radiation is higher on higher-lying rock-glacier lobes, regardless of their size, while more poleward mountain belts have colder average temperatures superimposed on similar altitudinal lapse rates. A striking result is that most of the rock-glacier lobes terminate within 250 vertical metres of the regional median elevation in each mountain range, regardless of climatic conditions (Figure 2.6).

We find that, depending on mountain belt, between 5% and 14% of the mapped rock glacier toes entered river channels, separating aggraded and widened channels upstream from much narrower and confined channels down-

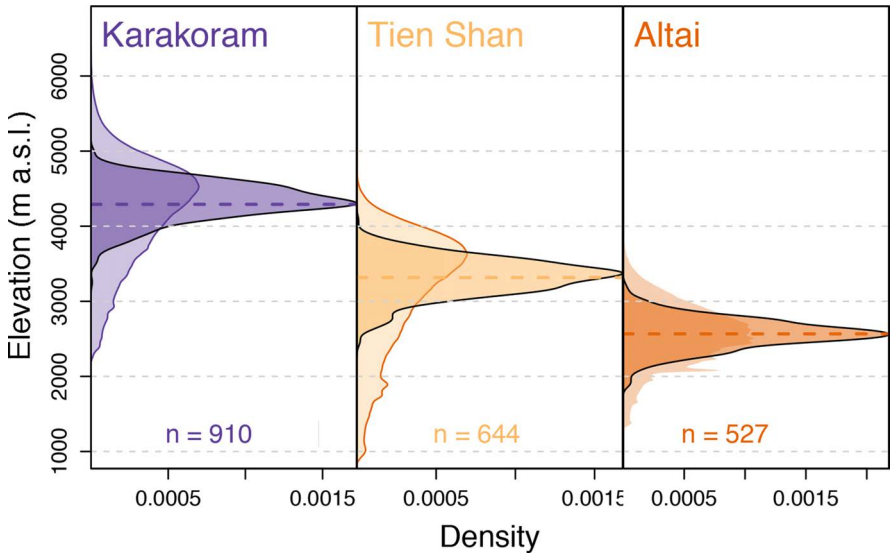

Figure 2.6: Distribution of study-area elevation (light tones) and rock glacier-toe elevations (dark tones with dark outlines) in the Karakoram, Tien Shan, and Altai. Dashed lines mark the median elevations of each study area. Toe elevations decrease by 140 m on average per degree of latitude in a northward direction.

stream. These geomorphic impacts are most frequent in the TS and ALT (Table 2.4). We estimate that at least 95 km of river channels are currently buried beneath 198 rock-glacier lobes; individual lobes blanket up to 1.8 km long tracts of valley floor beneath 30-50 m of debris, such as in the upper Chon Kemin River, Kyrgyz Tien Shan (42.91°N 77.12°E). In the KS, TS, and ALT river-impacting rock glaciers make up some 7%, 34%, and 26% of the total rock-glacier area, respectively, so that in the latter two mountain ranges larger rock glaciers play a larger role in burying, constricting, or otherwise impacting mountain rivers. Few of the lobes that buried, diverted or disrupted river channels have also impounded lakes (1%), and we identified a similarly small number of dams that have failed in the past (Table 2.4). The catchment area lying upstream of river-disrupting rock glaciers is 7.2%, 11.5%, and 18.8% of each study area in the KR, ALT, and TS, respectively, summing up to a total of 3600 km^2; again, local variations are pronounced (Figure 2.7).

Our logistic regression identifies only few credible predictors for discerning rock glaciers with visible river impacts. Among the 59 candidate predictors,

Table 2.4: Rock glaciers and their geomorphic impact on rivers in three High Asian mountain belts.

Rock glaciers	**Total** (>0.025 km^2)	**Impact**[1,2]	**Current dam**[2] (lake)	**Former dam**[2] (breached)
Karakorum				
(#)	911	47 (5.2%)	5	11
(km^2)	178.7	670.6 (7.2%)	142.4 (1.5%)	176.5 (1.9%)
Tien Shan				
(#)	644	88 (13.7%)	9	14
(km^2)	171.7	1528.1 (18.8%)	256.6 (3.2%)	286.5 (3.5%)
Altai				
(#)	527	63 (12.0%)	7	6
(km^2)	101.9	1434.7 (11.5%)	229.9 (1.8%)	151.3 (1.2%)
Total				
(#)	2082	198	21	31
(km^2)	452.3	3633.4 (12.1%)	628.9 (2.1%)	614.3 (2.0%)

[1]Derived using Euclidean distance from drainage network within 90-m (3 pixel) window
[2]Area refers to upstream catchment area (% to total study area)

we selected 13 first-5 order topographic, climatic, and geographic location metrics; many of the remaining predictors are more or less derivatives thereof. We observe that only 7 out of these 13 metrics, i.e. the size of the rock glacier and its feeder basin, the rock-glacier toe elevation, geographic latitude and longitude, and mean annual temperature and precipitation have credible non-zero weights. Other predictors such as steepness or mean aspect of the feeder basins have non-credible weights. The 95% highest density interval (HDI) of the posterior distributions of all other regression weights include zero values, so that we can credibly discard these predictors as irrelevant or at least ambiguous (Figure 2.8). This model has a median AUC of 0.78 with a very narrow 95% HDI.

Limiting our analysis to only two predictors, we find that the planform area of rock glaciers and their toe elevation roughly distinguish rock glaciers that impact mountain rivers from rock glaciers that do not. We obtain very similar results if replacing toe elevation by maximum PISR (Figure 2.9). The logistic regression classifies larger rock glaciers at lower elevations (or lesser exposure to solar radiation) as more likely to impact rivers. The median AUC value for rock-glacier area and rock-glacier toe elevation (maximum PISR on the rock glacier) is 0.77 (0.77). Given that PISR correlates strongly with elevation in our study areas, we find that rock-glacier toe elevation does not add any credible weight to the classification; indeed the posterior

distribution of the regression weight of elevation contains zero in its 95% HDI. In essence, elevation and PISR are nearly equally valid and mutually exchangeable predictors. We obtain similar results if replacing rock-glacier area by the area of its feeder basin. In this case, the median AUC value for feeder-basin area and rock-glacier toe elevation (maximum PISR on the rock glacier) is 0.76 (0.71). Feeder-basin size has a slightly higher weight in discerning rock-glaciers that impact rivers, whereas minimum elevation and maximum PISR retain a comparable influence (Figure 2.10). This is reflected in the spread of credible decision boundaries, which we map as sampled 50% probability contours of classifying a rock glacier as disrupting a mountain river (Figure 2.8).

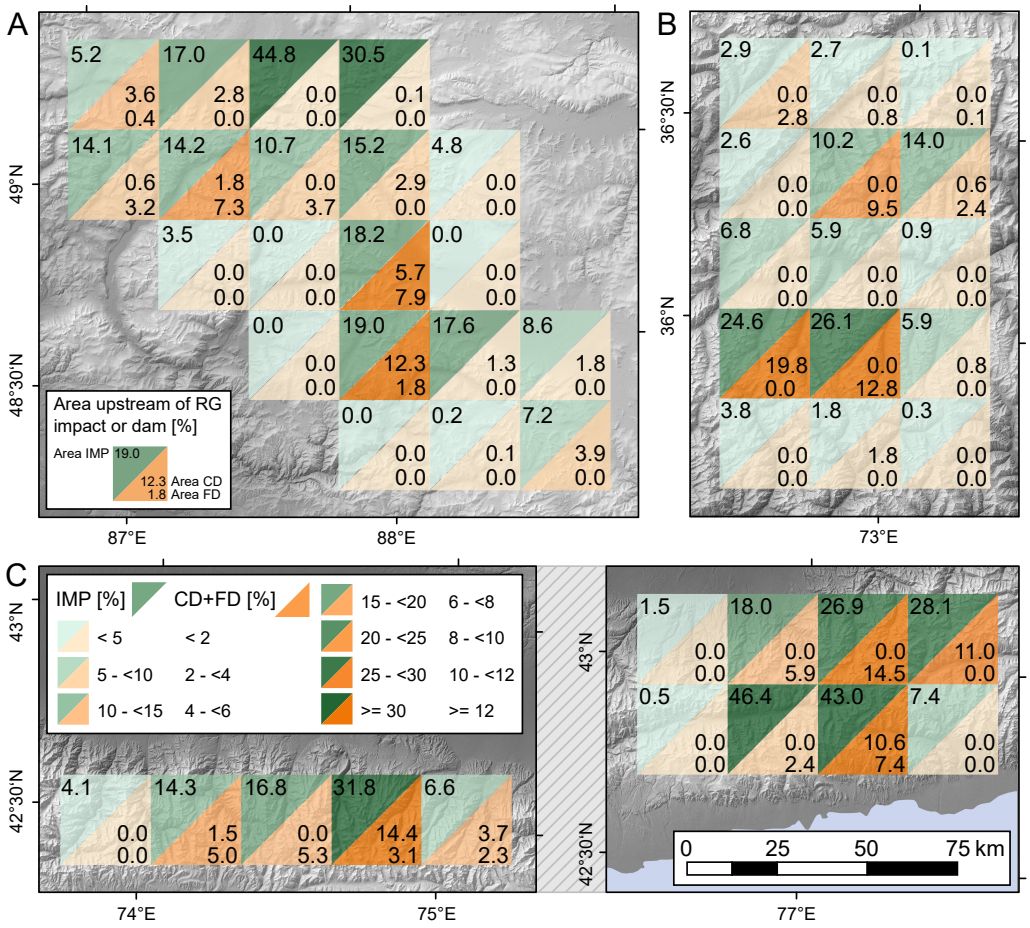

Figure 2.7: Rock glacier (RG) impact on river systems in High Asia. A, B, and C. Detailed maps of the three regions Altai (B), Karakoram (C), and Tien Shan (D) with squared grid cells of 25x25 km^2 each, colour coded by the fraction of area lying upstream of RG that impact the drainage system in green shadings and RG that currently dam (CD) and formerly dammed (FD) the river system in orange shadings (numbers indicate exact fraction). See Figure 2A for location of panels A, B, C.

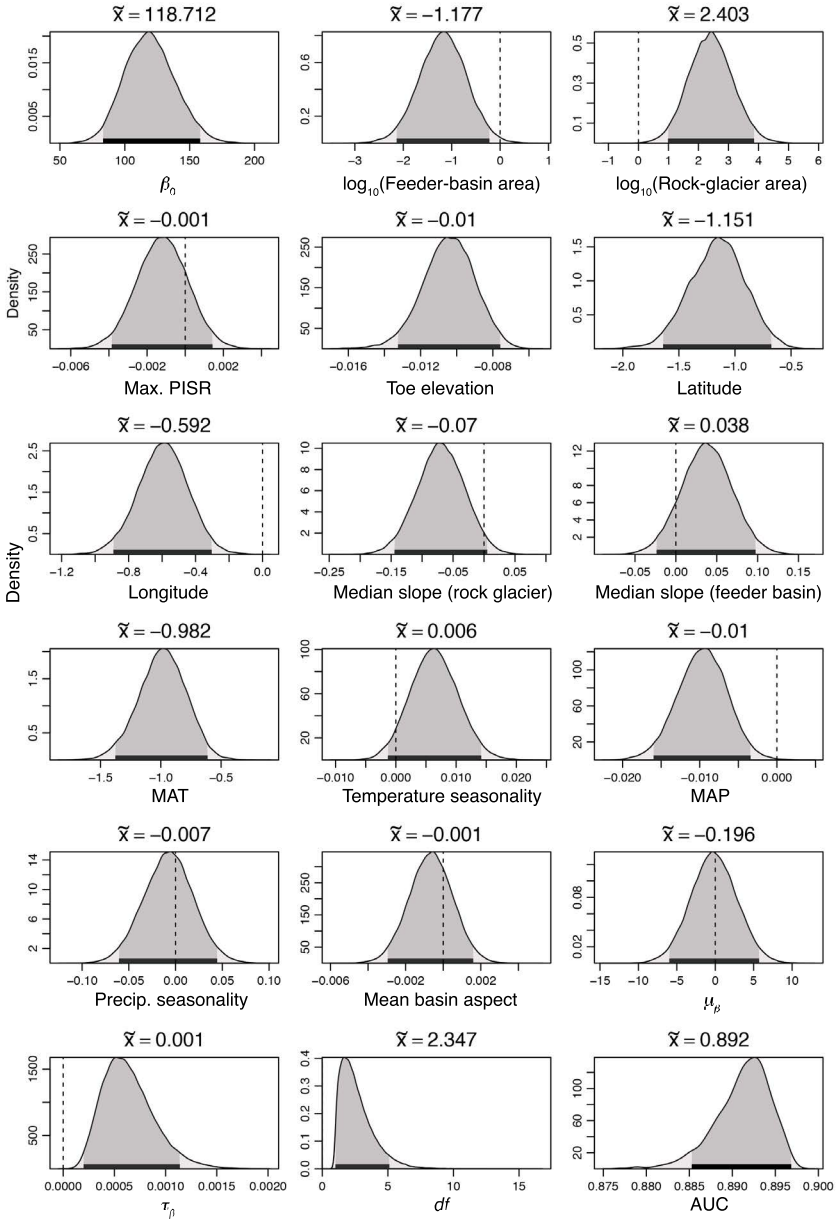

Figure 2.8: Posterior distributions of Bayesian robust logistic regression intercept β_0 and weights β_j of $j = 13$ topographic and climatic predictors, the hyperpriors μ_β, τ_β, and df of their underlying t-distribution, and the resulting area under the receiver-operator characteristic curve (AUC). We report the distributions of the weights and their medians x in unit regression weights, not in the original parameter scales. Most predictors except for feeder-basin area and mean aspect, maximum PISR, and geographic latitude have zero values (dashed lines) in their 95% highest density intervals (thick black lines), and are thus not credible weights for the classification.

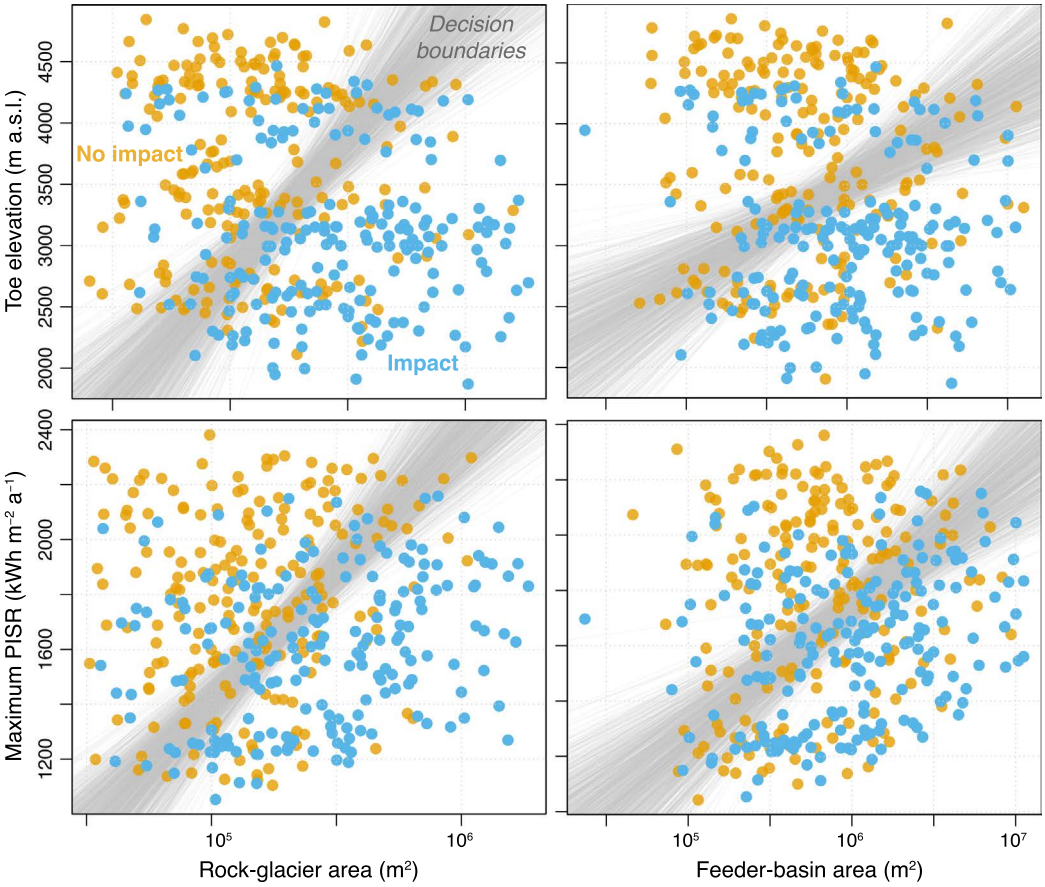

Figure 2.9: Results of Bayesian robust logistic regression with credible decision boundaries sampled from the posterior distribution. These grey lines are contours of 50% probability (sampled from the posterior) that any out of $n = 392$ rock glaciers is classified as impacting (impounding or partly constricting) a mountain river in our study areas. Elevation and potential incoming solar radiation (PISR) are highly correlated predictors and thus perform nearly equally well (Figure 2.10). Feeder-basin area is a slightly better predictor than rock-glacier area, with more bundled decision boundaries.

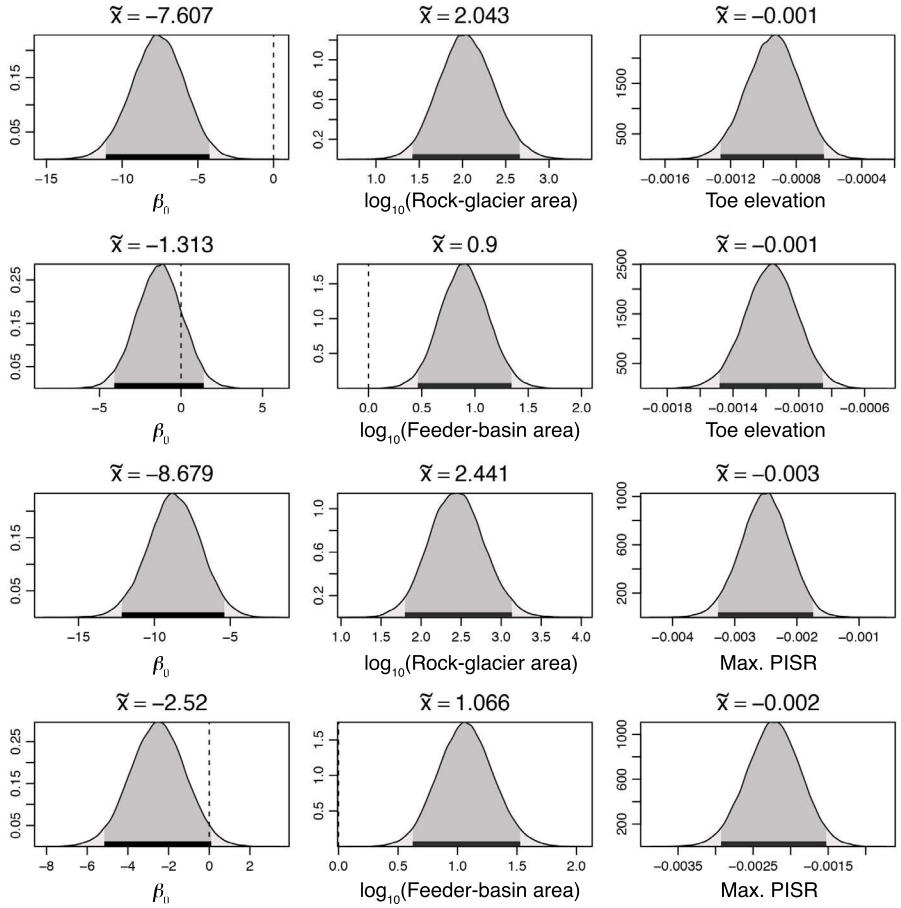

Figure 2.10: Posterior distributions of logistic regression intercepts and weights for predictors shown in Figure 2.9. For better comparison, we show each model in a row, and omit the priors and hyperpriors here; see Figure 2.8 for all other parameter definitions. Note the minor differences in the weights of minimum elevation and maximum PISR.

We learn that the first eight principal components explain >80% of the variance of the 59 topographic and climatic characteristics that we collected for rock glaciers and their catchments (Table 2.5). Using the scores of these eight principal components as predictors in our Bayesian robust logistic regression, we find that only five principal components have regression weights that are credibly different from zero, largely combining influences of elevation, PISR, and geographic latitude; summer temperature and its evenness; and relief and steepness of the feeder basin (Figure 2.11). This dimensional reduction of the original parameter space reveals how redundant the original parameters were, and also reflects our choice of a t-distributed prior for modelling regression weights. The median AUC value for a model with these eight PCs is 0.82. The negative weights of PC1 and PC6, and the positive weights of PC2, PC4, and PC8 indicate that lower-lying, larger rock glaciers in drier, less exposed, and thermally less stable settings have a higher chance of disrupting river channels (Figure 2.11).

Table 2.5: Interpretation of the first eight principal components 5 of 59 topographic and climatic candidate predictors; last column indicates whether these principal components have credible non-zero weights in their posterior distributions derived from Bayesian robust logistic regression (Figure 2.10)

Principle component	**Interpretation**	**Cumulative proportion of total variance explained**	**95% HDI excludes zero?**
PC1	Elevation, potential incoming solar radiation, geographic latitude, and wet-season temperature	0.308	**Yes**
PC2	Warm-season temperature	0.465	**Yes**
PC3	Wet-season precipitation	0.598	No
PC6	Temperature evenness	0.671	**Yes**
PC5	Rock-glacier steepness	0.715	No
PC9	Feeder-basin relief	0.757	No
PC4	Rock-glacier and feeder-basin size	0.795	**Yes**
PC8	Feeder-basin steepness	0.831	**Yes**

In terms of predicting rock-glacier impacts on rivers, we limit ourselves here to the bivariate cases, because these can be best visualised. The median predictive posteriors for the bivariate classification indicate that lower and larger catchments with rock glaciers receiving less PISR are more prone to feed lobes that disrupt rivers (Figure 2.12). We use the standard deviations

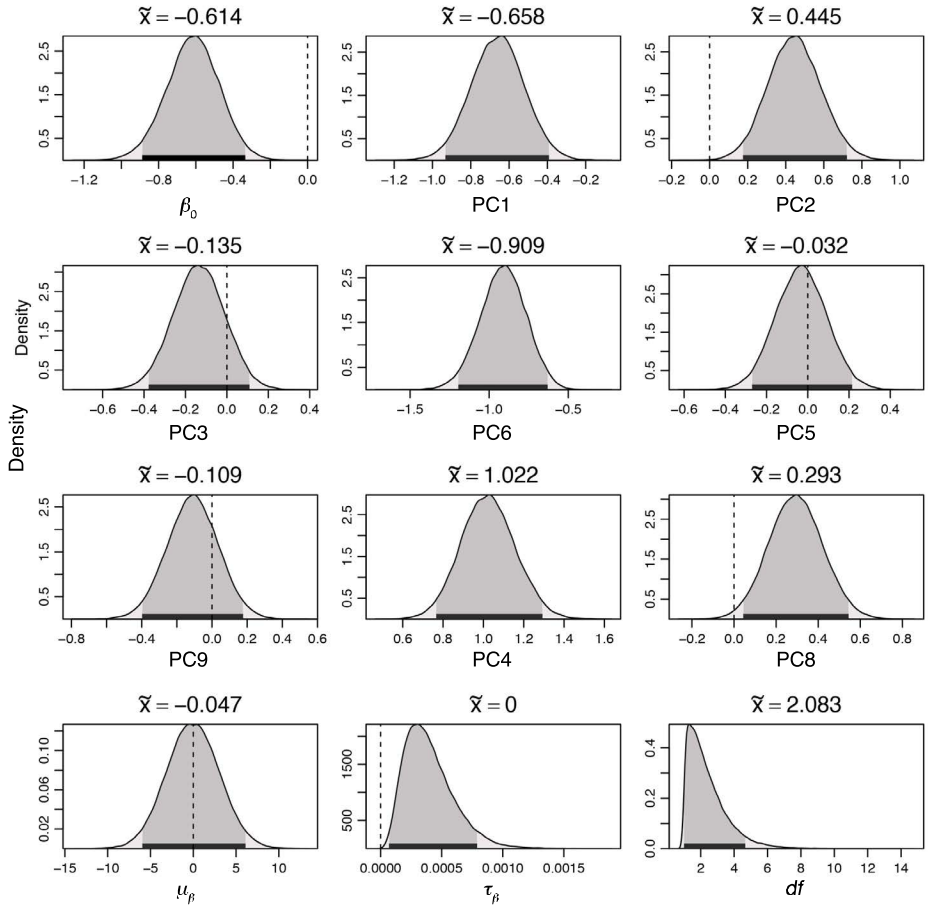

Figure 2.11: Posterior distributions of logistic regression intercept β_0 and weights of the first eight principal components (PCs) sorted by decreasing fraction of total variance that they explain (Figure 2.5). Except for β_0, PC1, PC2, PC4, PC7 and PC8 do not contain zero values (dashed lines) in their 95% HDIs (thick black lines), and are thus credible weights for the classification; see Figure 2.8 for all other parameter definitions.

of the approximately Gaussian posteriors to express the uncertainty in our predictions. For example, a 1-km^2 rock glacier terminating at 4000 m asl has a 70% probability of impacting a mountain river, with an uncertainty of ± 10% (± 2 standard deviations or a 95% HDI).

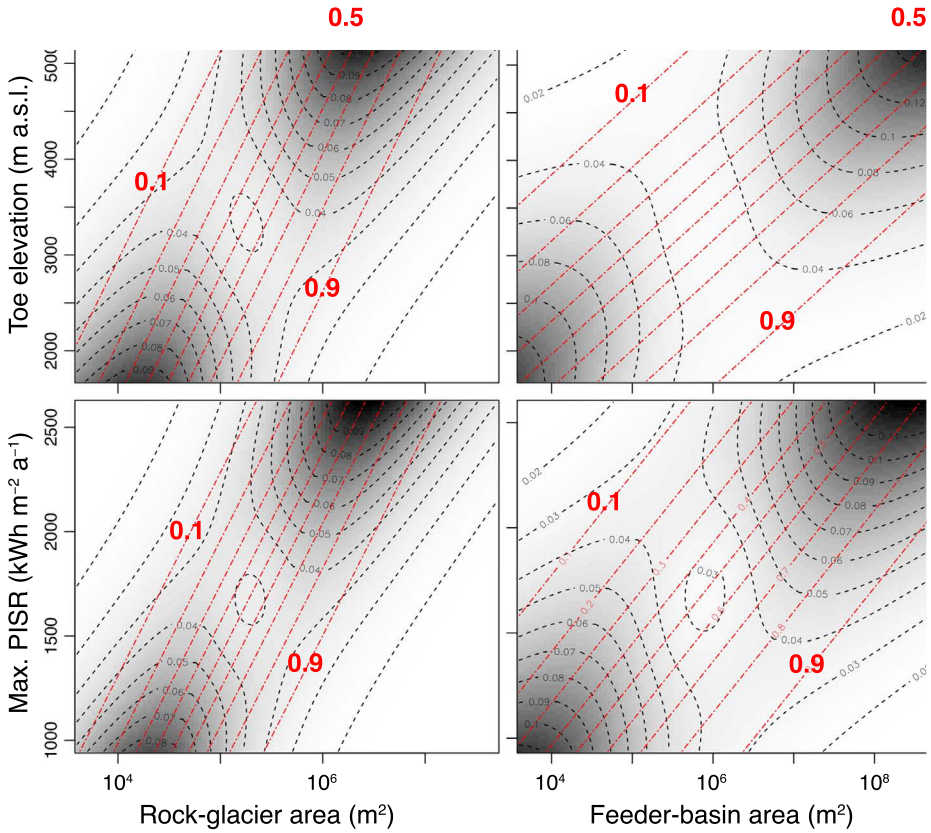

Figure 2.12: Median predictive posterior probabilities (red lines) of a rock glacier disrupting a mountain river for the predictors shown in Figure 2.9. These predictions are for rock glaciers not contained in our inventory. Dashed contours are standard deviations of these probabilities estimated from the approximately Gaussian posterior distributions; brighter and darker areas mark lower and higher uncertainties in the predictions, respectively.

2.5 Discussion

We can credibly discern from our sample of 2082 High Asian rock glaciers those that have impounded rivers or notably aggraded river reaches, largely on the basis of elevation, potential incoming solar radiation, rock-glacier size, and feeder-basin size (Figure 2.9, Figure 2.12). We obtain very similar results if collapsing the original set of 59 mostly topographic and climatic candidate predictors with principal component analysis (Table 2.5, Figure 2.11). Only five principal components have credible weights and combine inputs of the rock-glacier source elevation and maximal PISR, geographic latitude, tem-

perature evenness, and wet-season precipitation, as well as the size of rock glaciers or their feeder basins. Rock-glacier size is one of the few predictors that might suffer from mapping bias that could systematically favour only larger or more distinct and recognisable lobes. However, the size distributions of rock glaciers in the three mountain belts are very similar across all elevation bands (Figure 2.4A, Figure 2.6), so that we exclude such size-effects in our analysis. The principal components also highlight the tight correlations between many topographic and climatic predictors, which produces overly confident classification models if remaining uncorrected: the best AUC values we obtained came from the model using 13 raw predictors.

Principal components warrant independence, but are harder to interpret than original attributes such as elevation or feeder-basin area. The overall performance may appear moderate with AUC values ranging between 0.71 and 0.82, but uses models with few and overly consistent predictors. We note that the classification performance changes little regardless of how we varied the hyperpriors, given the large amount of data. It is remarkable how consistently the predictors separate rock glaciers in terms of their impact on mountain rivers, given that we intentionally sampled rock glaciers across broad environmental gradients, particularly with respect to elevation, latitude, temperature, and precipitation. We note that stratifying the data and running the classification for individual mountain belts slightly improves the performance of the logistic regression model, at least judging from the AUC values, so that we can exclude substantial group effects in our predictions. Our inventory also contains different types of rock glaciers, including those derived from or mainly nourished by talus, moraines or debris-covered lower parts of glaciers. Such distinction might also contain valuable information on the fraction and thickness of debris cover and ice content (Barsch, 1996; Berthling, 2011; Janke et al., 2015). Yet the geographic scope of our study makes representative site assessments of mixed complexes of debris-covered glaciers and rock glaciers impractical. We recall that our classification is concerned more with the geomorphic impact than with the ice content of rock glaciers. Some uncertainty is also tied to the climatic parameters from the WorldClim data. These data, like some other satellite-derived products for

mountain areas with few climate stations, rely heavily on topographic interpolation (Gruber et al., 2017). For example, the WorldClim data indicate a mean annual precipitation of ∼570 mm for rock glaciers in the Tien Shan, whereas Bolch and Gorbunov (2014) estimate this at ∼1000 mm, at least for 74 rock glaciers in the region. However, our elevation and PISR estimates are highly consistent with those of the authors for that region. Irrespective of potential topographic artefacts in our climatic data, the clustering of rock glaciers to narrow bands remains striking, and points to a distinct topographic niche in each mountain belt (Figure 2.4, Figure 2.6).

With these uncertainties in mind, our results offer a testable prediction of the geomorphic consequences of flowing ice and debris in mountain belts. Logistic regression enjoys frequent use in studies on rock glaciers as proxies of permafrost distribution in mountains (Boeckli et al., 2012; Brenning and Trombotto Liaudat, 2006; Etzelmüller et al., 2006). Our Bayesian variant has the advantage that it depicts the full distribution of uncertainties in our classification, and it does so in a probabilistically consistent and reproducible manner for multiple predictors and our initial assumptions about them (Figure 2.9). Our predictions of how likely and under which conditions rock glaciers disrupt river channels go beyond simple point estimates, and have explicit uncertainties learned from the data (Figure 2.12). Using a t-distributed prior on the regression weights avoids overfitting, especially for many predictors and few sample points, and undue influence of outliers, thus ensuring that we end up with as few credible predictors as possible (Figure 2.3).

For most applications, it may be desirable to use the original data on the size of rock glaciers as well as elevation or PISR in logistic regression. In that case we can state that larger rock glaciers from larger catchments have a higher likelihood of interfering with river systems (Figure 2.9). The size of the feeder basin has a very similar relevance, but is less ambiguous and more robust to determine. Several rock-glacier lobes that we mapped grade into glaciers upstream, compromising a clear distinction of lobe size, whereas the locations of active rock-glacier toes were distinct throughout. Regardless of whether we use original predictors or principal components, we infer that

larger and lower-lying rock glaciers have higher probabilities of disrupting rivers; for example, for lobes >1 km^2 flowing down to 4000 m asl this probability is at least 70% ± 10% (Figure 2.9, Figure 2.12). This finding is far from trivial, because we would expect that smaller headwater catchments have a higher potential for coupling hillslope and channel processes. We would thus anticipate that many more rock glaciers entered low-order channels. Instead, we observe that most river impoundments occur in the larger valleys below, often linked to the majority of rock-glacier lobes that advanced down to the median elevation of each mountain belt (Figure 2.6).

The clustering of rock-glacier toes near the median elevation of each study area might indicate a narrow lower limit of sporadic mountain permafrost (Figure 2.6), and support the notion of a frost-cracking window encompassing only a few Kelvin (Hales and Roering, 2007); this window could be vital in producing and feeding sediment to many High Asian rock glaciers (Figure 2.4). We note that our logistic regression takes in widely used determinants of regional permafrost distribution (Figure 2.9). In particular, elevation and PISR have been key for predicting the regional distribution of mountain permafrost from rock-glacier toes (Brenning and Trombotto Liaudat, 2006). Our data thus support the idea that the lower-lying and river-disrupting rock glaciers are likely closer to non-equilibrated permafrost conditions. In the Tien Shan, for example, Bolch and Gorbunov (2014) found that they could not fully explain the low-lying locations of several large rock glaciers with climatic or topographic variables alone. They argued that these rock glaciers were not equilibrated with the current climate, and suggested topography, weathering, and seismic activity as additional drivers. Local effects also come into play, as the temperature regime below large blocks can be several degrees lower compared to surrounding soils (Harris et al., 1998), thus stabilising rock glaciers or permafrost patches below the 0°C isotherm (Marchenko and Gorbunov, 1997). The two credible predictors from our principal component analysis encapsulate mostly temperature- and precipitation-related variability, and therefore support this possibility.

In our study area, 21 rock glaciers fully block rivers and impound small lakes, disconnecting a total of 630 km^2 of upstream catchment area from

the sediment cascade. Rock glaciers that not fully block channels, but enter valley floors and divert or constrict rivers, likely reduce sediment delivery from another 3000 km^2 (Table 2.4). These fractions vary widely across the study areas (Figure 2.7). Nonetheless we infer that river-impacting rock glaciers might play a significant and hitherto unrecognised role in altering the flux and storage of sediments in high mountains. Judging from numerous case studies on landslide and glacier dams, we suspect that a full blockage requires both highly mobile and mostly impermeable lobes; otherwise the lobes would be undercut and trimmed by the larger rivers before being able to progress across the valley floor. A high flow velocity in particular could indicate a local disconnection from regional climatic conditions as Bolch and Gorbunov (2014) suggested. Another option is that some of the rock-glacier dams formed in deposits of catastrophic landslides, which abound in all the mountain areas that we sampled. Compared to the dimensions of a sample of large dams formed by catastrophic landslides worldwide, we find that our rock-glacier dams occupy the lower size spectrum. Rock-glacier dams can be as high and wide (measured along-stream) as some major landslide dams, and share similarly low ratios of dam height over width; yet the ones we sampled remain well below the size of the largest landslide deposits (Figure 2.13). Similarly, lakes associated with rock glaciers in our study area are limited to small ($<$11 km^2) headwater catchments with a total relief of less than 1800 m. This first-order comparison points at the possibility that at least the dimensions of some rock glaciers are compatible with those of landslide deposits, but does not guarantee that rock glaciers did indeed evolve from them.

A final point to consider is whether the rock glaciers actively impounded lakes or simply advanced over pre-existing natural dams formed by landslides or moraines. Such a polygenetic origin is plausible, especially for rock-glacier lobes that emanate from debris-covered glaciers. In this scenario, rock glaciers could simply override and reinforce a previous landslide or moraine dam. More work will be necessary to establish morphological similarities of rock-glacier lobes with deposits of catastrophic long-runout landslides.

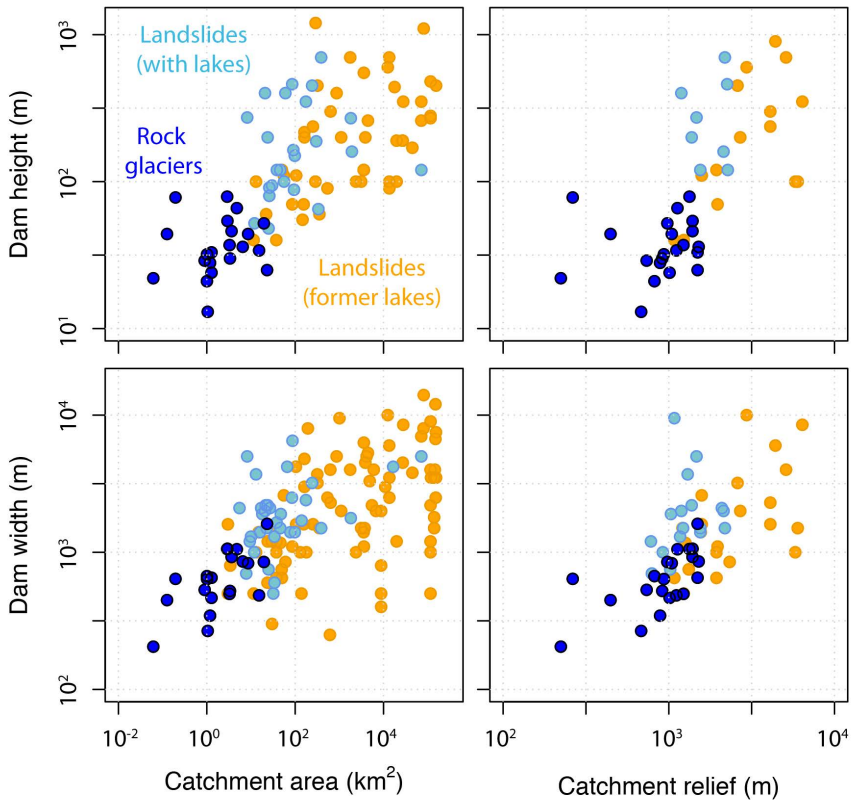

Figure 2.13: Rock-glacier dam height and dam width (measured along-stream) versus upstream catchment area and relief (maximum elevation difference), measured above the point of blockage, in High Asian mountain belts compared to a sample of large landslide dams from around the world.

2.6 Conclusions

We present an inventory of more than 2000 rock glaciers, distributed over three mountain ranges of High Asia. In contrast to other studies on rock-glacier inventories, we offer a first quantitative appraisal of the geomorphic impacts of rock glaciers on rivers. Despite covering 13 degrees of latitude and more than 3000 m in vertical difference, rock glaciers consistently occupy narrow thermal niche between –5 and –4 °C in the KS and TS, and about 4-5 K lower in the ALT. Bayesian logistic regression reveals that elevation, potential incoming solar radiation, and the size of rock glaciers and their feeder basins can credibly separate rock glaciers that disrupt mountain

rivers from those that do not, while consistently identifying redundant predictors. Our classification indicates that larger and low-lying rock glaciers that receive commensurately less PISR are more likely to impact on river processes, forming lakes, backwater sediment wedges, and constricting channels over at least 95 km of the drainage network, and involving between roughly 7% and 36% of the total rock-glacier area sampled in each study area. If using principal components instead, we can identify only two credible predictors that eliminate a lot of correlation in these (and 59 original) parameters and boil down to combined influences of low elevation, PISR, temperature variability, geographic latitude, wet-season precipitation, and the size and steepness of feeder basins. The geometries of rock glacier lobes that we classified as disrupting mountain rivers are comparable to those of large landslide dams. Whether some rock-glacier lobes out of equilibrium with regional climatic conditions rapidly advanced over existing landslide or moraine dams, or whether the lobes formed their own impoundments, deserves future detailed fieldwork. In either case, rock glaciers are understudied as forming, or at least contributing, factors of natural dams and disrupting or partially disturbing the sediment flux in semiarid mountain belts.

Acknowledgements

Funded by the German Ministry for Education and Research (BMBF TIPTIMON, 03G0809), the Potsdam Research Cluster for Georisk Analysis (PROGRESS), the Potsdam Graduate School, the University of Potsdam, and German Research Foundation (DFG), and the VolkswagenStiftung. Kanatbek Abdrakhmatov kindly organised our field support in the Kyrgyz Tien Shan. We thank Mansoor Ahmadi, Atyrgul Dzhumabaeva, Angela Landgraf, Anina Sorg, Friedrich Volkmer, and Martin Zeckra for fieldwork collaboration, Wolfgang Schwanghart and Christoff Andermann for computational support, and Jan Seidemann for helping with rock-glacier mapping. We used the free R software environment (https://cran.r-project.org/) for data processing, including the JAGS module by Martyn Plummer (https://cran.r-

project.org/web/packages/rjags/index.html) and code kindly shared by John Kruschke and Rasmus Bååth.

Chapter 3

Late Pleistocene outburst floods from Issyk Kul, Kyrgyzstan?

Abstract

Elevated shorelines and lake sediments surrounding Issyk Kul, the world's second largest mountain lake, record fluctuating lake levels during Quaternary times. Together with bathymetric and geochemical data, these markers document alternating phases of lake closure and external drainage. The uppermost level of lake sediments requires a former damming of the lake's western outlet through the Boam gorge. We test previous hypothesised ice or landslide dam failures by exploring possible links between late Quaternary lake levels and outbursts. We review and recompile the chronology of reported changes in lake site, and offer new ages of abandoned shorelines using ^{14}C in bivalve and gastropod shells, and plant detritus, as well as sand lenses in delta and river sediments using Infrared Stimulated Luminescence. Our dates are consistent with elevated lake levels between ∼45 ka and 22 ka. Cosmogenic ^{10}Be and ^{26}Al exposure ages of fan terraces containing erratic boulders (>3 m) downstream of the gorge constrain the timing of floods to 20.5–18.5 ka, postdating a highstand of Issyk Kul. A flow-competence analysis gives a peak discharge of $>10^4$ m^3 s^{-1} for entraining and transporting these boulders. Palaeoflood modelling, however, shows that naturally

dammed lakes unconnected to Issyk Kul could have produced such high discharges upon sudden emptying. Hence, although our data are consistent with hypotheses of catastrophic outburst floods, average lake-level changes of up to 90 mm yr^{-1} in the past 150 years were highly variable without any outbursts, so that linking lake-level drops to catastrophic dam breaks remains ambiguous using sedimentary archives alone. This constraint may readily apply to other Quaternary lakes of that size elsewhere. Nonetheless, our reconstructed Pleistocene floods are among the largest reported worldwide, and motivate further research into the palaeoflood hydrology of Central Asia.

3.1 Introduction

Issyk Kul is the world's second largest mountain lake, and located in the tectonically active Tien Shan mountains of Central Asia (Figure 3.1). Today, the lake is endorheic with its water surface at ∼1606 m asl. Distinct shorelines partly surround the lake, and mark prominent former highstands at ∼1620 and ∼1660 m asl; the same goes for >10-m thick stacks of lake sediments exposed as far as 30 km to the west of the present-day lake shore. A number of sedimentary archives document lake-level changes of ∼180 m during the past 10 kyr, and up to 400 m during the past 0.5 to 1 Myr (Trofimov, 1978) (Figure 3.1E). Historical records confirm that lake levels changed by as much as 90 mm yr^{-1} (Ricketts et al. (2001); Romanovsky (2002) and references therein; Table S1). Submerged channels and terraces also require lake levels ∼110 m lower than today (De Batist et al., 2002), possibly attained in Late Pleistocene (Bondarev and Sevastianov, 1991; Markov, 1971) and Middle Holocene times (Trofimov, 1978). The isotopic composition of Holocene ostracods indicates alternating opening and closing of the lake basin (Ricketts et al., 2001). Noble gases from lake sediments in drill cores record ∼300 m lower lake levels inferred from increased salinity at ∼8 ka (Kipfer (2011), pers. comm.), though geomorphic evidence remains elusive (Korjenkov (2011), pers. comm.). Overall, however, the climatic and tectonic drivers of lake-level changes remain disputed (De Batist et al., 2002), leav-

ing the Quaternary history of the lake largely unresolved (Grosswald et al., 1994).

The Chu River that passes by the western edge of Issyk Kul through the Kok Moinok basin and the Boam gorge has played a major role in controlling the lake's in- and outflow during the Quaternary. At present, the river does not drain the lake. Burgette (2008) proposed that a former landslide dam on the river prompted some of the Late Pleistocene lake highstands. Other scientists argued that the Chu River's shifting fan delta blocked and deflected the channel away from the lake's western shores (Gerasimov, 1953; Maksimov, 1985; Sevastianov et al., 1980). Grosswald et al. (1994) speculated that Issyk Kul was partly ice-dammed during the last glaciation, and that multiple phases of damming and breaching caused the lake level to fluctuate. According to this hypothesis, glacier dams or clusters of floating icebergs upstream of the Boam gorge would have blocked the lake's western outlet, diverting the course of the Chu River, while episodic outburst floods would have carved the Boam gorge. Lakes impounded by large landslides or glaciers in the Tien Shan (Strom and Korup, 2006), like in other mountain belts (Bookhagen et al., 2005; Hermanns and Strecker, 1999; Korup et al., 2007), can exist for hundreds to thousands of years before suddenly releasing large volumes of water during outburst floods. Yet such catastrophic origin of the gorge remains disputed (Grosswald et al., 1994) in favour of a more gradual incision responding to localised uplift or changing lake levels (Berg, 1904).

Our objective is to test the hypothesis of outburst floods from Issyk Kul in the light of new absolute age constraints. Understanding the dynamics of the lake's western outlet is key to validating links between lake-level changes and outbursts or, alternatively, longer-term controls of climate, basin hydraulics, subsidence, and altered water and sediment fluxes (García-Castellanos, 2006). A natural dam could have also formed anywhere inside or near the Boam gorge. Without any diagnostic remnants of a former dam, however, we resort to study lake and backwater sediments and boulder-littered outburst deposits. The exit of the Boam gorge, where it widens to the Chu foreland basin of the Tien Shan, is an ideal place to look for geo-

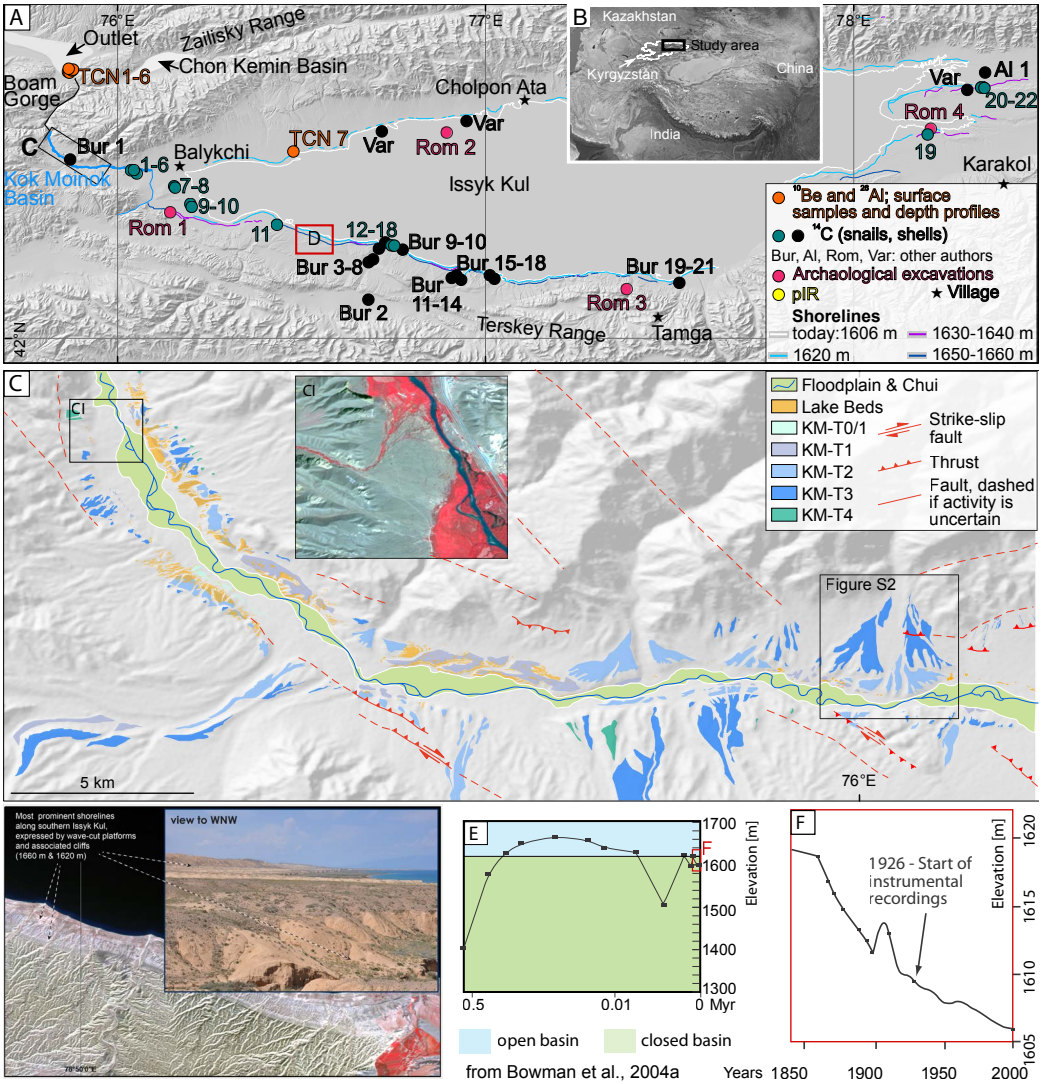

Figure 3.1: (A) Shaded relief of study area in north Kyrgyzstan (Google Earth, (B)), based on SRTM90 data showing sampling locations of terrestrial cosmogenic nuclides, ^{14}C, and IRSL. Sample sites of previous studies are marked by a prefix of the authors' name: (Bur = Burgette (2008), Al = Aleshinskaya et al. (1971), Rom = Romanovsky (2002), Var = various authors cited in Romanovsky (2002). The shorelines have been mapped on 2.5 m resolution SPOT 5 data. Outlet refers to the fan terrace at the exit of Boam gorge. (C) Mapping of fluvial/alluvial terraces, lake beds, and faults overlain on a SRTM hillshade model. At least four sets of terrace levels are clearly distinguishable along the length of Chu in Kok Moinok (KM) at different heights above the recent channel (all approximate numbers: KM-T4 – 150 m; KM-T3 – 90–100 m; KM-T2 – 70 m; KM-T1 - 50 m; KM-T0 – 10 m). Note the distributed faulting. Insets CI and S2 are locations discussed in the Text as examples of potential river blockage from alluvial fans. (D) SPOT satellite image and field photo showing the most prominent shorelines with wave-cut platforms and cliffs. (E) Issyk Kul lake-level changes (Bowman et al., 2004a) since the Mid-Pleistocene, and in higher detail from 1860 to 2000 (F).

morphic and sedimentary evidence of past outburst floods to chronologically match the lake sediments upstream. We found numerous boulders embedded in three fan terraces at the gorge exit, and used cosmogenic ^{10}Be and ^{26}Al exposure dating to determine the timing of potential lake outbursts. Palaeo-competence and -flood models helped to estimate peak discharges that dam failures could produce anywhere between the western end of Issyk Kul and the gorge exit. Specifically, we tested whether ephemeral lakes unconnected to Issyk Kul could have delivered large enough outburst floods. To put these events into context, we reviewed and expanded the lake-level history of Issyk Kul by sampling bivalve and gastropod shells (further referred to as shells and snails), and plant detritus for ^{14}C dating from several lake sediments, and infrared stimulated luminescence (IRSL) dating of fluvial backwater sediments to detect past outburst signals.

3.2 Study area

Issyk Kul is lodged in a tectonically active intramontane basin between the Kungey and Terskey Ranges of the northern Kyrgyz Tien Shan (Figure 3.1A, B). The Tien Shan mountains spread out over 2500 km from east to west, and 300 to 500 km from north to south; the highest peaks exceed 7000 m asl. The basement of the Tien Shan consists of three Precambrian micro-continents that have controlled most of the orogenic deformation later on (Buslov et al., 2003). The modern orogeny results from ongoing far-field deformation of the colliding Indian and Eurasian tectonic plates (Tapponnier and Molnar, 1979). Northward-directed shortening rates between the northern and southern shores of Issyk Kul measured by GPS are 5-6 mm yr^{-1} (Zubovich et al., 2010), and seismic profiles reveal shortened sediment layers on the lake-basin floor (De Batist et al., 2002). North of Issyk Kul, the prominent Ak-Teke anticline shows Quaternary deformation with a record of up to 17 possible earthquakes (Korjenkov et al., 2007), and slip rates of 0.1-1.5 mm yr^{-1} (Selander et al., 2012) along faults bordering the Kungey Ranges.

Pleistocene seismites amongst shallow lacustrine, beach, and fluvial deposits indicate episodic strong ground motion (Bowman et al., 2004a,b). The strongest historical earthquakes include those at Verny (1887, Ms 7.3), Chilik (1889, Ms 8.3), Chon Kemin (1911, Ms 8.1), and Kemino-Chu (1938, Ms 6.9) (Abdrakhmatov and Strom, 2002). South of the lake, south verging faults and folds accommodate active deformation, so that flights of Quaternary fluvial terraces are tilted progressively to the north (Burgette, 2008). Issyk Kul has an area of ~6,200 km^2 and is up to 670 m deep (De Batist et al., 2002). Its water level dropped by an annual average of 42 mm since 1926, interspersed by periods of rapid rise of up to 320 mm from 1956 to 1960 (Romanovsky, 2002) (Figure 3.1F). Highstands occur mostly in August to September owing to seasonal changes in water inflow and evaporation (Romanovsky, 2002). The Djyrgalan and Tjup rivers entering the lake from the east are its primary sources of water and sediment (De Batist et al., 2002). The lake has been endorheic for the past 150 years (Giralt et al., 2003) and was formerly drained by the Chu River (De Batist et al., 2002). Today the 'Kutemaldinsky threshold' (Grosswald et al., 1994) separates the river from the lake at 1620 m asl. This topographic high (or 'sill') seems a natural location for suspecting former river blockages that would have raised the lake level of Issyk Kul. West of this sill lies the 30-km long Kok Moinok basin featuring an aggraded valley floor with the meandering gravel bed of the Chu River. A distinct knickpoint in its longitudinal profile (Figure 3.2A, Figure 3.3A) marks the entrance to the steep, bedrock-walled Boam gorge. The knickpoint also separates the gorge from the aggraded reaches upstream, and coincides with the westernmost outcrops of perched lake sediments (Figure 3.2B) that cap beds of fluvial gravel and bouldery debris flows. The Boam gorge slices through Precambrian and Palaeozoic metamorphic and magmatic rocks, and conglomerates, covered locally by patches of Neogene and Quaternary sediments. Near the exit of the gorge the Chu meets the Chon-Kemin River that drains the Zailisky and Kungey Ranges, just upstream of the Chu foreland basin. We refer to this area, where both rivers form a large alluvial fan at the range front of the Tien Shan, as the outlet area. Several large, boulder-rich terraces (T1–3 at 1280, 1320, and 1340 m asl, respectively) line the fan sur-

face. A network of braided channels covers terrace T2 (Figure 3.2A inset). This terrace is cut into T3, which in turn has clast-supported boulders and fluvial gravels lacking any current structures or erosional features (Figure S3 E).

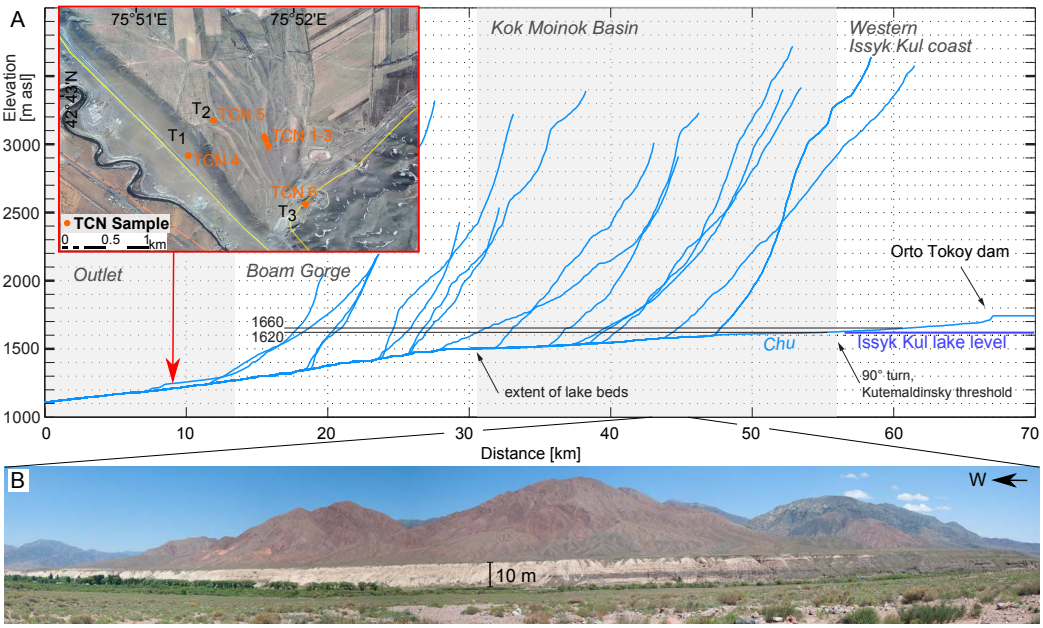

Figure 3.2: (A) Longitudinal profile of Chu River and its tributaries from Orto Tokoy dam to Boam-gorge outlet; Google Earth satellite image shows dated terraces T1–3 (TCN 4-6), dated boulders (TCN 1-3), and distributary channels (upper left). (B) Lake sediments in Kok Moinok basin flank the Chu's river banks for up to 30 km west of the Kutemaldinsky Threshold.

3.3 Methods

3.3.1 Exposure dating with ^{10}Be and ^{26}Al

We sampled the surface (uppermost ∼5 cm) of three 3–4 m large granitic and gneissic boulders embedded in terrace T2 at the gorge exit for cosmogenic ^{10}Be and ^{26}Al exposure dating (Figure S3 D). Some of the boulders had slightly cracked surfaces from incipient weathering. We also collected amalgamated gravel- to cobble-sized sediment samples from four depth profiles (>2 m) of terraces T1-3 and the northern Issyk Kul shore (Figure S3

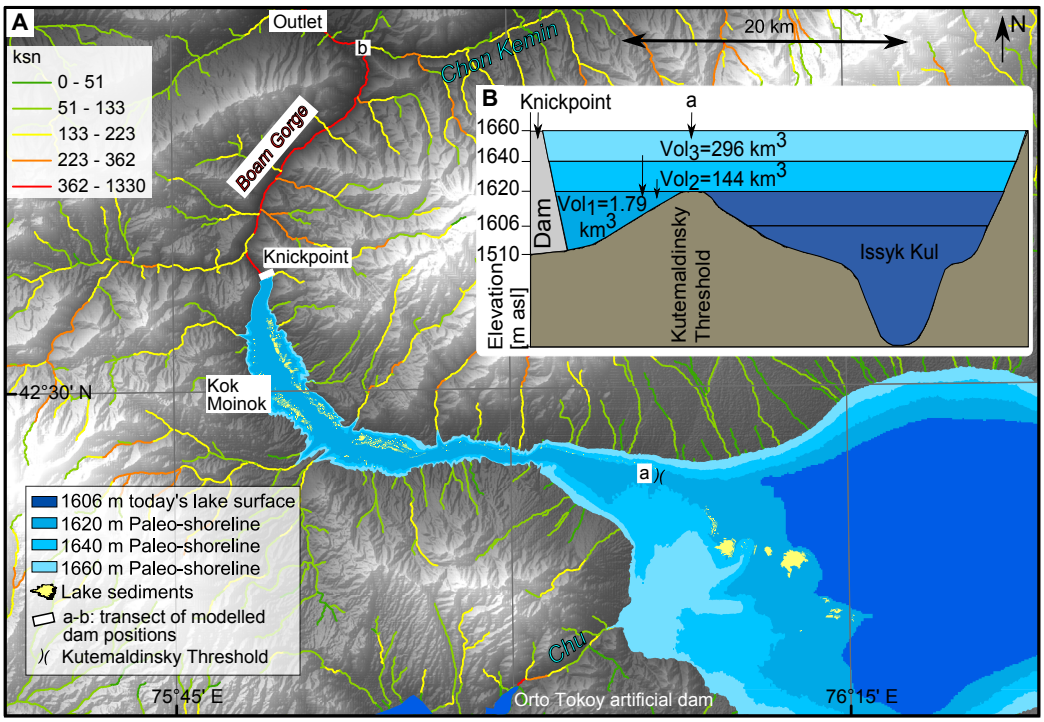

Figure 3.3: (A) SRTM (30 m) of western Issyk Kul and Boam gorge area. Rivers are colour-coded to their normalized steepness indices (ksn). Different blue tones refer to lake highstands; exposed lake sediments are highlighted in yellow (we only refer to their position, their maximum elevations are ~1620 m asl). Peak discharges were modeled for hypothetical dam sites in reach between 'a' and 'b'. (B) Estimated outburst flood volumes for different lake elevations, assuming a dam at the Chu knickpoint.

A–C, E–F, Table 3.1), and kept with mechanical and chemical sample treatment standards (Supplementary Online File S7). AMS measurements were conducted at the DREAMS facility using the in-house standard SMD-Be-12 (Akhmadaliev et al., 2013), which is traceable to the NIST SRM 4325 standard with $^{10}Be/^{9}Be = 2.79 \pm 0.03 \times 10–11$; (Nishiizumi et al., 2007), and in-house standard SMD-Al-11 with $^{26}Al/^{27}Al = 9.66 \pm 0.14 \times 10–12$ (Rugel et al., 2016), which is traceable to the primary standards described by Merchel and Bremser (2004). We calculated the boulder exposure ages and modelled depth profiles using a MATLAB Input GUI (Hidy et al., 2010) with a ^{10}Be reference production rate at high-latitude sea level of 4.76 atoms g^{-1} a^{-1}, recalibrated according to Nishiizumi et al. (2007), the time-dependent scaling scheme of Lal and Stone (Stone, 2000), and a ^{10}Be half-life of 1.387

± 0.012 Ma (Chmeleff et al., 2010; Korschinek et al., 2010). We measured topographic shielding in the field, but neglected duration and thickness of snow cover, which could reduce the in-situ production by 10% (Schildgen et al., 2005).

Table 3.1: TCN sampling locations and results for exposure ages.

Name	Depth [mm]	Location	Type	Latitude [°N]	Longitude [°E]	Elevation [m asl][a]	Shielding factor	^{10}Be conc. [10^3 at g^{-1}]	^{26}Al conc. [10^3 at g^{-1}]	^{10}Be age [kyr][b]	^{26}Al age [kyr][b]
TCN 1	0	Outlet T2	Boulder	42.7125	75.8652	1332	–	260.2 ± 9.2	–	19.5 +3.7 -3.8	–
TCN 2	0	Outlet T2		42.7125	75.8652	1332	–	262.5 ± 16.6	1870.0 ± 90.0	20.0 +6.1 -7.1	20 +9.3 -10
TCN 3	0	Outlet T2		42.7120	75.8654	1331	–	268.8 ± 3.9	1670.0 ± 259.0	20.5 +1.6 -2.2	18.6 +8.6 -8
TCN 4	0	Outlet T1		42.7111	75.8569	1289		144.1 ± 2.1	–	6.2 +NaN -0.1 –11.4 +0 -10*	–
	42.5							103.8 ± 1.7	–		–
	77.5							135.9 ± 1.9	–		–
	117.5							133.6 ± 1.8	–		–
	172.5							137.3 ± 1.8	–		–
	240							98.5 ± 2.0	–		–
TCN 5	0	Outlet T2	Depth profile	42.7146	75.8597	1325		295.9 ± 5.0	–	18.6 +4 -5	–
	95							213.1 ± 3.7	–		–
	110							154.8 ± 2.3	–		–
	130							96.5 ± 1.9	–		–
	180						0.999	98.7 ± 2.0	–		–
	235							99.6 ± 2.1	–		–
TCN 6	0	Outlet T3		42.7062	75.8689	1357		823.9 ± 8.1	–	66.3 +10.8 -12.4	–
	32.5							569.1 ± 4.6	–		–
	52.5							449.1 ± 3.8	–		–
	77.5							289.1 ± 3.1	–		–
	110							218.1 ± 2.5	–		–
	180							143.8 ± 2.1	–		–
TCN 7	0	Issyk Kul North, Delta		42.5043	76.4662	1633		1382.2 ± 10.3	–	22.2 +7.4 -2.1	–
	28.5							1254.8 ± 9.3	–		–
	134							1016.7 ± 7.6	–		–
	155							1138.1 ± 8.5	–		–
	191							983.0 ± 8.1	–		–
	280							1105.5 ± 9.3	–		–

[a]Sample elevations were measured with GPS or dGPS with an accuracy of about 3 m and 10 cm, respectively.
[b]Bayesian most probable ages and 2 uncertainty calculated with MATLAB Input GUI (Hidy, 2010).
*Ranges of two ages based on model of two interpreted depositional phases (Figure S10). Note that uncertainties can be even larger, because the upper deposit interpretation is based on two data points only, please refer to Table S11 for data statistics.

3.3.2 Radiocarbon dating

We radiocarbon-dated gastropod and bivalve shells that we found in platforms or cliffs cut into the lake sediments around Issyk Kul (Figure 3.1A, Figure S3I–L) to estimate the timing of former lake highstands. The shells likely predate the shoreline close to its sampling elevation, as we cannot exclude that we dated reworked material. All samples were analysed in the Poznan Radiocarbon Laboratory, Poland. We calibrated all previously published and new samples using OxCal software (`https://c14.arch.ox.ac.uk/`) and the IntCal13 curve (Reimer et al., 2013).

3.3.3 Infrared stimulated luminescence

We sampled fluvial backwater sediments covered by the lake sediments in the Kok Moinok basin (pIR1), and delta sediments (pIR2) associated with Issyk Kul's 1620 m shoreline (Figure 3.1A, Figure S3 G–H). The low luminescence sensitivity of the quartz grains in active mountain belts (Preusser et al., 2006) motivated us to use feldspar luminescence with the post-IR IRSL protocol, and a stimulation temperature of the second readout at 150°C, using sampling procedures, preparation, and measurement set-up outlined in Supplementary Online File S8.

3.3.4 Lake levels and chronology

In an approach similar to Oviatt et al. (1992), we reviewed and synthesised published data on shoreline elevations, lacustrine and fluvial deposits to reconstruct age-elevation relations for Quaternary sediments fringing Issyk Kul (Table 3.2, Table 3.3). Where possible, we also determined sediment provenance of boulders in the field. Two prominent shorelines at ∼1660 m and ∼1620 m asl have reported ^{14}C ages of ∼25 ka and ∼0.5 ka, respectively (Burgette, 2008). Aided by SPOT 5 satellite imagery, we mapped remnants of the younger shoreline around most of the lake; in the field a wave-cut platform below a distinct cliff marks this former highstand along the southern shore, whereas in the north this cliff is less clearly preserved along the trimmed

Table 3.2: Assumptions for shoreline and lake-highstand deposit comparison.

Description	Sample altitude and age relative to lake level
Shoreline angle marked by wave-cut platform/cliff couple	Altitude ∼ lake level
Deltaic deposits	Sample altitude ∼ lake level; sample age > lake age at that altitude
Fluvial backwater deposits	Sample altitude ∼ lake level; sample age > lake age at that altitude
Lacustrine marl	Sample altitude < lake level; sample age > age of lake transgression

toes of alluvial fans (Figure 3.1A, Figure 3.1D). Traces of the older, higher, and more eroded shoreline are limited to the southern shore of Issyk Kul, and generally more clear from satellite imagery (Figure 3.1A, Figure 3.1D). Erosional remnants of another shoreline at ∼1640 m also dot the southern shore. All former shorelines feature sand or gravel bars, and one can trace distinct subparallel sand and gravel beach ridges tied to falling lake levels below the 1620-m shoreline.

3.3.5 Palaeoflood modelling

We measured the principal axes of 89 subangular to subrounded boulders embedded in the three fan-terrace levels $T_{1–3}$ at the Boam gorge outlet (Figure S4, Table S5). The intermediate boulder axes have medians of 0.8 m, 1.4 m, and 1.1 m for $T_{1–3}$, respectively. From these intermediate axes diameters $d[m]$ we inferred the minimum flow velocity $v[ms^{-1}]$ needed to entrain and transport the boulders following the palaeo-competence equations of Costa (1983) (Figure 3.4B):

$$v = 0.18d^{0.487} \tag{3.1}$$

We derived the flow velocity for the largest boulder surveyed (3.1 m, Table S5) assuming that it was transported by a flood rather than a debris flow. This velocity estimate is a minimum that further reflects the uncertainties tied to the empirical relation between clast diameter and flow conditions (Costa, 1983; Jacobson et al., 2003).

Based on v, we calculated the minimum discharge $Q[m^3s^{-1}]$ at the fan head where the cross-sectional area $A[m^2]$ is well constrained by the adjacent

hillslopes. We solved Manning's equation (Manning, 1904):

$$Q = v \times A = 1/n \times AR^{2/3}S^{1/2} \tag{3.2}$$

with a numerical optimisation scheme to find values of the hydraulic radius R (the ratio between the cross-sectional area $A[m^2]$ and the wetted perimeter $P[m]$) and the area given the flow velocity $v[ms^{-1}]$, a mean channel gradient $S = 0.01[mm^{-1}]$, and varying roughness values $n[sm^{-1/3}]$ (Supplementary Online File S6). Since n is unknown for past outburst floods, we computed solutions for 100 equally-spaced values of n between 0.05 (natural stream with stony bed and irregular slopes) and 0.1 (very rough channel). This upper bound of n accounts for flow obstacles such as shrubs or trees on floodplains, and energy losses due to sediment bulking (Fread, 1992).

We tested three different highstand scenarios for Issyk Kul at 1620, 1640, and 1660 m asl, and estimated the corresponding peak discharge for glacier and earthen-dam failures positing the overflow point at the westernmost tip of the lake sediments perched in the Boam gorge. We also computed the maximum volume of water storable behind possible dams in the Boam gorge. To test whether the outburst of temporary lakes in the Boam gorge, separated from Issyk Kul by the Kutemaldinsky Threshold, could have moved the boulders to the foreland, we calculated the maximum water volumes for ten dam-crest elevations between 1350 and 1660 m asl along the entire gorge (Figure 3.3), using SRTM1 (Land Processes Distributed Active Archive Center, USGS/EROS, `http://lpdaac.usgs.gov`) data and TopoToolbox 2 (Schwanghart and Scherler, 2014). We used Walder and O'Connor (1997) dam-break model in its revised form (O'Connor and Beebee, 2009), and estimated peak discharge from the outflow volume $V_0[m^3]$, dam height $D[m]$, breach depth $h[m]$, and breach rate $k[ms^{-1}]$. The model considers only geometry and energy losses, and mostly applies to dam failures by overtopping and piping (Walder and O'Connor, 1997):

$$Q_0 = \begin{cases} 1.42\left(g^{1/2}h^{5/2}\right)^{0.006}\left(\frac{kV_0}{h}\right)^{0.94} \text{ for } \eta <\sim 0.6 \\ 1.79\left(g^{1/2}h^{5/2}\right)\left(\frac{D}{h}\right)^{3/4} \text{ for } \eta >\sim 1 \end{cases} \tag{3.3}$$

and

$$\eta = \frac{V_0 k}{h^{7/2} g^{1/2}} \tag{3.4}$$

Obtaining V_0 and D from the SRTM1 data, we simplistically assumed the dam would fully incise (i.e. $h = D$) upon failure at a rate $k = 33mh^{-1}$, which is the median value reported for case studies worldwide (Walder and O'Connor, 1997). We did not systematically analyse flood sources from other Chu tributaries except for the Chon Kemin River, which has a large enough catchment to produce major outburst floods.

3.3.6 Channel steepness

We surmise that catastrophic outburst floods through the Boam Gorge would be erosive enough to undercut the mouths of small, steep tributary channels, thus forming hanging valleys. To test this idea, we extracted an index of normalised channel steepness (ksn) from digital topographic data from the Shuttle Radar Topography Mission (SRTM) at 90-m resolution with the Stream Profiler tool (`http://www.geomorphtools.org/`; Wobus et al. (2006)) in ArcGIS and MATLAB. We analysed the river network automatically using a 1-km smoothing window and 20-m contour intervals, with a reference concavity of 0.45.

3.4 Results

3.4.1 Boulder provenance

The boulders at the outlet of Boam gorge are mostly granites, granodiorites, gneisses, and conglomerates. This composition differs from the locally outcropping rocks, leaving instead only the Boam gorge, the Chon Kemin valley, or the Kok Moinok basin as possible sources. The Chon Kemin valley in particular could have delivered the gneissic boulders on the lowest terrace T_1. Granodiorites are absent in the Boam gorge, whereas granitic and conglomeratic boulders could have come from anywhere in the western Issyk Kul

area (Figure 3.4D, Figure 3.4E).

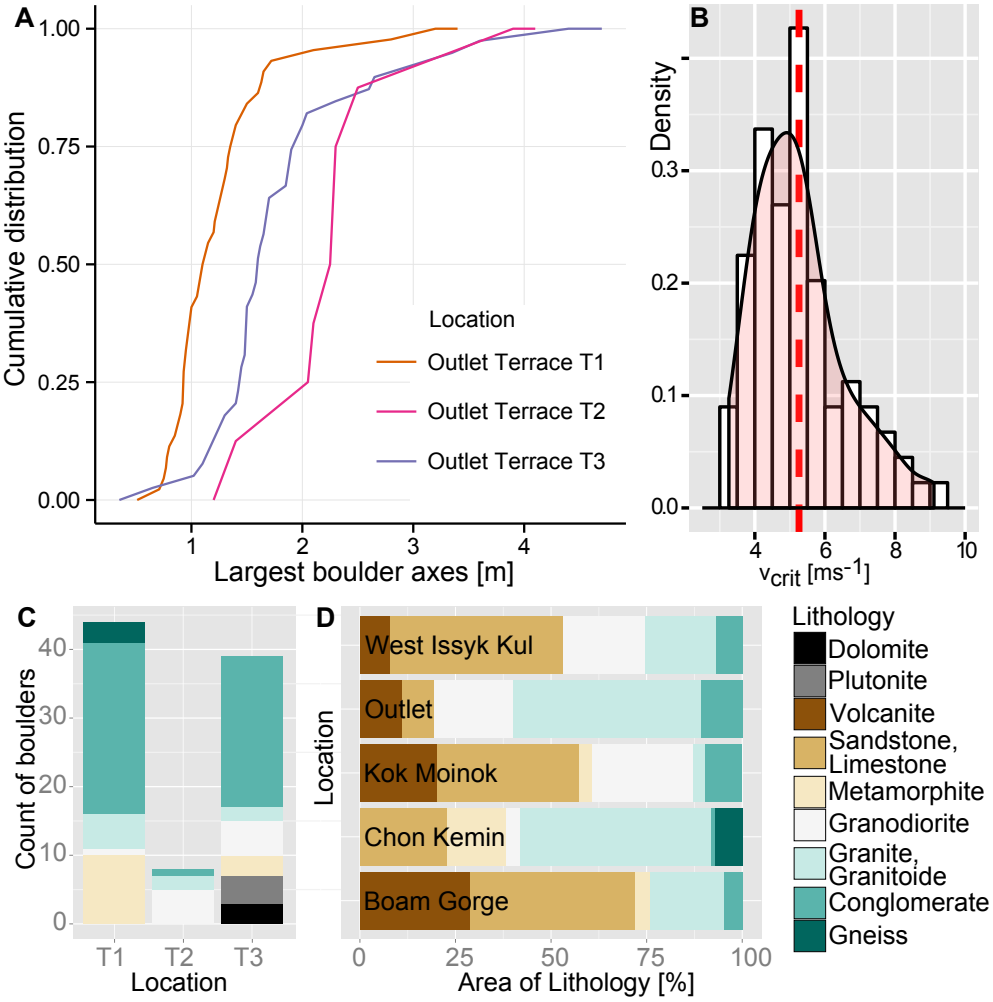

Figure 3.4: Cumulative distribution of the largest boulder axes on the different terrace levels (T_1 = lower terrace, T_2 = upper terrace, T_3 = higher level on upper terrace) at the outlet (A) and density estimate of the critical velocity vcrit of their incipient motion (density units are reciprocals of vcrit) (B). Composition of lithologies of the outlet terraces (C) compared with local bedrock classes (D).

3.4.2 Palaeoflood modelling

Any former blockage near the Chu River's major knickpoint between Kok Moinok basin and Boam gorge must have been 130 m and 150 m high at least, if its impoundment were to link up with the Issyk Kul highstands at

1640 m and 1660 m asl, respectively. Sudden lake-level drops from these positions would have released water volumes of up to 144 km^3 and 296 km^3, respectively, exceeding the critical flow velocity of ∼9 m s^{-1} to move the largest boulders at the gorge outlet, irrespective of whether the dam was earthen or glacial (Figure S9). These Issyk Kul outburst scenarios entail peak discharges of the order of 10^6 to 10^7 m^3 s^{-1} at the gorge outlet (Figure 3.5). However, the Kok Moinok basin could have stored water volumes of up to

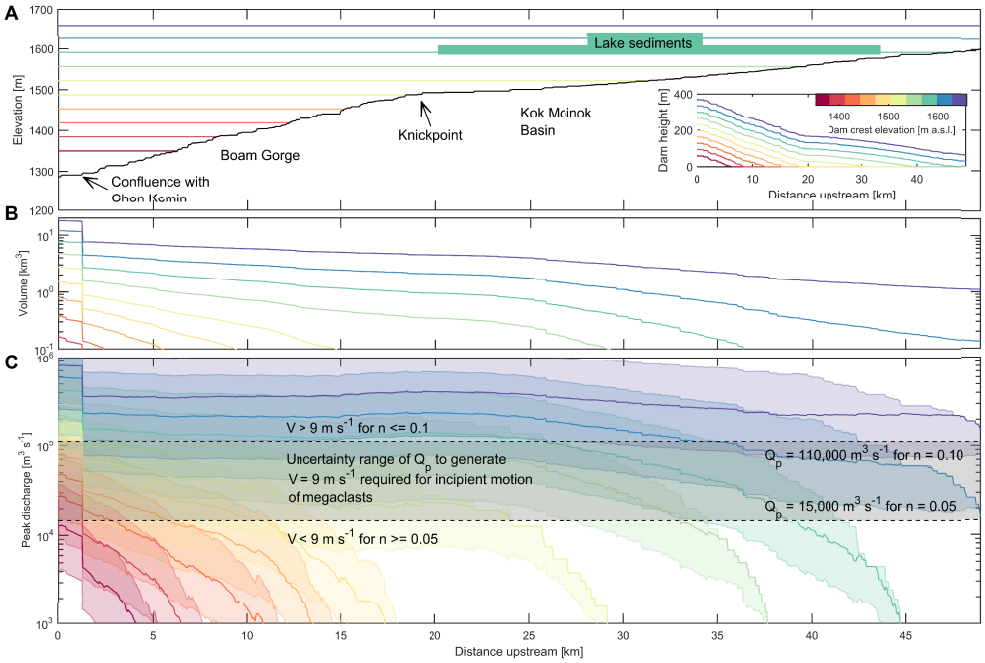

Figure 3.5: Modelled outburst flood scenarios from the outlet of Boam Gorge (0 km) to the Kutemaldinsky Threshold and Kok Moinok basin (∼50 km upstream). (A) River longitudinal profile and assumed dam-crest elevations. Inset shows these dam heights relative to the river bed. (B) Potentially impounded water volumes; the sharp increase of volumes near the outlet arises from additional backflooding of the Chon Kemin valley. (C) Peak dis- charge derived from the model by Walder and O'Connor (1997) as a function of water volume, dam height and breach rate. Solid, coloured lines are for a breach rate of 33 mh^{-1}; shaded areas derived for breach rates varying between 10 and 100 mh^{-1}. Peak discharges capable of moving megaclasts to the outlet require dams >150 m high anywhere in the gorge.

∼1.8 km^3 without being connected to Issyk Kul. Our computations also show that only earthen (but not glacial) dams between the Boam gorge outlet and the Kutemaldinsky Threshold could have impounded isolated and large enough lakes to produce peak discharges of up to 10^6 m^3 s^{-1} upon catastrophic

failure, well above the 10^4–10^5 m^3 s^{-1} needed to entrain and deposit the boulders on the foreland fan (Figure 3.5, S9).

3.4.3 Cosmogenic exposure ages

Depth-profile modelling of the outlet terraces gives Late Pleistocene to Holocene ages of T_3 to T_1 in stratigraphic order (Table 3.1 and Figure S10), and we report most likely ages following the Monte Carlo method by Hidy et al. (2010) (Table S11). T_3 has a ^{10}Be exposure age of ∼66 ka. The underlying terrace T_2 has a ^{10}Be age of 18.6 ± 4.5 ka, and the three embedded boulders have ^{10}Be and ^{26}Al exposure ages of 20.5 ± 1.9 to 18.6 ± 8.3 ka, roughly consistent with the timing of the youngest Pleistocene highstands of Issyk Kul (Figure 3.6). The uncertainty of the measurements allows no distinction between the ages of terrace T_2 and the boulders. ^{10}Be concentrations in the lowest terrace T_1 have little variance. We assumed two depositional phases (Figure S10) resulting in ages of ∼6 ka and ∼11 ka. A depth profile in delta deposits at the northern Issyk Kul coast yields an exposure age of ∼22 ka, which is consistent with previous dates of the former shoreline at 1620 m asl (Table 3.3).

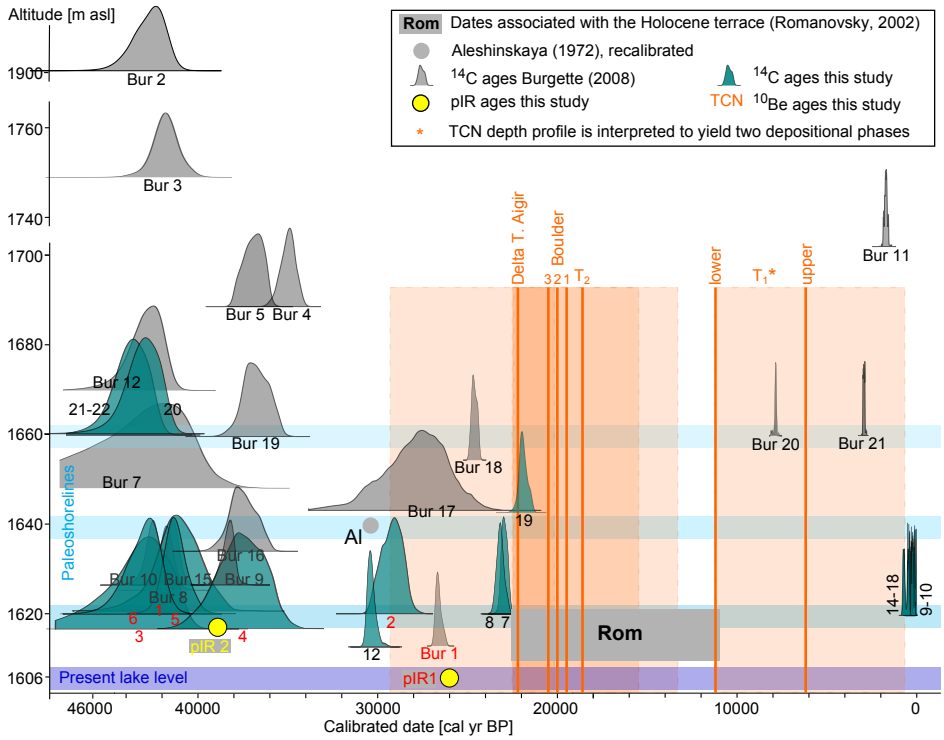

Figure 3.6: Probability densities of calibrated radiocarbon ages with respect to their sampling elevations (bottom line of distribution). PIR ages of flu- vial deposits (pIR 1) sampled below lake sediments and delta deposits (pIR 2) are highlighted in yellow. Terrestrial cosmogenic nuclide (TCN) results (dark orange verticals) are shown with external uncertainties (light orange boxes). Present-day and palaeo-lake levels are highlighted in dark and light blue, respectively. Age-elevation relations of data cited by Romanovsky (2002) are approximate only. Samples west of the Kutemaldinsky Threshold are highlighted in red. Note that 14C and pIR represent sedimentation ages, while TCN dates are exposure ages postdating sedimentation.

Table 3.3: Radiocarbon sampling locations and dating results.

Altitude [m asl]	**Abbreviation****	**Name**	**Material**	**Lithology#**	**Height [m]§**	**Latitude [°N]**	**Longitude [°E]**	**Radiocarbon age [yr B.P.]**	**Error [yr]**	**Calibrated age [yr B.P.]**	1μ **[yr]**
1613	Bur14	RBTG0805-5	charcoal	sl, fs-ms	-4.7	42.158	76.933	325	30	388	48
1614	12	180512-2-1	bivalve shell	sl, fs, lam		42.251	76.747	26550	270	30751	236
1614	13	180512-2-2	bivalve shell	c		42.251	76.747	>45000		> 45000	
1614	14	180512-3a	bivalve shell	sl		42.251	76.747	695	30	643	39
1614	15	180512-3b	plant	sl		42.251	76.747	140	30	145	82
1616	Bur1	RWKM082704-S	bivalve shell		-10	42.486	75.870	22710	100	27053	173
1616	Bur13	RBTG0805-1	charcoal	sl, fs-ms	-1.5	42.155	76.933	209	30	181	94
1617	3	140512-2-1	bivalve shell	sl, thin g layers		42.447	76.055	41400	1700	45469	1649
1617	4	140512-2-2	bivalve shell	sl, thin g layers		42.447	76.055	33800	1100	38268	1315
1620	5	140512-2A	bivalve shell	sl, thin g layers	-3	42.447	76.055	36900	1400	41462	1323
1620	16	180512-3A	bivalve shell	sl	-2	42.251	76.747	645	30	609	36
1620	Var5	Various5		sl				1190	160	1107	155
1620	Var6	Various6		sl				1400	120	1316	127
1621	1	090512-1-1	bivalve shell	c, thin fs and sl layers	-1.5	42.455	76.039	37300	800	41723	646
1621	2	090512-1-2	bivalve shell	c, thin fs and sl layers	-1.5	42.455	76.039	37300	800	29605	570

Continued on next page

Table 3.3 – *Continued from previous page*

Altitude [m asl]	**Abbreviation****	**Name**	**Material**	**Lithology#**	**Height [m]§**	**Latitude [°N]**	**Longitude [°E]**	**Radiocarbon age [yr B.P.]**	**Error [yr]**	**Calibrated age [yr B.P.]**	1μ **[yr]**
1621	6	140512-2B	bivalve shell	sl, thin g layers	-3	42.447	76.055	39000	1200	43262	1032
1621	9	120512-1-1	gastropod shell	sl, thin g layers		42.364	76.201	190	30	166	91
1621	10	120512-1-2	gastropod shell	sl, thin g layers		42.364	76.201	290	30	370	53
1621	17	180512-3B	bivalve shell	sl	-2	42.251	76.747	1150	60	1077	75
1622	18	180512-3C	plant	sl	-2	42.251	76.747	140	30	145	82
1625	Bur8	RB70305.1	bivalve shell		-5	42.257	76.730	37710	470	42055	330
1628	Bur10	RB70305.3	bivalve shell		-13.9	42.239	76.775	38880	530	42852	403
1628	Bur15	RWPRI-7	bivalve shell	sl, fs-ms and g layers	-15.46	42.170	77.012	37560	540	41948	392
1628	Bur9	RB70305.2	bivalve shell		-5.9	42.239	76.775	34320	310	38873	348
1631	7	070512-3-2	bivalve shell	fs, sl, c, lam	-2	42.412	76.157	19390	100	23342	162
1631	8	070512-3-5	bivalve shell	fs, sl, c, lam	-2	42.412	76.157	19560	140	23561	201
1631	Bur7*	RBAT0824-V	ox. wood		-5	42.242	76.710	40500	2800	45165	2268
1635	Bur16	RBPRI-5	bivalve shell	sl, fs-ms and g layers	-12.58	42.169	77.012	33680	540	37964	720
1640	Al1	Aleshinskaya	plant detritus					26000		30319	165
1640	Var1	Various1						9950	200	11533	339

Continued on next page

Table 3.3 – *Continued from previous page*

Altitude [m asl]	**Abbreviation****	**Name**	**Material**	**Lithology#**	**Height [m]§**	**Latitude [°N]**	**Longitude [°E]**	**Radiocarbon age [yr B.P.]**	**Error [yr]**	**Calibrated age [yr B.P.]**	**1μ [yr]**
1640	Var2	Various2						13540	400	16363	586
1640	Var3	Various3						16500	700	20071	857
1640	Var4	Various4						18600	400	22502	476
1643	19	081012-2-2	gastropod shell	ms, sl, cs and g layers		42.553	78.204	18470	150	22313	179
1645	Bur17	RWPRI-4	root	sl, fs-ms and g layers	-7.04	42.167	77.013	23070	1650	27828	1932
1654	Bur18	RWPRI-1	bivalve shell	sl, fs-ms and g layers	-1.2	42.167	77.015	20650	70	24869	174
1660	Bur19*	RBTAM-1	bivalve shell		0.2	42.149	77.527	33540	550	37801	718
1660	Bur20*	RBTAM-2	bivalve shell	2.5		42.149	77.527	7178	41	7996	42
1660	Bur21*	RBTAM-3	charcoal	3.9		42.149	77.527	2950	15	3112	32
1661	21	091012-1-2	gastropod shell	c, sl			42.682	78.352	40800	1100	44558	1028
1661	22	091012-1-2	gastropod shell	c, sl			42.682	78.352	40700	1100	44477	1018
1662	20	091012-1-1	gastropod shell	c, sl	-3		42.682	78.352	40000	1100	43947	958
1665	11	120512-5	gastropod shell	c, sl			42.307	76.436	123.92	1.48	post bomb, recent	
1670	Bur12*	RBTG092804	charcoal		-16	42.166	76.920	39850	1430	44067	1333
1689	Bur6*	RBAT091404-1	charcoal		-10.7	42.213	76.694	>43200	46330	207	
1690	Bur4*	RBAT0912-2	charcoal		2.5	42.209	76.694	30960	420	34939	418
1690	Bur5*	RBAT91604-1	charcoal		2.6	42.209	76.694	33030	360	37244	543

Continued on next page

Table 3.3 – *Continued from previous page*

Altitude [m asl]	**Abbreviation****	**Name**	**Material**	**Lithology#**	**Height [m]§**	**Latitude [°N]**	**Longitude [°E]**	**Radiocarbon age [yr B.P.]**	**Error [yr]**	**Calibrated age [yr B.P.]**	1μ **[yr]**
1716	Bur11*	RBTG091604	charcoal		1.8	42.162	76.906	1955	40	1906	46
1759	Bur3*	RBAT0906-1	bivalve shell		0.2	42.205	76.681	37640	930	42021	757
1905	Bur2*	RBAT0906-2	bivalve shell		0.2	42.105	76.681	39300	1100	43435	929

**Code 1–22 refers to samples of this study, code Bur1–21 to Burgette (2008), Al1 to Aleshinskaya et al. (1971), and Var1–6 to various studies cited in Romanovsky (2002).

Most samples are from lake beds, those marked by an asterisk are from river terraces.

#Abbreviations: fs (fine sand), ms (medium sand), cs (coarse sand), c (clay), sl (silt), g (gravel), lam (laminated).

§Height above top of gravel for river terraces, and height below top of lake beds (negative heights).

3.4.4 Radiocarbon, IRSL, and pIR ages

Our calibrated radiocarbon ages of the lowest-lying lake sediments associated with prominent shorelines around Issyk Kul are between 45 and 22 cal ka BP (Table 3.3, Figure 3.6). We discarded reservoir effects given minor limestone outcrops in our study area, assuming that snails offer robust ages (Pigati et al., 2004). Although Ricketts et al. (2001) found that modern shells from Issyk Kul surface sediments had ages of 840 cal yr BP, and referred to a reservoir effect, we cannot assume this to have been constant over time. Two of our modern shell samples had much younger ages (∼170 to 370 cal yr BP, Table 3.3, Code 9-10), arguing against a significant reservoir effect. Our IRSL and pIR ages differ substantially (Table 3.4), likely because anomalous fading underestimates the IRSL ages (Buylaert et al., 2012). On the other hand, pIR ages may be overestimated in some fluvial environments (Lowick et al., 2012). The age of sample pIR 1 (26.6 ± 1.5 ka) fits well with radiocarbon dates from lake beds nearby (Bur 1, 27.1 ± 0.2 cal ka BP). The delta deposits of sample pIR 2 likely date the high-stand of Issyk Kul at 1620 m asl. The ∼19-ka large discrepancy between IRSL and pIR dates is unlikely due to fading only; rather, the pIR is overestimated due to partial bleaching of the signal prior to deposition. We expect the real deposition age to lie between the two age estimates.

Table 3.4: IRSL/ pIR sampling locations and dating results

Code	pIR1	pIR 2
Name	070913-2-2	250912-2-1 A
Latitude [°N]	42.47	42.653
Longitude [°E]	75.98	77.208
Depth [cm]	600	200
Elevation [m]	1605	1618
Grain size [µm]	200-250	100-125
W [%]	8 ± 4	8 ± 4
K [%]	2.7 ± 0.2	3.5 ± 0.4
Th [ppm]	11.8 ± 0.6	14.9 ± 0.9
U [ppm]	2.9 ± 0.3	3.0 ± 0.3
D [Gy ka-1]	4.7 ± 0.2	5.6 ± 0.3
De IRSL [Gy]	93.4 ± 3.8	111.9 ± 2.8
De pIR [Gy]	126.3 ± 2.5	228.7 ± 8.7
Age IRSL [ka]	19.7 ± 1.3	20.0 ± 1.3
Age pIR [ka]	26.6 ± 1.5	40.9 ± 2.9

3.5 Discussion

Geomorphic and sedimentary evidence west of Issyk Kul consistently indicates a larger lake, potentially sustained by local blockage, in the late Quaternary. Massive lake beds in the Kok Moinok basin west of Issyk Kul terminate abruptly at a pronounced knickpoint on the Chu River, where it drops from a broad aggraded valley floor into the narrow bedrock channel of Boam gorge. The gorge is extremely steep as indicated by the high ksn values (Figure 3.3) irrespective of whether we include the endorheic basin Issyk Kul in the gorge's catchment area or not. Together with tributary fluvial hanging valleys, the gorge thus appears to be in a transient state indicative of a recent gain in drainage area assuming no major, localized tectonic control. These massive lake beds are well below 1620 m asl, and geomorphic evidence of higher lake levels is elusive around Kok Moinok, with the exception of an isolated spot at 1650-1670 m (Figure 3.1C). Unfortunately, this spot was only observed on satellite data and not verified in the field. There is the possibility that high reflectance typical for lake sediments is actually of different origin. Instead, lacustrine marls in Kok Moinok either onlap fluvial and alluvial gravel and terrace surfaces (up to KM-T_3, Figure 3.1C) proximal to the potential dam site) or interfinger with fan gravels from tributaries. Terrace level KM-T_1 has bevelled the surface of the lake beds and thus postdates this phase of impoundment (Figure 3.1C).

Distinct abrasion platforms and cliffs mark the 1660-m shoreline south of Issyk Kul. This observation has two possible implications: First, the 1660-m lake highstand did not involve the Kok Moinok basin and Boam gorge, thus requiring a dam farther to the east. A candidate location is near the Kutemaldinsky Threshold, where the Chu flows through a narrow bed and where prograding alluvial fans could have coalesced to raise the lake level (Figure 3.1C and S2). Based on a mapping of (Selander et al. (2007): Figure 3.3), we correlate a large alluvial fan, which corresponds to KM-T_2, with an alluvial-terrace tread that Selander et al. (2012) dated to ~86 ka with cosmogenic ^{10}Be. Around that time the Chu River was flowing at ~1640 m. Several coalescing alluvial fans, now conspicuously toe-trimmed and aban-

doned in KM-T_3 might have blocked the drainage at 1660 m (Figure S2). To test this idea, we reconstructed the original fan surface based on dissected and toe-trimmed remnants that we mapped from digital elevation data and satellite images. Assuming that a former course of the Chu River had incised KM-T_3, we find that an extrapolated fan surface now stranded >50 m above the present channel would have been able to completely buried former channel courses. Compared to surface ages reported by Selander et al. (2012) from north of Issyk Kul, this fan would have aggraded before 86 ka, but probably after 126 ka ago, perhaps coinciding with major glacial advances in the northern and eastern Kyrgyz Tien Shan (Koppes et al., 2008). Alternatively, dissected Neogene pediments and Quaternary fan-delta deposits recording former eastward inflows into Issyk Kul could be remains of a former higher dam. Today, for example, an aggrading alluvial fan protruding into the modern floodplain nearly chokes the Chu River (Figure 3.1CI), so that during high sediment loads from tributaries the river might be temporarily blocked.

Second, the highest outcrops of the Kok Moinok lake beds (1620 m asl) might be remnants of a local isolated water body. In either case, the landforms and sediments marking former lakes above the Kutemaldinsky Threshold require at least one major blockage at the western tip of Issyk Kul, and most likely in the Boam gorge. Yet, clear footprints of such a barrier are elusive. A gradual, non-catastrophic lowering of these former highstands by seepage and evaporation (García-Castellanos, 2006) would have favoured preserving any former dam, so that its catastrophic removal during a lake-outburst flood seems more likely.

Our new dates consolidate previous work on Issyk Kul's late Quaternary history, while providing more constraints on potential dams at its western end. All our ages, regardless of dating method, largely corroborate published dates of former shorelines east of the Kutemaldinsky Threshold. To the west, lake beds near Kok Moinok are >10 m thick (Figure 3.2B, Figure S3I), for which (Burgette, 2008) reported a ^{14}C date of 27.1 ± 0.2 cal ka BP (Bur 1, Figure 3.6). Our pIR dating of fluvial sands directly below largely inorganic lake beds at 1605 m asl returned a similar age of 26.6 ± 1.5 ka (Ta-

ble 3.4). Conservatively assuming mean lake sedimentation rates of 0.3 mm yr^{-1} (De Batist et al., 2002), the impoundment could have lasted for ∼33 kyr, and at least ∼23 kyr of continuous sedimentation are recorded around Issyk Kul (Figure 3.6, Table 3.3). Smaller isolated lakes might fill in much faster, though, while rivers cutting into older lake sediments could be blocked episodically, thus likely creating multiple blocking and breaching phases (Figure S3 J–K). This is consistent with younger lake beds documenting a Holocene impoundment east of the Kutemaldinsky Threshold to levels as high as 1620 m asl, up to the present elevation of the sill (Figure 3.6). Also, larger gaps in the sedimentary record begin at ∼20 ka and overlap with a major lake-level fall to 1,500 m asl (Bowman et al., 2004a), well below the present lake surface, from 10 ka to 5 ka (De Batist et al., 2002). Shells from lake beds between ∼1,000 and 150 cal yr BP at 1620 m asl record a renewed highstand of Issyk Kul (Samples 9 and 10, Figure 3.6). Nonetheless, this synthesis of available age constraints only partly resolves individual lake highstands, mainly owing to the differing sampling environments (lake, delta, and river sediments, Table 3.2) and their differing elevations. Our oldest radiocarbon dates are also at the limit of the method's resolution, and we cannot exclude older ages. A tentative correlation of alluvial fans in Kok Moinok suggests that the upper highstand dates back to the early Late Pleistocene. Yet sediments and landforms tied to lower lake levels could have been reworked and overprinted by subsequent lake-level rise (Garcin et al., 2009) or wave erosion (Nelson, 2012). Active tectonic deformation may play another important role, as the Kok Moinok area has many NW-trending lineaments and active faults that displace Quaternary alluvial sediments (Figure 3.1C). Single segments, however, are not traceable for more than 5 km suggesting distributed shear in this area. It is intriguing that in contrast to the younger shoreline, only remnants of the 1660m-highstand are limited to a broken record from the south (Figure 3.1A). Subsequent to lake regressions, the lacustrine sediment might has been uplifted along the southern shore. Burgette (2008) suggests a growing crustal-scale active structure emanating from the Terskey range, which could be responsible for this uplift. In contrast, the northern slopes are steeper and dominated by deposition of glacial and fluvioglacial sediment

that potentially covers older lacustrine sediment (De Batist et al., 2002).

Evidence for lake highstands postdating 22 ka is limited. Instead, we find that a boulder-littered fan terrace formed at the Boam gorge outlet around this time. The sedimentology of this fan terrace is largely reminiscent of deposits of glacial lake outburst floods (Maizels, 1997), and its morphology strongly resembles that of an expansion bar downstream of a spillway in the Boam gorge, featuring channel fills, chute channels, and imbricated boulder lag. The ^{10}Be and ^{26}Al exposure ages of the boulders fall within the last glacial maximum (LGM). However, glaciers did not advance below 2,000 m asl during LGM Koppes et al. (2008); Narama et al. (2009): Table 3). In contrast, Grosswald et al. (1994) reported glacial deposits 10 km upstream of the Boam gorge in support of their glacier-dam theory, though without any absolute age control. The boulders that we dated are located at 1,300 m asl and show no glacial striations, making a glacial-drift origin unlikely. The polymict lithologies of the boulders on the Late Pleistocene Chu River fan-terrace T_2 exclude local sources such as rock falls or debris flows (Figure 3.4C,Figure 3.4D), while their size requires catastrophic transport by water flows of the order of 10^4–10^5 m^3 s^{-1} (Figure 3.5C). These peak discharges are well above the range of meteorological floods (Table S12): major spillway discharges of the Orto-Tokoy reservoir are 240 m^3 s^{-1} at a catchment area of 5,930 km^2 (Pelli, 2005). The catchment area upstream of the Chu and Chon Kemin confluence is 7,140 km^3. Even a linear increase of peak discharge with catchment area could not generate floods large enough to entrain the observed boulders. Indeed, the peak discharges from our modelled dam-breach scenarios are among some of the largest Quaternary floods worldwide, e.g. ranking about one order of magnitude below the Pleistocene ice-dam breach Missoula flood O'Connor and Beebee (2009); Figure 3.7). Our scenarios are in line with the hypothesis of one or several catastrophic outburst floods through the Boam gorge. Sedimentary structures in T_3 show rapid deposition of clast-supported pebbles to boulders without current structures as ripples or erosion features, indicating high-velocity, turbulent flow, possibly during older megafloods (Figure S3E).

Palaeoflood modelling shows that flood discharges large enough to en-

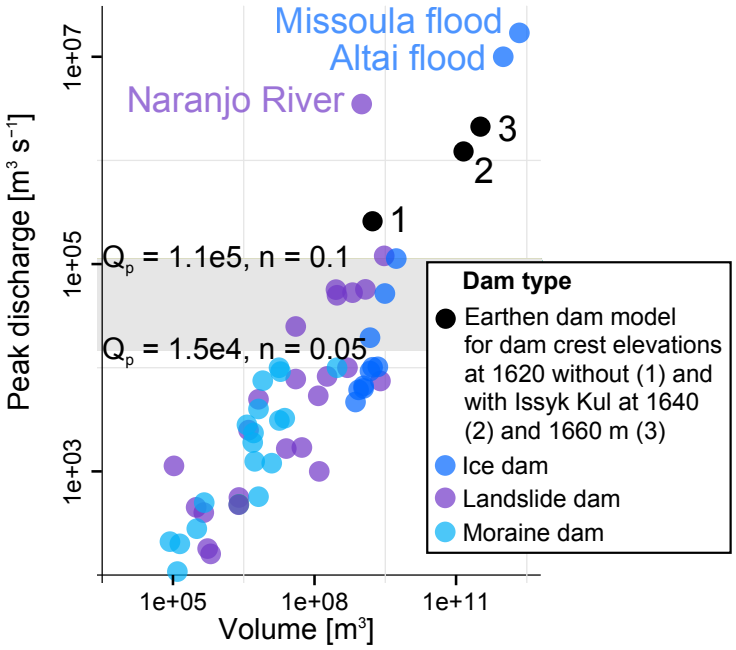

Figure 3.7: Peak discharge and flood volume of large Quaternary floods of different dam breach types (blue and purple dots, O'Connor and Beebee, 2009) compared with modelled outburst flood peaks from and nearby Issyk Kul (black dots). Q_p refers to peak discharges for the minimum and maximum values of Manning's (1904) n needed to entrain the boulders.

train the boulders could have come from lakes solely contained within Kok Moinok basin, and unconnected to Issyk Kul (Figure 3.5). Sudden drainage may significantly erode the lake and channel floors (Johnsen and Brennand, 2004), so that we might overestimate the total water volume released. In any case, the boulders at the outlet of Boam gorge are no conclusive evidence of Pleistocene catastrophic outbursts of Issyk Kul. Lake levels of Issyk Kul oscillated rapidly and up to 160 mm yr^{-1}; thus lake-level changes captured in the sedimentary record may record drivers other than catastrophic outbursts. Taking modern lake-level drop rates of >40 mm yr^{-1} as a reference, the lake level could have fallen within 450 or 900 yr without any sudden drainage. These time intervals are short enough to be contained in the measurement errors of the existing Pleistocene lake-level chronology (Figure 3.6). We conclude that the current sedimentary archives of past lake-level changes may easily mask signals of past outburst floods, such that we cannot map directly

major lake-level drops to outburst floods of Issyk Kul.

3.6 Conclusions

Our study gives new insights into the late Quaternary history of Issyk Kul. Palaeoflood modelling reveals that peak discharges of 10^4–10^5 m^3 s^{-1} are necessary to entrain and transport dozens of exotic boulders that were deposited at 20.5–18.5 ka below the exit of the Boam gorge, a proposed former drainage route for the lake's Pleistocene highstands. Meteorological floods are insufficient to move these boulders, such that we infer one or several catastrophic floods through the Boam gorge in the late Pleistocene. The exposure ages of these boulders and of delta sediments at the northern Issyk Kul shore postdate last Pleistocene lake highstands inferred from previous and our new ^{14}C data. Together with our pIR data they are consistent with one or several lake levels reported earlier. This temporal succession of lake-level drop and boulder deposition supports a link between both. Palaeoflood modelling, however, shows that catastrophic lake outbursts in the Boam gorge or the Kok Moinok basin unconnected to Issyk Kul could have also produced the necessary peak discharges for moving the boulders at the gorge exit. Although the overall geomorphic and sedimentary evidence around Issyk Kul records some of the largest ($\gg 10^4$ m^3 s^{-1}) catastrophic outburst floods in the Tien Shan mountains, if not Central Asia, direct links to documented lake-level changes of Issyk Kul remain elusive. Similar constraints may apply to deciphering catastrophic outburst floods from other large Quaternary lakes, such as those in the Siberian Altai (Herget, 2005) or former Lake Missoula in the Channelled Scablands (Baker, 1973). Our findings might also motivate research on megafloods towards also considering sequences of smaller events instead of focusing solely on the idea of few large events (Larsen and Lamb, 2016). The setting at Issyk Kul is particularly instructive in this regard, because even the worst-case scenario would have involved the catastrophic release of only a fraction of the total lake volume, while alternative plausible sources of outburst floods along the former flood route call for more flexible

palaeoflood analyses.

Acknowledgements

Funded by the German Ministry for Education and Research (BMBF TIP-TIMON contract no. 03G0809), the Potsdam Research Cluster for Georisk Analysis (PROGRESS), and the German Research Foundation (DFG, LA 3078/1-1). We thank the Volkswagen Foundation for funding our collaboration with A. Dzhumabaeva (contract no. 86 860). K. Abdrakhmatov kindly organised our field support. Thanks to S. Tofelde, P. Thöle, L. Pollozek, D. Käter, E. Rhode, J. Artel, D. Kauschus, H. Wilborn, and M. Lüdicke, who helped prepare samples for cosmogenic nuclide dating, and A. Musiol for ICP measurements. Luminescence measurements at the Department of Physical Geography and Quaternary Geology, Stockholm University, were kindly supported by S. Bjursäter, N. Gribenski, and J. Wolff. Gamma spectrometric measurements were done by S. Szidat, Department of Chemistry and Biochemistry, University of Berne. We used the free R software environment (https://cran.r-project.org/) for some of the data processing. SPOT satellite imagery has been made available to us via the ISIS-CNES program. SPOT 5 satellite data have been provided by ASTRIUM via the ISIS program (ISIS 732)

Supplementary material

Supplementary material can be found in Appendix B.

Chapter 4

Discussion

4.1 Rock-glacier activity

In the following discussion I revisit, in the light of the previous three studies (and core chapters of this thesis), the main research questions that I introduced earlier.

> **Q1:** *Is the resolution from lichenometric dating high enough to distinguish with confidence between ages of rock glaciers and their lobes?*

In my introductory notes, I emphasised in Chapter 1 the difficulties that arise from the lichenometric dating method and the benefits of the Bayesian statistic approach that we chose to capture some of these uncertainties objectively and in the light of limited data. The largest errors attached to the method arise both for the youngest and the oldest ages. Ages from young lichens are difficult to determine particularly, as lichens need time to get stabilised on a rock surface before they are visible, at least in my study area. Other work, however, supports that this colonisation phase depends on lichen species and microclimate. To this end, for example, Bull et al. (1998) developed a mathematical approach to approach the colonisation phase. They determined colonisation ages of up to 30 years, where they found that lichen colonies are stabilized (Figure 4.1). Direct studies, where aerial photography has been used to bracket the earliest time of lichen colonisation, showed

much shorter colonisation times between eight and ten years (Andres et al., 2015). Here most of the discrepancy likely results from the different methods used. While Bull et al. (1998) seek to find the minimum age of the colony establishment, the method used by Andres et al. (2015) aims to find the age of the first colonisers.

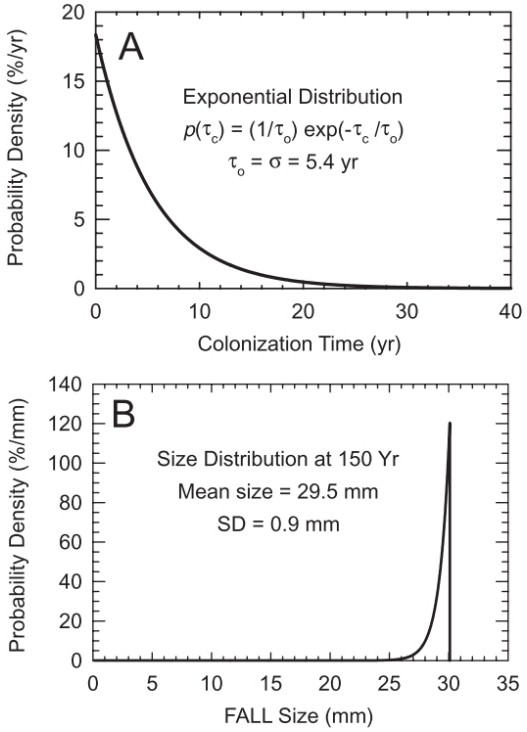

Figure 4.1: Distribution for lichen colonisation time. A. Predicted distribution for arrival times of the first lichen. B. Distribution of lichen sizes after 150 years, assuming that the only variation is in colonisation time. Figures from Bull et al. (1998).

The main difficulties with older ages arise 1) from the low number of specimens that have survived, and 2) when the largest lichens, which represent the age of the surface, might not be found or 3) when the largest lichen might be inherited from the rock's original surface, and thus represents an older surface. Because of the low number of older specimens, the determination of growth rates also becomes more imprecise towards older individuals, i.e. those centennial ages that we are potentially most interested in when trying to unravel long-term deformation and advance rates of rock glaciers. Different lichen species have their own specific and favourite conditions. Therefore,

colonisation of different species, or only one species occurring, may mostly reflect rather specific site conditions. For example, Figure 4.2 shows that a) lichen species in the study area tend to be more abundant in lower elevations, and b) different species dominate at different elevations. Other microclimatic effects, which are correlated with elevation, might also strongly affect lichen growth and could have been underrepresented when evaluating ages derived from lichenometric dating. For example, snow cover can limit lichen growth or even kill lichens under specific circumstances, including moisturised lichens and cold winds (Benedict, 1990a,b). Neglecting such and other biological aspects has been criticised, and some scientist have worked to understand these influences on lichen growth and mortality better (Armstrong, 2011).

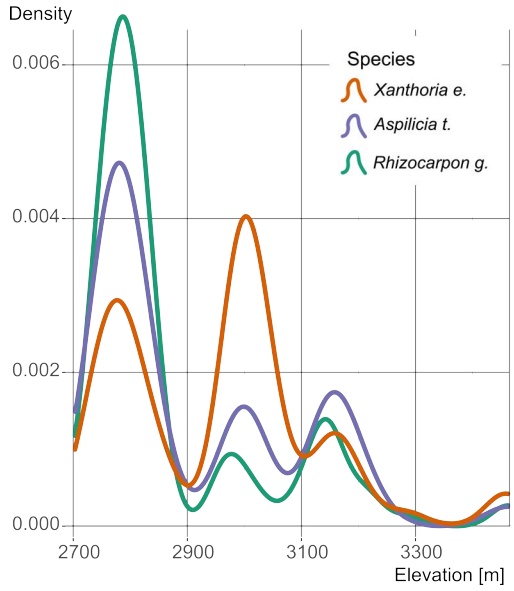

Figure 4.2: Elevation distribution of *Xanthoria elegans*, *Aspilicia tianshanica*, and *Rhizocarpon geographicum* from our study area in the northern Tien Shan. Density plot of the abundance of lichen species over elevation at all visited rock-glacier sites. Note that lichens were measured at specific elevations mostly dictated by the positions of selected rock-glacier lobes.

Furthermore, lichen growth varies with temperature and humidity (Matthews and Trenbirth, 2011). Taking the biological background and climatic influences on lichen growth into account is therefore inevitable if we wish to make lichenometry more accurate and representative of the myriad local site

conditions. Local "reference lichens" of known age matching the conditions of the object of interest are also necessary, if not essential, to give reasonable growth curves. Dated rock surfaces containing a lichen population of at least some tens of intact lichen specimens are not always easy to find, especially in some of the more remote mountain valleys of the northern Tien Shan. Only very few rock-fall deposits of known age and several cemeteries provided a basic amount of local lichen specimens for the growth curve determination in Chapter 1 (Figure 4.3). Some of the different methods for the application of lichenometry coexist, whereas others contradict each other. The traditional use of the largest lichen diameter to represent the oldest lichen, and thus minimum age, of the exposed rock surface has been found to be disadvantageous by some practitioners as there is always the probability of not finding these representative lichens. Size-frequency methods were established to avoid this error, given that abnormally large lichens can be identified (Innes, 1985). Bayesian statistic models fed with probabilistic distributions, e.g. lichen diameter vs. age data, offers updates on these distributions conditioned on the data at hand as a result. Taking the data scarcity into account, we also used bootstrapping with multiple calculation circles using randomly selected training samples to get a better grip on the variability of the growth curves. Even with scarce data, this method is useful to provide results with estimated error propagation.

Figure 4.3: Lichen measurements on dated gravestones for growth-curve calibration in northern Kyrgyzstan.

While many studies favour one lichen species for their study, the abundance of different species in my study area made it reasonable to test them

in combination. Thereby each species tells a different story. The dating resolution of lichenometry depends on the lichen species. In Chapter 1 I showed that some fast growing species (*Xanthoria elegans*) are more suited to resolve surface ages <200 years, and some slow growing species (e.g. *Aspilicia tianshanica*, *Rhizocarpon geographicum*) still exist to allow estimating the exposure ages of older rock surfaces. My general conclusion about applying lichenometry to rock glaciers is that the method is unable to date absolutely, but offers relative age differences between rock glaciers and single rock-glacier lobes. This view of lichens being more suitable for relative age dating has been recently supported by other authors (Decaulne, 2016). Despite its many applications and its long history, the method is still developing. Recently approaches restricted themselves to measure only small lichens, which are not biased towards the larger or largest lichens, which may not always be detected at a given site (Heindel et al., 2017).

One reason of concern in the mountainous regions of Central Asia is the hazard of earthquakes. It was stressed that earthquakes may also have an effect on rock-glacier advance (Bolch and Gorbunov, 2014). One working hypothesis I started off with was that the age of earthquake-derived debris stored on rock-glacier surfaces could be tracked with lichenometry. I measured thousands of lichen diameters on 37 lobes of six different rock glaciers. Using lichenometry as relative dating method and not as absolute age dating tool avoids the errors arising from varying methodological approaches and their respective problems. Used as a relative dating method on a regional basis as presented in Chapter 1, lichenometric dating remains difficult for comparing derived ages with other established chronologies, but is useful for interpreting local patterns of lichen growth. Rock glaciers respond on changing environmental conditions following long term regional trends, but their behaviour on a short and local scale has been found to be much more variable (Sorg et al., 2015). Therefore lichenometry used as relative method gives a detailed comparison of neighbouring rock glacier or rock-glacier lobe exposure, as presented in Chapter 1. Yet such local case studies remain important for documenting current and predicting future trends in rock-glacier dynamics for the next decades. Nevertheless as colonisation timing and growth

rate also depend on microclimatic conditions especially in cold environments (Golledge et al., 2010), relative age dating also inherits undefined errors.

In any case, my results show that movement and reactivation of these lobes is very localised and thus difficult to reconcile solely with regional climatic or seismic triggers. I conclude that the topographic location of rock glaciers cannot be used to infer to climatic conditions alone. This result is very important for permafrost research, since rock glaciers are widely used as proxies of the lowermost boundary of sporadic mountain permafrost (Janke, 2005). The local variability of rock-glacier response on climate change has been shown previously by isotherms generated from front temperature measurements of relict and active rock glaciers (Frauenfelder and Kääb, 2000). As monitoring becomes more easy and accessible to a larger community through high-resolution satellite images, fieldwork is still necessary to validate such research, even if only locally. One important lesson I learned during the fieldwork is that rock glaciers, which have large vegetated parts, and might appear relict in a satellite image, can still have highly active parts. We discovered, for example, a trekking route along the edge of one rock glacier, which had been buried by part of the advancing rock-glacier mass recently.

4.2 Rock glaciers as natural dams

Former studies (Bolch and Gorbunov, 2014), and my field- and remote-sensing mapping investigations in the northern Tien Shan pointed out that some rock glaciers advanced down to the point where they disturbed the river flow, diverting its course or even impounding small lakes (Figure 2. Rock glaciers influence the hydrology in mountain regions (Hewitt, 2014), but to which degree has not been quantified in detail as yet. In the context of climate warming and decaying permafrost, the occurrence of river-damming rock glaciers may become a new, though still poorly understood, hazard, possibly culminating in dam breaching and downstream flooding. Bolch and Gorbunov (2014) noted that low-lying rock glaciers are more of an exception in a specific area; in fact some of the rock glaciers lie very low compared to

other rock glaciers in their direct vicinity. This discrepancy should not be expected if their elevations were only dependent on climatic parameters. For example, Figure 4.4 shows the elevation distribution of rock-glacier toes and highlights that active rock glaciers have their highest elevation density (3400 m asl), so roughly 400 m above inactive rock glaciers (3000 m asl); many examples of both activity states of rock glaciers seem to deviate from the regional sporadic permafrost boundary. Rock glaciers appear shortly below the snowline. This has been seen in other regions of the world and underlines this curious topographic niche that rock glaciers seem to occupy. Whereas ice glaciers develop in environments where snow accumulation exceeds talus input, rock glaciers rely on a large amount of talus to develop. These topoclimatic conditions that rock glaciers favour have been described for Greenland (Humlum, 1998) and the Andes (Brenning and Trombotto Liaudat, 2006).

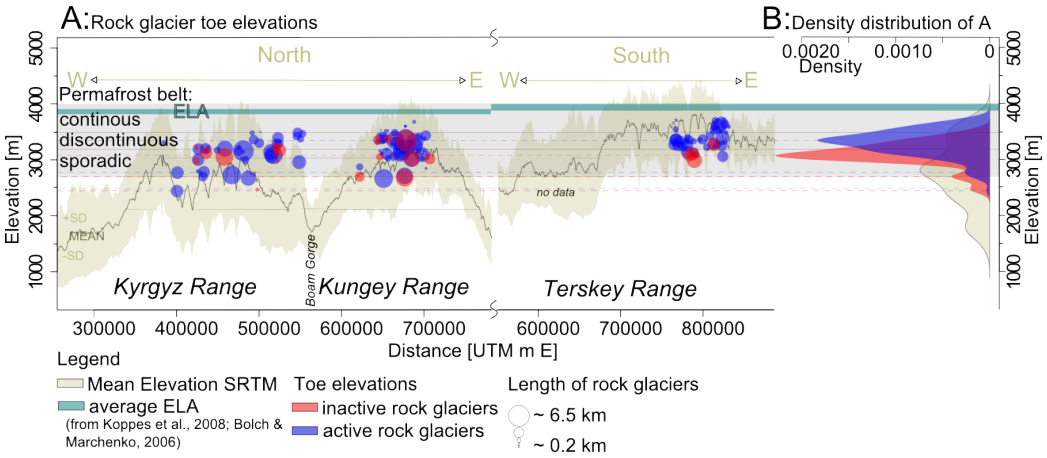

Figure 4.4: Some rock glaciers lie low. A: Rock-glacier toe elevation of inactive (red dots) and active rock glaciers (blue dots); dots are scaled by the length of the rock glaciers. Mean STRM elevation (beige), permafrost elevation (grey belts), and ELA (equilibrium line altitude, i.e. the point where snow accumulation and depletion are equal; turquoise belts) are shown for the northern Tien Shan mountains, i.e. the Kyrgyz, Kungey, and Terskey ranges. B: Density distribution of rock-glacier elevations.

Several factors promote rock-glacier advance (e.g. slope, solar radiation, vicinity to earthquakes). As shown in other studies (Bolch and Gorbunov, 2014), and in Chapter 1, climatic and seismic factors cannot explain the unusual or "outlier" topographic location of some rock glaciers alone. To answer the central question of Chapter 2:

Q2: *Which parameters are more likely to lead to the ability of rock glaciers to dam rivers?*

we examined how 69 different climatic and topographic parameters were likely influencing factors of rock-glacier damming. From Bayesian logistic regression we derived correlations between catchment area and rock-glacier length, and an increasing likelihood of river-damming with lower elevations of the rock glaciers. The elevation in the latter correlation might thereby be exchangeable with mean annual temperature and potential incoming solar radiation, as these values were strongly correlated, mainly because of topographic interpolation of few climate station data in sparsely populated mountain terrain. Another source of error includes the origin of the lakes. Satellite images do not yield information about the timing of the lake formation. So it may be possible that in some cases the rock glacier had merely advanced over an existing dam and partly into an already existing lake, dammed by a landslide, moraine, or fan. Analyses of time series of satellite images and air photos, together with geomorphometric analyses of the valley floor might help to constrain the age and formative processes of some lakes, although we found this to be largely intractable in our study area, even for only several dozens of water bodies currently associated with rock glaciers. We compiled our rock-glacier inventory aiming to include only active examples. Information about the activity status came solely from visual inspection of local slope, vegetation, and the state of surface erosion. The identification (or subjective classification) of a rock glacier as active, inactive, or relict from satellite images always bears some error of misinterpretation. More accurate and higher resolved data might be one way to constrain these errors. For example, airborne laser scanning was successfully used to determine the activity status in measuring thickness changes and displacement of rock glaciers (Bollmann et al., 2015). The authors determined an index of the activity status and compared their results to a regional rock-glacier inventory. They found that 77% of the active rock glaciers had been classified correctly using their index. I therefore must assume that the rock-glacier inventory presented in Chapter 2 also bears an unknown uncertainty concerning a misinterpretation of

the activity status. The error largely arises from the visual decision making process of determining the activity status from satellite images. Without any further constraints, I must assume that the error is in the same order as the error found by Bollmann et al. (2015), as the visual interpretation of steepness, vegetation cover, and state of erosion also reflects the parameters of activity, the thickness changes, and the displacement.

4.3 Natural dams in Central Asia

River damming and lake outbursts are common scenarios in high mountain landscape, especially in active orogens with seismic activity, such as the northern Tien Shan. To gain insight into the lake outburst history of the study area, I focused on one famous example of possible lake outbursts in prehistoric times. The lake Issyk Kul shows evidence of pronounced lake level changes probably resulting from multiple damming and outburst events. Boulders of diameters of up to 4 m are deposited at the end of the spillway of the potential flood, i.e., the outlet of the Boam gorge. In order to find a link between outburst flood and lake level changes, I aimed to answer the question:

> **Q3:** *Do ages of deposited rocks indicate one or more flood events, and are these connected to lake level drops?*

In my third core chapter exposition ages of boulder at the Boam gorge outlet and delta deposits in vicinity of today's Boam gorge were dated using cosmogenic ^{10}Be and IRSL. Boulders turned out to have younger ages (20.5–18.5 ka) than lake-level highstands (45–22 ka). This succession in time of declining lake-level and deposition of large boulders downstream of the Boam gorge is an evidence of a possible linkage between these processes. These ages fall into the last glacial maximum, similar to ages Herget (2005) modelled for the Altai floods in Siberia (13–40 ka), and the formation of other large scale glacier-dammed lakes in Eurasia (Mangerud et al., 2004). Yet the latter two studies were concerned with flood magnitudes that were likely a few orders of magnitude larger than those we propose for the western edge of Issky Kul.

Modelled drainage velocities for a potential Issyk Kul outburst flood, as presented in Chapter 3, of $>10^4$ m^3 s^{-1} are necessary for moving the inspected boulders, and thus exceed the regional meteorological floodplain and point to catastrophic lake outbursts. The study also shows that an outburst of a smaller lake, separated and downstream of Issyk Kul, would have been able to reach this transportation force. Hence a direct link to lake-level fluctuations and catastrophic outburst floods along a western pathway remains elusive. In either case the outbursts would have been among the larger, if not largest, documented floods in Central Asia. This is interesting in the light of other studies, which tend to focus on, and perhaps over-emphasise, megafloods instead of smaller floods, which might also have long-lasting effects on rivers and their surrounding landscape (Larsen and Lamb, 2016). The geomorphic inheritance of prehistoric megafloods (Baker, 1973; Herget, 2005) has long been invoked for a better need to understand landscape evolution and for future hazard assessment. I echo this view, and our study around Issyk Kul demonstrates the many potential pitfalls when trying to reconstruct and reconcile different facets of Quaternary landscape evolution such as lake and delta sediments, sediment age and provenance, former drainage paths, and outburst deposits in the context of catastrophic events. Combining palaeoflood modelling, dating of potential flood deposits and former lake sediments is necessary to evaluate a possible connection of lake-level changes and outburst floods. Further and more detailed analyses on the sedimentology in the Baom gorge might give further information on flood velocities

4.4 Future challenges

Several key challenges for future research emerged from my PhD thesis. These challenges are often multidisciplinary and veer off into different and often young research directions, some of which have merely been established yet. First, clearly more direct lichen growth measurements are needed to establish the abundance of growth curves worldwide. The large uncertainties that remain tied to the method make it difficult to comparing results between

studies. Independent verification or cross-dating with other methods seems a viable approach to validate lichenometric derived ages. The same could go for a dedicated study on the local environmental conditions that limit lichen growth in arid to semi-arid mountain ranges such as the northern Tien Shan.

Second, since rock-glacier movement is mostly between few centimeters to several meters per year, their probable connectivity to the river system should be relatively easy to monitor and predict. Nevertheless monitoring is necessary as rock-glacier activity is locally variable and depends on several climatic and geomorphic parameters. Monitoring via laser scanning, either airborne or terrestrial, can be used in combination with long-time series of satellite images to record patterns of movement and velocities over a long period; here standard techniques known from glacier monitoring may help. Short-term monitoring via photogrammetry is helpful to gain insights to their finer-scale activity. Dendrochronology is also a promising tool to track distinct zones of activity on a rock glacier, at best on annual to centennial scales. Rock glaciers have different response times to atmospheric warming than clear ice glaciers, and may thus store water in volumes that may become important in a future world of higher water stresses and demands. But still, it is unclear how rock glaciers respond in detail to atmospheric warming and what time delay can be expected. More research about inactive rock glaciers could help to find answers under which conditions rock glaciers became inactive. Similarly, a major line of research could follow the question whether earthquake-induced rock falls might contribute to nourish sediment supply to rock glaciers, and thereby change their activity status or advance rates. As Haeberli et al. (2006) pointed out: *"significant advance in understanding most periglacial phenomena requires the close integration of field and theoretical studies, and will greatly benefit from ideas and techniques in other disciplines within the geosciences and beyond."*

Third, rock-glacier dams or the influence of rock glaciers on the stream network needs to be quantified around the world to resolve their abundance. A comparison of different mountain regions with different morphological and climatic parameters will be needed to oppose and compare the key criteria sufficient and necessary for damming. Criteria that are relevant for clear

ice glaciers might also help to analyse rock glaciers. For example, Golledge et al. (2010) introduced the positive degree day (PDD) for analysing snow kill of lichens, as it represents the local "felt" temperature. The method, which is a statistical relationship between air temperature and snow melt, is applied to melt models for ice-sheets (Hubbard et al., 2009), but as rock-glaciers turned out to respond on their environment locally very different, the PDD may pose a valuable alternative to other temperature variables or proxies. Furthermore the areas downstream of rock glaciers need to be checked for evidence of historic rock-glacier lake outbursts. As for natural dams, also for rock-glacier dams, evidences of historic outburst floods will help to understand their hazard potential. Further research is also necessary to elucidate more the past potential of catastrophic outbursts from Issyk Kul. For example, field evidences for lake highstands or outburst floods in the tributaries of the Chu Rriver could be an important addition to the study presented in my third core chapter. After all, the lake is still prone to rapid lake-level changes so that learning from the past might inform us critically about future dynamics.

Chapter 5

Conclusions

Glaciers and permafrost related phenomena as rock-glaciers are threatened by atmospheric warming worldwide, and with them the water availability and food security, which is already the case in Asia and Central Asia (Immerzeel et al., 2010). After the break-up of the Soviet Union the different countries which are mutually depending on the resources of their neighbours (hydrocarbon, hydropower), are having political disputes with regards to managing and exchanging their resources (Malone, 2010). Furthermore science and politics need to meet rising challenges of related hazards as permafrost and glacier thawing to find solutions for risk mitigation, especially for densely populated areas. Basic research such as trying to date rock glaciers or to understand how they form and decay is surely bound for gaining more importance, as better access to water resources becomes necessary in a warming world. With my thesis I contributed to test the practicability and usage of lichenometry to date rock glaciers and their lobes. I found that lichenometry is useful as a relative dating method. It might be even more powerful, when linked to other dating methods such as dendrochronology, which cannot be applied in many of the subalpine to alpine settings that rock glaciers occupy. The temporal resolution of lichenometry depends on the lichen species. When available it is useful to measure different species, even though they might display different time spans. Different studies including the lichenometric method presented in this thesis found rock glaciers to be highly variable bodies in terms of

their activity. Osborn et al. (2015) criticised lichenometry after using it for decades due to methodological drawbacks. It is still a recommended method in glaciology, however (Garibotti and Villalba, 2017). The scarce information on directly measured lichen growth limits the use of lichenometry, as growth is highly dependent on microclimatic conditions. I recommended the technique for relative age information only. Bayesian statistics offers a smooth way to deal with less abundant lichen data for old lichen ages, which are of most interest as they provide information about the minimum exposure age, and gives a valuable error prediction. Furthermore, I could separate rock glaciers, which have a geomorphic influence on mountain rivers from those that have not, again by using Bayesian data analysis, this time in the form of a robust multiple logistic regression. In this context, I found that elevation, potential incoming solar radiation, and the size of rock glaciers and their feeder basins are credible predictors. Comparison with large landslide dams showed geometries similar to rock glacier dams. Finally, combined absolute age dating and palaeoflood analysis tentatively associated some lake level drops with outburst floods and records some of the largest ($\gg 10^4$ m^3 s^{-1}) catastrophic outburst floods in the Tien Shan mountains, specifically west of Issyk Kul. Yet direct links to documented lake-level changes of Earth's second largest mountain lake remain elusive. Palaeoflood back-calculations also showed that a smaller lake downstream of, and unconnected to, Issyk Kul could have produced floods strong enough to explain the transportation of what we interpret as outburst flood boulders in the foreland of the Tien Shan. This finding might also motivate research on megafloods to also consider sequences of smaller events instead of focusing solely on the idea of few large and catastrophic events. Similar constraints towards a focus on sequences of smaller events was proposed by Larsen and Lamb (2016) for the formation of the Channelled Scablands, and may apply to deciphering catastrophic outburst floods from other large Quaternary lakes, such as those in the Siberian Altai (Herget, 2005).

Appendix A

Supplementary material

Limits to lichenometry

Table S1. Posterior probability of the contrasts (or difference from the common mean) of lichen diameter and predicted ages (Figure 1.3). Rows contain comparisons between six rock glaciers (KT = Kugalan Tash, TA = Turgen Aksu, O = Ordzhonikidze, K = Karakorum, DK-N = Djassik Kul North, and DK-S = Djassik Kul South) in 15 possible pairs using all largest lichen for species X. elegans, A. tianshanica, and R. geographicum. Grey shades are credible contrasts for lichen diameter and ages, for which a zero contrast probability is outside the 95% highest density interval (HDI).

		Diameter					Predicted Age Median					Predicted Age Upper 95					Predicted Age Lower 95				
Species	Compared rock glacier pairs	Difference of means	HDI min	HDI max	Smaller Zero Prob [%]	Larger Zero Prob [%]	Difference of means	HDI min	HDI max	Smaller Zero Prob [%]	Larger Zero Prob [%]	Difference of means	HDI min	HDI max	Smaller Zero Prob [%]	Larger Zero Prob [%]	Difference of means	HDI min	HDI max	Smaller Zero Prob [%]	Larger Zero Prob [%]
Xanthoria elegans	KT vs. TA	16.5	7.29	25.9	0	100	20.7	1.82	38.90	1.2	98.8	31.7	-1.96	63.7	2.9	97.1	20.4	2.09	38	1.2	98.8
	KT vs. O	0.529	-8.14	6.97	56.1	43.9	-0.1	-14.2	14.30	50.5	49.5	-1.38	-26.8	24.4	54.4	45.6	0.52	-13	14.9	47	53
	KT vs. K	3.53	-4.05	10.7	17.5	82.5	4.7	-9.37	19.10	26.1	73.9	11	-14	37.1	19.9	80.1	5.03	-8.38	19.3	23.6	76.4
	KT vs. DK-N	13.4	-0.63	27.2	2.5	97.5	22.2	-3.51	50.20	4.6	95.4	33.2	-10.8	82.5	7.4	92.6	22.1	-2.94	48.9	4.1	95.9
	KT vs. DK-S	18.6	3.6	34.2	0.6	99.4	26.7	-2.14	56.50	2.9	97.1	37.1	-9.45	89.2	6.3	93.7	26.5	-1.79	55.1	2.6	97.4
	TA vs. O	-17.1	-25.8	-8.19	100	0	-20.8	-38.4	-2.97	99.0	1.0	-33.1	-63.4	0.77	97.9	2.1	-19.9	-36.5	-2.5	99	1
	TA vs. K	-11.5	-20.5	-2.9	99.5	0.5	-16.1	-32.4	0.70	97.3	2.7	-20.7	-50.6	7.37	91.8	8.2	-15.4	-30.9	0.89	97.2	2.8
	TA vs. DK-N	-2.49	-16.2	11.3	64.3	35.7	1.5	-23.4	28.20	47.1	52.9	1.49	-41.7	47.3	49.5	50.5	1.7	-22.4	27.5	46	54
	TA vs. DK-S	2.74	-12	17.4	36.5	63.5	6.0	-19.9	34.70	35.1	64.9	5.39	-39.2	53.9	43.3	56.7	6.13	-18.7	34.3	34.1	65.9
	O vs. K	4.18	-2.6	11.1	11.6	88.4	4.7	-8.57	17.90	24.4	75.6	12.4	-11.5	36.7	15.7	84.3	4.5	-8.08	17.6	24.7	75.3
	O vs. DK-N	14	0.74	28	1.8	98.2	22.2	-2.84	49.40	4.0	96.0	34.5	-8.69	83.1	6.1	93.9	21.6	-3.19	47.6	4.1	95.9
	O vs. DK-S	19.3	4.58	34.8	0.4	99.6	26.8	-1.04	56.50	2.5	97.5	38.4	-6.94	90.4	5	95	26	-1.62	54.1	2.6	97.4
	K vs. DK-N	9.72	-3.65	23.3	7.4	92.6	17.5	-6.85	44.60	8.5	91.5	22.1	-19.4	69.4	16.4	83.6	17.1	-6.3	43.5	8.4	91.6
	K vs. DK-S	14.9	0.537	30.2	1.9	98.1	22.1	-4.85	51.20	5.4	94.6	26	-18.1	75.6	13.6	86.4	21.5	-4.54	49.5	5.3	94.7
	DK-N vs. DK-S	5.22	-12	22.9	27.7	72.3	4.5	-25.9	37.10	39.1	60.9	3.9	-49.4	58.5	44.3	55.7	4.43	-25.3	35.6	39	61

Aspilicia tianshanica	KT vs. TA	-41.6	-51.6	-31.2	100	0	-59.9	-87.5	-31.1	100.0	0.0	-84.1	-145	-22.1	99.6	0.4	-45.5	-69.7	-21.5	100	0
	KT vs. O	-55.2	-64.3	-45.9	100	0	-86.3	-112	-61.2	100.0	0.0	-144	-199	-88.9	100	0	-64.7	-87.1	-42.9	100	0
	KT vs. K	-20.6	-31.7	-9.89	100	0	-30.9	-59.7	-2.17	98.2	1.8	-51.3	-115	10.4	94.7	5.3	-29	-54.2	-3.33	98.7	1.3
	KT vs. DK-N	-29.7	-48.1	-11.7	99.9	0.1	-35.8	-85.3	12.1	92.6	7.4	-37.5	-143	70.1	75.5	24.5	-29.5	-68.3	8.14	93.5	6.5
	KT vs. DK-S	-92.3	-110	-74.4	100	0	-192	-242	-143	100.0	0.0	-460	-567	-353	100	0	-141	-181	-102	100	0
	TA vs. O	-13.6	-22.5	-4.68	99.8	0.2	-26.4	-50.6	-2.26	98.4	1.6	-60.3	-114	-8.34	98.7	1.3	-19.2	-37.6	-0.63	97.9	2.1
	TA vs. K	21.1	10.4	31.7	0	100	29.0	1.06	57.2	2.1	97.9	32.8	-29.5	91.9	14.6	85.4	16.5	-5.99	39.3	7.7	92.3
	TA vs. DK-N	11.9	-6.29	29.8	9.9	90.1	24.1	-23.5	73.1	16.4	83.6	46.5	-56.7	154	19.4	80.6	15.9	-20.1	53.3	19.7	80.3
	TA vs. DK-S	-50.7	-68.2	-32.8	100	0	-133	-182	-84.9	100.0	0.0	-376	-480	-270	100	0	-95.4	-132	-57.5	100	0
	O vs. K	-34.7	25.1	44.3	0	100	55.4	30.6	80.7	0.0	100.0	93.1	38.9	147	0	100	35.7	15.8	56.7	0	100
	O vs. DK-N	25.5	8.22	43.2	0.2	99.8	50.5	3.78	97.3	1.7	98.3	107	8.11	212	1.9	98.1	35.2	-0.36	70.4	2.5	97.5
	O vs. DK-S	-37.1	-54.2	-20.1	100	0	-106	-153	-65	100.0	0.0	-316	-417	-215	100	0	-76.1	-112	-41.1	100	0
	K vs. DK-N	-9.2	-27.5	8.71	84	16	-4.9	-53.8	43.8	58.1	41.9	13.8	-91.4	120	40	60	-0.528	-38.1	37	51.2	48.8
	K vs. DK-S	-71.8	-90	-54	100	0	-162	-211	-113	100.0	0.0	-409	-513	-300	100	0	-112	-150	-73.4	100	0
	DK-N vs. DK-S	-62.6	-85.9	-39.5	100	0	-157	-222	-95.5	100.0	0.0	-423	-562	-286	100	0	-111	-159	-62.5	100	0
Rhizocarpon geographicum	KT vs. TA	-23.1	-33.8	-12	100	0	-125	-301	25.40	94.0	6.0	-152	-371	36.8	93	7	-97.2	-250	33	91.7	8.3
	KT vs. O	-28.5	-39.1	-17.8	100	0	-138	-309	14.50	96.2	3.8	-172	-386	22	95.8	4.2	-108	-259	21.7	94.4	5.6
	KT vs. K	-16	-27.9	-4.23	99.6	0.4	-49.3	-209	86.40	72.5	27.5	-71	-271	100	75.6	24.4	-37.5	-176	83.1	69.6	30.4
	KT vs. DK-N	-12.4	-28.5	3.41	93.9	6.1	-26.9	-227	160	61.8	38.2	-37.5	-285	192	63.2	36.8	-20.5	-194	142	60.7	39.3
	KT vs. DK-S	-23.5	-39	-8.33	99.9	0.1	-87.4	-289	78.9	82.7	17.3	-123	-377	88.7	85.2	14.8	-60.1	-231	84.3	77.3	22.7
	TA vs. O	-5.44	-11	0.149	97.2	0.28	-12.8	-102	74.0	61.6	38.4	-20.3	-130	89.5	64.5	35.5	-10.7	-90.8	65.3	61	39
	TA vs. K	4.69	-1.47	10.8	6.7	93.3	75.5	-15.8	170	5.6	94.4	81.2	-29.5	198	8.3	91.7	59.7	-19.6	145	7.8	92.2
	TA vs. DK-N	7.77	-5.58	21.8	13	87	97.8	-68.0	293	13.2	86.8	115	-86.8	361	14.8	85.2	76.7	-63	248	15.6	84.4
	TA vs. DK-S	-3.36	-14.2	7.48	73	27	37.4	-101	181	29.0	71.0	28.9	-140	210	36.2	63.8	37.1	-78.8	168	27	73
	O vs. K	10	4.5	15.6	0	100	88.3	-3.28	176	2.7	97.3	102	-9.55	211	3.7	96.3	70.3	-7.64	150	4.1	95.9
	O vs. DK-N	13.1	-0.16	26.8	2.5	97.5	111.0	-48.0	308	9.4	90.6	135	-61.8	382	9.9	90.1	87.3	-47.1	259	11.4	88.6
	O vs. DK-S	1.98	-8.68	12.3	35.1	64.9	50.2	-81.7	192	22.2	77.8	49.2	-115	226	26.8	73.2	47.7	-66.2	173	20.5	79.5
	K vs. DK-N	3.15	-10.2	16.8	32.6	67.4	22.3	-140	203	42.7	57.3	33.5	-167	259	40.5	59.5	17	-122	175	44.1	55.9
	K vs. DK-S	-7.99	-18.7	2.6	93.2	6.8	-31.1	-179	96.7	71.9	28.1	-52.3	-233	112	73.6	26.4	-22.6	-145	93.4	65.8	34.2
	DK-N vs.	-11.1	-27.2	5.18	91.4	8.6	-60.4	-276	127	72.0	28.0	-85.8	-366	140	74.6	25.4	-39.6	-255	120	66.9	33.1

DK-S							

Table S2. Posterior probability of the contrast (or difference from the common mean) of lichen diameters and calibrated ages, i.e. the median, upper, and lower boundaries of the 95% bootstrap confidence interval, Kugalan Tash rock glacier. Rows contain the 15 possible pairwise comparisons of the six sampled lobes (#27-32) for lichen species X. elegans, and A. tianshanica. No specimens of A. tianshanica were found on lobe 29, while R. geographicum was completely absent. Grey shades are credible contrasts for lichen diameter and ages, for which a zero contrast probability is outside the 95% highest density interval (HDI).

			Diameter					Predicted Age Median					Predicted Age Upper 95					Predicted Age Lower 95				
Location	Species	Compared lobes	Difference in means	HDI min	HDI max	Smaller Zero Prob [%]	Larger Zero Prob [%]	Difference in means	HDI min	HDI max	Smaller Zero Prob [%]	Larger Zero Prob [%]	Difference in means	HDI min	HDI max	Smaller Zero Prob [%]	Larger Zero Prob [%]	Difference in means	HDI min	HDI max	Smaller Zero Prob [%]	Larger Zero Prob [%]
Kugalan Tash	X. elegans	27 vs. 28	14.8	4.43	24.9	0.3	99.7	37.6	14.1	60.4	0.1	99.9	69.6	21	119	0.3	99.7	37.5	14.6	60.6	0.1	99.9
		27 vs. 29	-5.05	-15.3	5.08	83.5	16.5	-15.1	-38.7	7.57	90.1	9.9	-35.8	-84.3	13	92.7	7.3	-15.1	-38.3	7.57	90.3	9.7
		27 vs. 30	26.6	16.3	36.8	0	100	57	33.5	80.1	0	100	97.6	48	147	0	100	57	33.8	80.1	0	100
		27 vs. 31	39	28.7	49.4	0	100	75.5	51.7	98.6	0	100	121	71.1	170	0	100	74.6	51.3	97.8	0	100
		27 vs. 32	42.6	32.3	53.1	0	100	79.6	56	103	0	100	126	76	175	0	100	78.5	55.7	102	0	100
		28 vs. 29	-19.8	-30.4	-9.77	100	0	-52.8	-76.3	-29.5	100	0	-105	-154	-56	100	0	-52.5	-75.5	-29.4	100	0
		28 vs. 30	11.8	1.29	21.8	1.2	98.8	19.4	-3.55	42.8	5	95	28.1	-19.6	76.9	12.5	87.5	19.5	-3.27	42.9	4.8	95.2
		28 vs. 31	24.3	13.9	34.4	0	100	37.8	14.9	61.3	0.1	99.9	51.8	3.62	101	1.9	98.1	37.1	14.2	60.2	0.1	99.9
		28 vs. 32	27.8	17.6	38.2	0	100	42	18.9	65.6	0	100	56.5	6.96	105	1.3	98.7	41	18	63.9	0	100
		29 vs. 30	31.6	21.2	41.9	0	100	72.2	48.4	95.3	0	100	133	84.8	184	0	100	72	48.6	95.3	0	100

	29 vs. 31	44.1	33.7	54.6	0	100	90.6	67.1	114	0	100	157	107	208	0	100	89.6	66	113	0	100
	29 vs. 32	47.7	37.3	58.2	0	100	94.8	70.9	118	0	100	162	111	212	0	100	93.5	70.3	117	0	100
	30 vs. 31	12.5	2.24	22.7	0.9	99.1	18.4	-4.53	41.8	5.9	94.1	23.7	-25.2	72	16.6	83.4	17.6	-5.24	40.8	6.5	93.5
	30 vs. 32	16	5.76	26.2	0.2	99.8	22.6	-0.118	46.3	2.8	97.2	28.4	-20.1	76.8	12.2	87.8	21.5	-2	43.9	3.3	96.7
	31 vs. 32	3.6	-6.78	13.7	24.3	75.7	4.18	-18.9	27.4	35.8	64.2	4.74	-45	52.7	42.4	57.6	3.86	-19	26.6	36.9	63.1
A. tianshanica	27 vs. 28	-12	-29.2	4.5	92.2	7.8	-16.2	-41.4	7.92	90.5	9.5	-14.3	-43.9	11.2	85.1	14.9	-10.1	-35.3	12.6	79.7	20.3
	27 vs. 30	-22	-35.9	-7.9	99.9	0.1	-26.6	-47.8	-5.13	99.3	0.7	-24.4	-48.9	1.49	97	3	-22.4	-44.2	1.42	97	3
	27 vs. 31	6.53	-6.4	19.8	16.1	83.9	6.28	-12.6	25.9	25.9	74.1	2.8	-18.8	24.7	40	60	1.93	-25	30.8	45.5	54.5
	27 vs. 32	3.66	-9.3	16.8	28.9	71.1	3.57	-15.9	22.6	35.4	64.6	1.71	-20.2	23.3	43.6	56.4	2.94	-18.4	24.5	39.4	60.6
	28 vs. 30	-10	-26.5	6.47	88.9	11.1	-10.4	-34.5	13.1	80.9	19.1	-10.1	-36.9	16.4	78	22	-12.3	-36.5	9.68	85.8	14.2
	28 vs. 31	18.5	1.56	35.8	1.6	98.4	22.5	-2.6	48.1	3.8	96.2	17.1	-9.37	46.3	11	89	12	-16.6	45.1	22.4	77.6
	28 vs. 32	15.7	-1.35	32.6	3.4	96.6	19.8	-4.39	45.2	5.6	94.4	16.1	-10.5	45.2	12.5	87.5	13	-10.9	39.9	15.6	84.4
	30 vs. 31	28.6	14	42.8	0	100	32.8	10.3	55.4	0.3	99.7	27.2	-0.601	51.9	2.1	97.9	24.3	-4.66	55.8	5.3	94.7
	30 vs. 32	25.7	11.5	39.9	0	100	30.1	7.7	51.7	0.4	99.6	26.1	-1.16	50.7	2.4	97.6	25.3	-1.12	49.5	2.7	97.3
	31 vs. 32	-2.87	-15.6	10.4	66.9	33.1	-2.71	-22	16.4	61	39	-1.09	-23.1	20.4	54	46	1.01	-27.7	29.4	46.1	53.9

Table S3. Posterior probability of the contrast (or difference from the common mean) of lichen diameters and calibrated ages, i.e. the median, upper, and lower boundaries of the 95% bootstrap confidence interval, Turgen Aksu rock glacier. Rows contain the ten possible pairwise comparisons of the five sampled lobes (#54-58) for lichen species X. elegans, A. tianshanica, and R. geographicum. No specimens of A. tianshanica were found on lobe 29, while R. geographicum was completely absent. Grey shades are credible contrasts for lichen diameter and ages, for which a zero contrast probability is outside the 95% highest density interval (HDI).

			Diameter					Predicted Age Median					Predicted Age Upper 95					Predicted Age Lower 95				
Location	Species	Compared lobes	Difference in means	HDI min	HDI max	Smaller Zero Prob [%]	Larger Zero Prob [%]	Difference in means	HDI min	HDI max	Smaller Zero Prob [%]	Larger Zero Prob [%]	Difference in means	HDI min	HDI max	Smaller Zero Prob [%]	Larger Zero Prob [%]	Difference in means	HDI min	HDI max	Smaller Zero Prob [%]	Larger Zero Prob [%]
Turgen Aksu	X. elegans	54 vs. 55	-29	-46.8	-10.4	99.9	0.1	-33.6	-65	-2.79	98.4	1.6	-39.5	-88.8	7.92	94.9	5.1	-32.2	-63.8	-1.87	98	2
		54 vs. 56	-24.3	-36.6	-11.6	100	0	-30.6	-52.5	-8.61	99.6	0.4	-41.8	-78.1	-4.99	98.7	1.3	-29.3	-51.6	-7.73	99.5	0.5
		54 vs. 57	-24.5	-36.9	-12	100	0	-27.1	-49	-5.59	99.2	0.8	-30.4	-64.9	4.32	95.7	4.3	-25.4	-46.6	-3.49	98.9	1.1
		54 vs. 58	27.1	14.4	39.4	0	100	16	-5.22	37.6	7	93	14.3	-19.3	47.7	19.8	80.2	15.5	-5.65	37	7.4	92.6
		55 vs. 56	4.68	-13.5	22.6	30.1	69.9	3.08	-26.7	33.1	42.2	57.8	-2.31	-48.8	42.9	54.9	45.1	2.87	-26.3	32.8	42.5	57.5
		55 vs. 57	4.44	-13.6	22.6	31.1	68.9	6.57	-23.5	36.4	33.3	66.7	9.12	-36.2	56	35.3	64.7	6.81	-22	37.5	32.7	67.3
		55 vs. 58	56.1	37.6	74.6	0	100	49.6	17.2	81.1	0.1	99.9	53.8	-0.131	102	1.6	98.4	47.7	16	80	0.2	99.8
		56 vs. 57	-0.236	-12.6	12.2	51.4	48.6	3.49	-17.8	24.7	36.9	63.1	11.4	-22.6	44.4	24.9	75.1	3.94	-17.1	25.1	35.3	64.7
		56 vs. 58	51.4	38.7	64.1	0	100	46.5	24.1	69.6	0	100	56.1	17.3	95.1	0.3	99.7	44.9	22.2	67.7	0	100
		57 vs. 58	51.7	39	64.4	0	100	43	20.2	65.3	0	100	44.7	6.7	80.3	0.9	99.1	40.9	18.1	63	0	100
	A. tianshanica	54 vs. 55	2.32	-14.7	18.8	39.4	60.6	5.63	-28.6	40.4	37.2	62.8	9.08	-64.3	87.1	40.5	59.5	3.96	-21.2	29	37.8	62.2
		54 vs. 56	19	1.46	37.2	1.7	98.3	27	-7.52	64.2	6.9	93.1	36.2	-37.5	117	17.7	82.3	21.8	-4.48	48.4	5.2	94.8
		54 vs. 57	-13.1	-30.4	3.93	93.6	6.4	-26.6	-63.2	8.23	92.9	7.1	-58.4	-142	19.6	92	8	-19.8	-46.2	6.21	93	7
		54 vs. 58	-8.7	-25.9	7.96	84.8	15.2	-15.9	-51.6	18	81.7	18.3	30.8	-110	42.8	78.6	21.4	-12.1	-37.9	12.9	82.6	17.4

	55 vs. 56	16.7	-0.479	33.7	2.7	97.3	21.3	-13.3	55.8	11.1	88.9	27.1	-46.1	103	23.8	76.2	17.9	-7.33	43.7	8.4	91.6
	55 vs. 57	-15.5	-32.4	1.51	96.5	3.5	-32.2	-68.4	3.84	96.1	3.9	-67.5	-153	11.5	94.6	5.4	-23.7	-49.6	2.96	96.1	3.9
	55 vs. 58	-11	-27.9	5.33	90.5	9.5	-21.5	-56.6	12.5	89.2	10.8	-39.9	-118	34.1	84.8	15.2	-16	-41.8	8.9	89.4	10.6
	56 vs. 57	-32.2	-51.2	-12.4	99.9	0.1	-53.6	-94.9	-9.01	99.3	0.7	-94.6	-183	4.36	97.5	2.5	-41.6	-72.4	-9.49	99.4	0.6
	56 vs. 58	-27.7	-46.4	-8.95	99.7	0.3	-42.9	-80.4	-1.9	98.5	1.5	-67	-149	14.5	94.3	5.7	-33.9	-62.1	-3.82	98.9	1.1
	57 vs. 58	4.45	-11.8	20.9	29.4	70.6	10.7	-23	44.9	26.5	73.5	27.6	-46.3	103	23.3	76.7	7.68	-16.8	32.8	27	73
R. geographicum	54 vs. 55	-2.03	-16.7	12.1	61	39	-9.09	-209	186	53.7	46.3	-14.7	-255	231	54.8	45.2	-6.36	-180	168	53	47
	54 vs. 56	-17.8	-32.8	-2.22	98.9	1.1	-138	-360	60	90.1	9.9	-192	-459	56.7	92.9	7.1	-97.5	-292	72.3	85.1	14.9
	54 vs. 57	-18.5	-33.8	-3.12	99.1	0.9	-147	-373	53.2	91.3	8.7	-206	-469	50.7	93.9	6.1	-107	-306	64.3	86.8	13.2
	54 vs. 58	8.4	-6.21	23	12.6	87.4	73.6	-114	288	23.5	76.5	96.3	-140	347	21.9	78.1	56.3	-111	241	26.6	73.4
	55 vs. 56	-15.8	-30.7	-0.7	98.1	1.9	-129	-347	66.6	88.8	11.2	-178	-439	71.2	91.3	8.7	-91.1	-285	75.3	83.7	16.3
	55 vs. 57	-16.4	-31.6	-1.48	98.4	1.6	-138	-354	63.8	90.1	9.9	-191	-455	59.5	92.8	7.2	-100	-299	67.6	85.7	14.3
	55 vs. 58	10.4	-4.29	25.1	8	92	82.7	-109	294	21.1	78.9	111	-129	362	18.6	81.4	62.7	-105	246	24.2	75.8
	56 vs. 57	-0.635	-15.4	13.3	53.6	46.4	-9.4	-209	187	53.8	46.2	-13.8	-252	232	54.7	45.3	-9.21	-182	163	54.3	45.7
	56 vs. 58	26.2	10.2	42.3	0.1	99.9	211	-19.6	446	3.8	96.2	289	-12.3	559	2.4	97.6	154	-31.9	365	7	93
	57 vs. 58	26.9	10.6	43.1	0.1	99.9	211	-17	457	3.6	96.4	302	-10.2	574	2.2	97.8	163	-30.7	377	6.4	93.6

Table S4. Posterior probability of the contrast (or difference from the common mean) of lichen diameters and calibrated ages, i.e. the median, upper, and lower boundaries of the 95% bootstrap confidence interval, Ordzhonikidze rock glacier. Rows contain the 28 possible pairwise comparisons of the five sampled lobes (#1-8) for lichen species X. elegans, A. tianshanica, and R. geographicum. No specimens of A. tianshanica were found on lobe 29, while R. geographicum was completely absent. Grey shades are credible contrasts for lichen diameter and ages, for which a zero contrast probability is outside the 95% highest density interval (HDI).

			Diameter					Predicted Age Median					Predicted Age Upper 95					Predicted Age Lower 95				
Location	Species	Compared lobes	Difference in means	HDI min	HDI max	Smaller Zero Prob [%]	Larger Zero Prob [%]	Difference in means	HDI min	HDI max	Smaller Zero Prob [%]	Larger Zero Prob [%]	Difference in means	HDI min	HDI max	Smaller Zero Prob [%]	Larger Zero Prob [%]	Difference in means	HDI min	HDI max	Smaller Zero Prob [%]	Larger Zero Prob [%]
Ordzhonikidze	X. elegans	1 vs. 2	11.6	-3.69	27.7	7.2	92.8	7.67	-25.3	41.8	32.8	67.2	5.83	-54.3	69.6	42.8	57.2	7.59	-24.1	40.3	32.2	67.8
		1 vs. 3	-14.6	-30.8	1.19	96.6	3.4	-28	-66.6	6.77	93.3	6.7	-38.4	-116	22.6	85.9	14.1	-27.3	-63.5	6.85	93.8	6.2
		1 vs. 4	11.7	-4.18	27.3	7.1	92.9	15.2	-17.9	50.7	19.2	80.8	16.7	-42.3	83.2	30.5	69.5	15.3	-15.7	50.4	18.1	81.9
		1 vs. 5	-12.9	-28.8	2.76	94.8	5.2	-22.8	-60.9	10.2	89.8	10.2	-25.2	-96.8	33.4	77.4	22.6	-22.4	-57.7	10.3	90.3	9.7
		1 vs. 6	-4.72	-20.1	10.7	72.8	27.2	-9.13	-43.1	23.8	70.3	29.7	-14.6	-80.4	45.3	67.5	32.5	-8.12	-41.6	22.8	69	31
		1 vs. 7	-0.489	-15.9	14.8	52.5	47.5	-1.08	-34.6	32	52.6	47.4	-3.17	-67.3	57.2	53.8	46.2	-0.258	-33.1	31.2	50.6	49.4
		1 vs. 8	5.66	-9.63	21.3	23.5	76.5	3.86	-28.7	37.7	41.1	58.9	0.927	-61.6	61.5	48.8	51.2	4.02	-28	36	40.4	59.6
		2 vs. 3	-26.2	-43.6	-8.17	99.8	0.2	-35.6	-75.3	3.46	96.3	3.7	-44.2	-126	17.2	88.5	11.5	-34.9	-72.9	3.51	96.6	3.4
		2 vs. 4	0.107	-15.4	15.3	49.4	50.6	7.54	-24.9	42.1	32.8	67.2	10.9	-47.3	77.8	36.7	63.3	7.73	-23.4	41.5	31.9	68.1
		2 vs. 5	-24.5	-42	-7.24	99.7	0.3	-30.5	-69.3	5.37	94.7	5.3	-31	-106	27	81.7	18.3	-30	-67.9	4.37	95.2	4.8
		2 vs. 6	-16.3	-32.3	-0.154	97.8	2.2	-16.8	-52.5	16.2	83.1	16.9	-20.5	-90.7	37	73.3	26.7	-15.7	-49.9	16.1	82.6	17.4
		2 vs. 7	-12.1	-27.8	3.66	93.6	6.4	-8.74	-43.5	23.8	69.6	30.4	-8.99	-73.6	50.8	61.2	38.8	-7.85	-40.8	23.9	68.4	31.6
		2 vs. 8	-5.92	-21.7	9.14	77.6	22.4	-3.8	-38.2	28.8	59	41	-4.9	-68.1	55.2	56.1	43.9	-3.57	-35.3	28.9	58.9	41.1
		3 vs. 4	26.3	8.29	43.7	0.2	99.8	43.2	-1.64	84.2	2.4	97.6	55	-13.6	143	8.5	91.5	42.6	-1.18	81.7	1.9	98.1

	3 vs. 5	1.68	-13.4	17	41.4	58.6	5.13	-28.2	38.5	38	62	13.1	-44.9	80.1	34.2	65.8	4.87	-27.2	37.4	38.4	61.6
	3 vs. 6	9.88	-5.48	25.6	10.5	89.5	18.8	-14	55.4	14.3	85.7	23.7	-34.3	94.9	23.8	76.2	19.2	-13.1	53.5	12.9	87.1
	3 vs. 7	14.1	-1.8	30.1	4	96	26.9	-7.59	65.2	7.3	92.7	35.2	-24.9	111	15.7	84.3	27.1	-6.88	63.6	6.4	93.6
	3 vs. 8	20.3	3.87	37.4	0.8	99.2	31.8	-5.43	70.3	4.9	95.1	39.3	-31.3	117	13.7	86.3	31.3	-4.67	68.5	4.5	95.5
	4 vs. 5	-24.6	-41.9	-7.05	99.7	0.3	-38	-78.1	2.39	96.9	3.1	-41.9	-123	18.6	87.3	12.7	-37.8	-76.4	1.59	97.4	2.6
	4 vs. 6	-16.4	-32.5	-0.0576	97.8	2.2	-24.3	-61.5	9.87	90.9	9.1	-31.3	-106	26.5	82	18	-23.4	-59	9.39	91.1	8.9
	4 vs. 7	-12.2	-28	3.65	93.7	6.3	-16.3	-52.4	16.3	82.4	17.6	-19.9	-87.9	39.6	72.6	27.4	-15.6	-50.2	15.9	82.5	17.5
	4 vs. 8	-6.02	-21.5	9.34	78.1	21.9	-11.3	-46.7	20.7	74.5	25.5	-15.8	-83.3	42.3	68.8	31.2	-11.3	-44.7	20.2	75.4	24.6
	5 vs. 6	8.2	-7.3	23.5	14.6	85.4	13.7	-18.8	49.3	21.4	78.6	10.6	-49.3	75	37.1	62.9	14.3	-17.1	48.6	19.5	80.5
	5 vs. 7	12.4	-3.08	28.7	5.9	94.1	21.8	-12.3	58.2	11.2	88.8	22	-36.5	91.7	25.1	74.9	22.2	-10.4	57.4	9.9	90.1
	5 vs. 8	18.6	1.87	34.7	1.2	98.8	26.7	-8.38	64.3	7.4	92.6	26.1	-31.5	98.3	21.8	78.2	26.5	-6.93	63	6.7	93.3
	6 vs. 7	4.23	-11.3	19.5	29.3	70.7	8.05	-24.5	42.7	31.9	68.1	11.5	-47.2	77.6	36.1	63.9	7.86	-23.9	40.7	31.5	68.5
	6 vs. 8	10.4	-5.19	25.9	9.4	90.6	13	-19.3	48.4	22.6	77.4	15.6	-42.4	83	31.5	68.5	12.1	-19.6	45.8	23.2	76.8
	7 vs. 8	6.14	-9.2	21.6	21.6	78.4	4.94	-27.7	39	38.6	61.4	4.1	-56.2	67.6	44.9	55.1	4.28	-27.6	36.9	39.8	60.2
A. tianshanica	1 vs. 2	-37.4	-52.3	-22.7	100	0	-48.9	-123	18.8	91.4	8.6	-127	-288	23.3	95	5	-37.1	-90.5	11.5	92.6	7.4
	1 vs. 3	-21.1	-35.9	-6.45	99.7	0.3	-25.2	-94.2	38	77.4	22.6	-49.6	-199	91.9	75.2	24.8	-18.1	-67	27.7	77.4	22.6
	1 vs. 4	2.52	-12.4	17	36.8	63.2	0.999	-65.5	63.8	48.7	51.3	-2.26	-146	142	51.4	48.6	-0.169	-46.8	45.8	50.2	49.8
	1 vs. 5	-35.3	-50	-20.4	100	0	-46.4	-120	19.9	90.4	9.6	-116	-272	35.8	93.4	6.6	-35.4	-88.3	12.8	91.6	8.4
	1 vs. 6	-68.2	-83	-53.1	100	0	-64.5	-132	5.16	96.9	3.1	-186	-342	-35.9	99.4	0.6	-47.3	-95.6	2.54	97.3	2.7
	1 vs. 7	-2.92	-18.4	12.7	64.6	35.4	-5.28	-72	61.7	56.3	43.7	-10.4	-161	138	55.6	44.4	-3.79	-51.7	44.6	56.3	43.7
	1 vs. 8	-14.6	-29.1	0.263	97.4	2.6	-16.3	-83.2	47	68.8	31.2	-30.4	-179	111	66	34	-12.4	-60.1	33.2	69.9	30.1
	2 vs. 3	16.3	1.56	31	1.5	98.5	23.6	-39.9	91.3	24	76	77.8	-69.4	227	14.8	85.2	19	-25.2	69.4	21.3	78.7
	2 vs. 4	39.9	25	54.7	0	100	49.9	-17.2	124	8.2	91.8	125	-27.1	283	5.2	94.8	36.9	-11.4	91	7.4	92.6
	2 vs. 5	2.11	-12.6	18.8	39	61	2.51	-62	66.8	47	53	11.8	-130	156	43.6	56.4	1.69	-44.6	47.6	47	53
	2 vs. 6	-30.8	-45.6	-16	100	0	-15.6	-75	41.1	70.7	29.3	-58.7	-188	69.4	81.9	18.1	-10.2	-52.7	30.4	69.2	30.8
	2 vs. 7	34.5	19	50.3	0	100	43.6	-22.9	121	11.6	88.4	117	-37.8	282	7.2	92.8	33.3	-15.5	89.6	10.1	89.9
	2 vs. 8	22.8	8.14	37.5	0.1	99.9	32.5	-31.4	103	17	83	97	-48.3	251	9.8	90.2	24.7	-21.3	75.2	15.6	84.4
	3 vs. 4	23.6	8.59	38.1	0.1	99.9	26.2	-35.5	96.9	21.8	78.2	47.3	-94.9	194	26	74	17.9	-27.2	67.1	22.8	77.2
	3 vs. 5	-14.2	-28.7	0.682	97	3	-21.1	-89.7	41.3	73.8	26.2	-66	-216	78.3	81.2	18.8	-17.3	-66.7	27.9	76.6	23.4
	3 vs. 6	-47.1	-61.9	-32.1	100	0	-39.3	-103	16.6	90.2	9.8	-137	-273	4.42	97.7	2.3	-29.2	-74.2	12.4	91	9

	3 vs. 7	18.2	2.58	33.8	1.1	98.9	20	-45.3	91.2	28.2	71.8	39.2	-109	193	30.4	69.6	14.3	-31.9	65.7	28.3	71.7
	3 vs. 8	6.49	-8.14	21.3	19.2	80.8	8.89	-54.2	75	39.5	60.5	19.2	-124	164	39.7	60.3	5.66	-40.1	53.4	40.6	59.4
	4 vs. 5	-37.8	-52.7	-23.1	100	0	-47.4	-122	18.4	90.8	9.2	-113	-271	33.5	93.2	6.8	-35.2	-88.7	12.4	91.6	8.4
	4 vs. 6	-70.8	-86	-55.7	100	0	-65.5	-134	6.96	97	3	-184	-335	-32	99.3	0.7	-47.1	-95.7	2.22	97.3	2.7
	4 vs. 7	-5.44	-20.8	10.3	75.5	24.5	-6.28	-73.3	61.1	57.8	42.2	-8.13	-157	140	54.4	45.6	-3.62	-52	44.1	56.2	43.8
	4 vs. 8	-17.1	-31.6	-2.22	98.8	1.2	-17.3	-84.7	45.7	70.2	29.8	-28.1	-172	116	65.1	34.9	-12.2	-60.4	33	69.7	30.3
	5 vs. 6	-32.9	-47.4	-17.9	100	0	-18.2	-78.1	38	73.8	26.2	-70.5	-203	53.2	86.3	13.7	-11.9	-53.5	29.8	72.2	27.8
	5 vs. 7	32.4	17	48.3	0	100	41.1	-26.2	117	12.7	87.3	105	-46.2	270	9.2	90.8	31.6	-17.1	86.4	11.3	88.7
	5 vs. 8	20.7	6.38	35.8	0.3	99.7	30	-33.2	100	18.6	81.4	85.2	-59.2	238	12.6	87.4	23	-22.7	73.1	17.2	82.8
	6 vs. 7	65.3	49.3	81.2	0	100	59.2	-7.23	130	4.3	95.7	176	15.8	329	1.1	98.9	43.5	-4.92	94.1	3.9	96.1
	6 vs. 8	53.6	38.6	68.4	0	100	48.2	-11.6	113	6.3	93.7	156	8.13	294	1.4	98.6	34.9	-7.74	81.1	5.9	94.1
	7 vs. 8	-11.7	-27.1	4.04	93.1	5.9	-11.1	-81	53.6	62.4	37.6	-20	-171	128	60.3	39.7	-8.63	-59.2	37.9	63.4	36.6
R. geographicum	1 vs. 2	-10.8	-18.8	-2.56	99.5	0.5	-209	-360	-59.2	99.6	0.4	-232	-407	-59.6	99.5	0.5	-183	-316	-44.3	99.5	0.5
	1 vs. 3	-19.2	-27.6	-11.1	100	0	-364	-520	-212	100	0	-404	-581	-224	100	0	-315	-456	-175	100	0
	1 vs. 4	4.98	-2.95	13.1	11	89	57.1	-89	207	22.2	77.8	80	-90.6	254	17.9	82.1	40.2	-92.8	176	27.5	72.5
	1 vs. 5	-13.6	-21.7	-5.43	99.9	0.1	-254	-404	-101	99.9	0.1	-272	-444	-94.2	99.9	0.1	-210	-345	-71.7	99.9	0.1
	1 vs. 6	-0.988	-9	6.98	59.7	40.3	-253	-405	-101	99.9	0.1						-210	-346	-72.2	99.8	0.2
	1 vs. 7	5.2	-2.89	13.2	10	90	42.7	-105	190	28.4	71.6	71.6	-96.8	246	20.6	79.4	29.9	-102	167	32.9	67.1
	1 vs. 8	-7.34	-15.4	0.717	96.4	3.6	-136	-284	14.2	96.3	3.7	-156	-331	14.4	96.3	3.7	-122	-258	11.8	96.2	3.8
	2 vs. 3	-8.45	-16.4	-0.316	98	2	-155	-305	-5.04	97.9	2.1	-171	-349	-1.04	97.4	2.6	-132	-267	2.03	97.3	2.7
	2 vs. 4	15.8	7.66	24	0	100	266	113	417	0	100	312	137	490	0	100	223	86.5	360	0.1	99.9
	2 vs. 5	-2.84	-10.8	5.33	75.7	24.3	-44.8	-191	106	72.5	27.5	-39.8	-212	132	67.7	32.3	-27.8	-161	106	66.1	33.9
	2 vs. 6	9.8	1.79	17.9	0.9	99.1	-44.3	-197	100	72.3	27.7						-27.7	-159	108	65.8	34.2
	2 vs. 7	16	7.87	24.2	0	100	252	98.4	401	0.1	99.9	304	129	480	0	100	213	73.4	348	0.1	99.9
	2 vs. 8	3.45	-4.4	11.7	19.7	80.3	72.7	-76.1	221	16.8	83.2	76.2	-93.9	249	19.1	80.9	60.9	-71	195	18.4	81.6
	3 vs. 4	24.2	15.8	32.6	0	100	421	263	577	0	100	484	303	668	0	100	355	212	497	0	100
	3 vs. 5	5.61	-2.38	13.7	8.4	91.6	110	-41.3	257	7.2	92.8	131	-43.4	302	6.7	93.3	104	-29.4	239	6.3	93.7
	3 vs. 6	18.3	10.2	26.6	0	100	111	-37	261	7.1	92.9						105	-30.3	283	6.3	93.7
	3 vs. 7	24.4	16.2	33	0	100	406	250	562	0	100	475	296	657	0	100	345	202	487	0	100
	3 vs. 8	11.9	3.82	20.1	0.2	99.8	228	78.3	380	0.2	99.8	247	69.9	420	0.3	99.7	193	56.6	329	0.3	99.7

Appendix B

Supplementary material
Late Pleistocene outburst floods from Issyk Kul, Kyrgyzstan?

Table S1 Historical lake-level change records

Elevation	High-/lowstand	Timing	Data origin	Open/closed lake	Reference
~1607	Reference level	recent	Lake surface		
~1610	regressive	1926 AD	Instrumental record	closed	(Ricketts et al., 2001)
just below 1620		1856 AD	Lake surface	closed	(Semenov, 1858)
above 1620		1755 AD	Lake surface	open?	(Romanovsky, 1990)
~1622	highstand	1500-1650 AD 1640-1960 AD	Lake sediments	open?	(Burgette, 2008)
1601-1604	lowstand	13th to 15th century	Trees, soils, settlements	closed	(Sevastianov et al., 1980)
~1615		580±40	Macrophytes	closed	(Rasmussen et al., 2001)
~1623	highstand	1200-1400 yr BP	Macrophytes	open	(Aleshinskaya et al., 1971; Berdovskaya and Egorov, 1986; Trofimov, 1978)
		4900-1000 cal yr BP	Ostracodes isotopes	transient open	(Ricketts et al., 2001)
		6900-4900 cal yr BP	Ostracodes isotopes	closed	(Ricketts et al., 2001)
		8300-6900 cal yr BP	Ostracodes isotopes	open - overflow	(Ricketts et al., 2001)
~1300	lowstand	~8000 yr ago	Isotopes	closed	(Kipfer, pers. comm., ICDP Workshop 2011)
~1497	lowstand	??	Relict submerged rivers	closed	(Trofimov, 1978)
1640-1675		~25 ka	Shoreline, wave-cut terrace	Open	(Burgette, 2008; Aleshinskaya et al., 1971; Trofimov, 1978)
			Erosive terrace, lacustrine sediment	Closed? (blockage)	(Trofimov and Grigina, 1979)

S2 Fan surface reconstruction

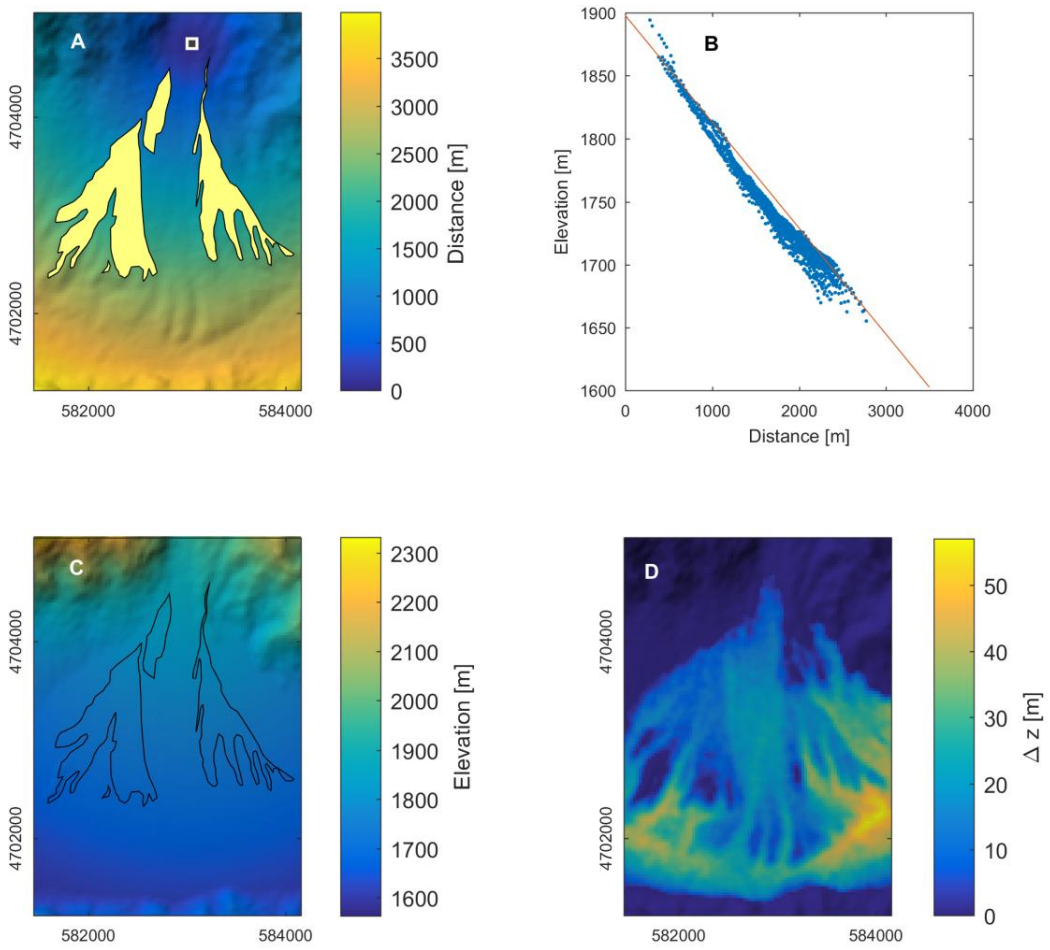

Figure S2: Fan surface reconstruction. (A) We calculated the euclidean distance transform seeded at the fan head (white square) and determined the relation between distance and elevations for all pixels of former fan surfaces (polygons in A) using a linear quantile regression (tau=0.95) (B). We chose a quantile regression to reconstruct the upper limit of the surface instead of its central tendency as a function of distance. We chose a straight line rather than a higher order polynomial since latter would easily overestimate fan surface elevations in distances beyond the mapped fan surface patches. The equation of the regression line is z_hat = 1897.7 -0.0843*d (d=distance in [m]). C) DEM of the reconstructed fan surface. D) Elevation difference between reconstructed and actual DEM.

S3 Selected field photos

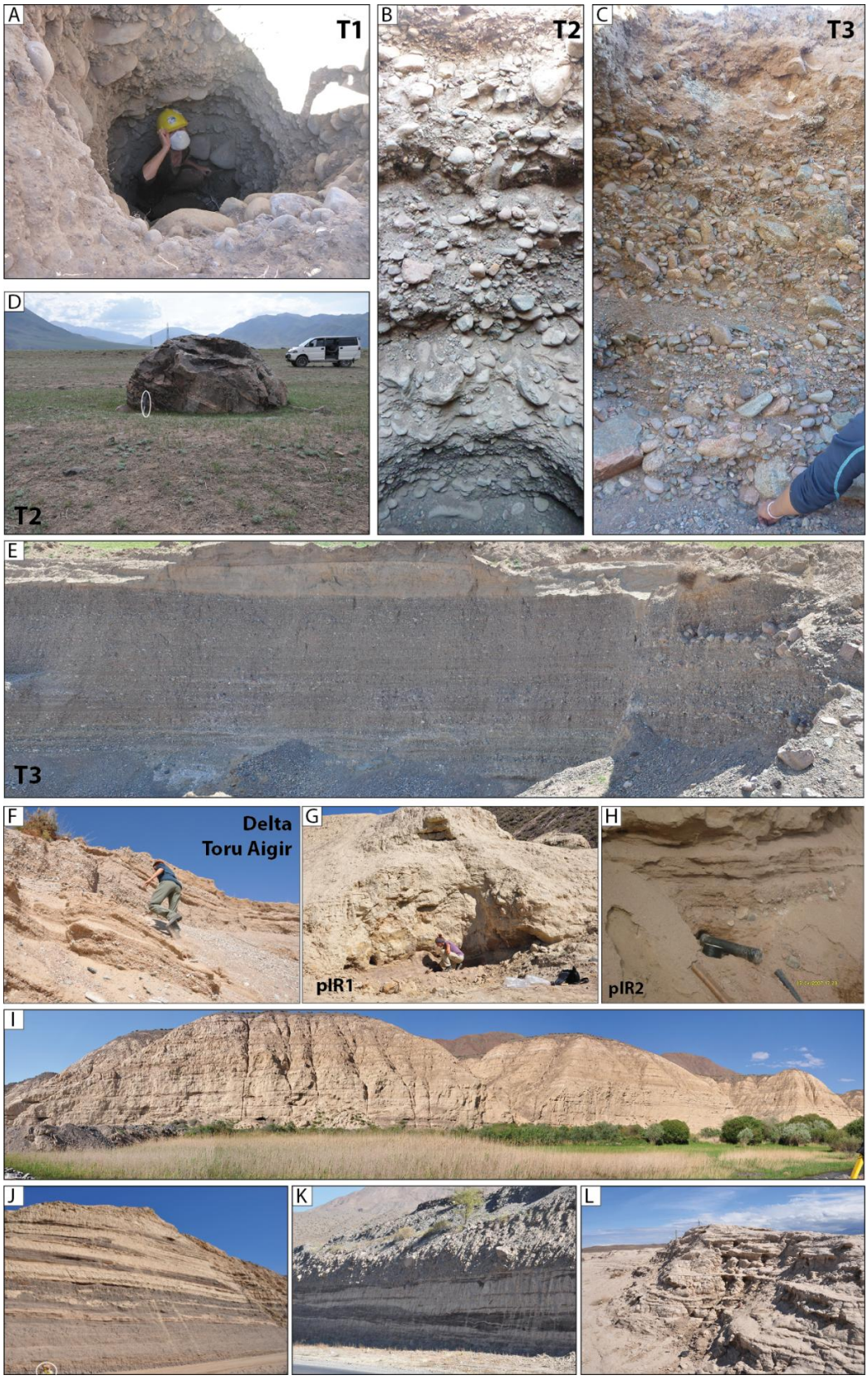

Figure S3: Selected field photos of sites or observations discussed in the main manuscript. (A-C) TCN (^{10}Be) sampling sites showing pit stratigraphy of T1, T2, and T3, respectively. (D) Example of boulders sampled on T2 using ^{10}Be and ^{26}Al, ellipse shows hammer for scale. (E) Excavation pit (height ~ 8 m) carved into T3 shows rapid deposition of clast-supported fluvial pebble to boulder. The lack of current structures as ripples etc. or erosion features indicates high flow velocities in turbulent water. (F) Excavation pit in delta sediments at northern coast of Issyk Kul. Upper profile has been sampled for ^{10}Be-determination (TCN7). (G) Sample site of pIR1. Fluvial sands and silt predate massive silt beds that we interpret as lake sediment. (H) Sample locality of delta sediment from northern Issyk Kul shore (pIR2). (I) Example of massive silty lacustrine deposits inside Kok Moinok. Note trees for scale. (J) Road cut exhibiting intercalations of fluvial pebble and silty lacustrine deposits, suggesting energetic flow conditions. Note person with GPS antenna for scale (white ellipse). (K) Similarly to J, but at a marginal lake location. Height ~ 5 m. (L) Lacustrine sediments that straddle lake Issyk Kul in the west; sample locality of radiocarbon-samples 7 & 8 (070512-3-2 and -5) Photo shows the upper approx. 5 m of thicker deposit.

S4 Boulder diameter distribution

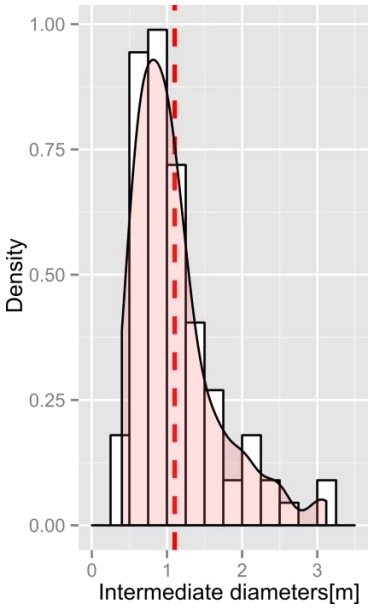

Figure S4: Density distribution [m^{-1}] of intermediate boulder diameters [m].

S5 Table of specifications for measured boulders at the outlet terraces

Diameter a axes [m]	Diameter b axes [m]	Diameter c axes [m]	Lithology	Longitude [°E]	Latitude [°N]	Elevation [m asl]
1.85	1.7	1.65	Dolomite	75.86561	42.70519	1335
1.5		1.1	Conglomerate	75.86561	42.70519	1335
1.95	1.6	1.1	Conglomerate	75.86561	42.70519	1335
3	2.55	1.7	Conglomerate	75.86561	42.70519	1335
2.3	1.1	1	Conglomerate	75.86561	42.70519	1335
1.7	1.3	0.7	Dolomite	75.86561	42.70519	1335
1.45	1	0.7	Granodiorite	75.86561	42.70519	1335
1.65	1.4	0.55	Metamorph/undefined	75.86561	42.70519	1335
1.5	0.5	0.25	Granodiorite	75.86561	42.70519	1335
1.3	1.15	0.45	Conglomerate	75.86561	42.70519	1335
1.15	0.7	0.4	Metamorph/undefined	75.86561	42.70519	1335
0.65	0.9	0.55	Granite	75.86561	42.70519	1335
1.02	0.9	0.45	Conglomerate	75.86561	42.70519	1335
1.48	0.8	0.4	Conglomerate	75.86561	42.70519	1335
2.04	1.62	1.4	Plutonite	75.86561	42.70519	1335
1.2	0.75	0.5	Conglomerate	75.86561	42.70519	1335
1.62	1.1	0.3	Granite	75.86561	42.70519	1335
1.6	1.26	1.15	Metamorph/undefined	75.86561	42.70519	1335
1.42	1.1	0.55	Plutonite	75.86561	42.70519	1335
1.45	0.8	0.95	Plutonite	75.86561	42.70519	1335
1.58	1.1	0.65	Conglomerate	75.86561	42.70519	1335
1.1	0.55	0.35	Conglomerate	75.86688	42.70343	1335
1.7	1.6	1	Granodiorite	75.86688	42.70343	1335
1.7	1.5	0.58	Conglomerate	75.86688	42.70343	1335
1.4	0.7	0.6	Granodiorite	75.86688	42.70343	1335
1.6	1.1	0.9	Granodiorite	75.86688	42.70343	1335
3.35	2.4	1.1	Conglomerate	75.86688	42.70343	1335
1.9	0.82	0.55	Conglomerate	75.86688	42.70343	1335
2	1.7	0.85	Plutonite	75.86688	42.70343	1335
1.5	0.9	0.75	Conglomerate	75.86688	42.70343	1335

1.55	0.75	0.7	Conglomerate	75.86688	42.70343	1335
1.5	0.97	0.45	Conglomerate	75.86688	42.70343	1335
1.25	0.85	0.8	Conglomerate	75.86688	42.70343	1335
1.9	1.85	0.8	Conglomerate	75.86688	42.70343	1335
2.65	2	1.75	Conglomerate	75.86688	42.70343	1335
4.4	3.12	1.5	Conglomerate	75.86688	42.70343	1335
2.6	2	1.75	Dolomite	75.86688	42.70343	1335
1.9	1.9	0.9	Conglomerate	75.86688	42.70343	1335
3.6			Conglomerate	75.86688	42.70343	1335
2.05	1.4	0.3	Granodiorite	75.86477	42.71485	1320
2.3	1	0.4	Granodiorite	75.86467	42.71432	1320
2.1	1.3	0.3	Granite	75.86492	42.71368	1321
2.3	1.3	0.76	Granodiorite	75.86538	42.71322	1322
2.5	2.15	1.2	Granodiorite	75.86538	42.71322	1322
3.9	2.45	1.2	Granite	75.86508	42.7128	1328
2.25	2.15	1.1	Granodiorite	75.86525	42.71258	1323
1.4	1.25	0.85	Conglomerate	75.86423	42.71248	1326
0.93	0.45	0.43	Conglomerate	75.85436	42.70912	1279
1	0.52	0.4	Conglomerate	75.85436	42.70912	1279
0.92	0.7	0.4	Metamorph/undefined	75.85436	42.70912	1279
0.71	0.63	0.42	Conglomerate	75.85436	42.70912	1279
1.2	0.8	0.3	Conglomerate	75.85436	42.70912	1279
0.9	0.41	0.31	Gneiss	75.85436	42.70912	1279
0.8	0.63	0.3	Metamorph/undefined	75.85436	42.70912	1279
1.32	1	0.38	Conglomerate	75.85436	42.70912	1279
0.9	0.9	1.15	Conglomerate	75.85436	42.70912	1279
1.3	0.95	0.58	Granite	75.85436	42.70912	1279
1.15	0.85	0.5	Conglomerate	75.85436	42.70912	1279
1.6	0.4	0.4	Metamorph/undefined	75.85436	42.70912	1279
1.35	0.66	0.6	Metamorph/undefined	75.85436	42.70912	1279
1.21	0.99	0.1	Metamorph/undefined	75.85436	42.70912	1279
1	0.73	0.35	Conglomerate	75.85436	42.70912	1279
1.63	1.32	1.12	Metamorph/undefined	75.85436	42.70912	1279
0.93	0.53	0.05	Metamorph/undefined	75.85436	42.70912	1279
0.93		0.57	Metamorph/undefined	75.85436	42.70912	1279
1.1	0.68	0.51	Gneiss	75.84755	42.70958	1266
1.15	0.5	0.2	Conglomerate	75.84755	42.70958	1266
1.5	0.75	0.4	Conglomerate	75.84755	42.70958	1266
0.77	0.54	0.31	Conglomerate	75.84755	42.70958	1266
1	0.6	0.35	Granite	75.84755	42.70958	1266
1.1	0.8	0.52	Conglomerate	75.84755	42.70958	1266
0.75	0.45	0.45	Conglomerate	75.84755	42.70958	1266
0.78	0.62	0.3	Conglomerate	75.84755	42.70958	1266
2.8	1.2	0.22	Conglomerate	75.84755	42.70958	1266
1.4	1.2	0.65	Conglomerate	75.84755	42.70958	1266
0.95	0.75	0.7	Conglomerate	75.84755	42.70958	1266
1.4	0.92	0.9	Conglomerate	75.84755	42.70958	1266
1.5	0.8	0.65	Conglomerate	75.84755	42.70958	1266
1	0.95	0.47	Granodiorite	75.84755	42.70958	1266
0.85	0.6	0.3	Conglomerate	75.84755	42.70958	1266
1.3	0.65	0.65	Metamorph/undefined	75.84755	42.70958	1266
3.2	3	1.7	Gneiss	75.84755	42.70958	1266
1.33		1.1	Granite	75.84755	42.70958	1266
2.1	1.4	0.7	Metamorph/undefined	75.84755	42.70958	1266
1.1	1	0.65	Granite	75.84755	42.70958	1266
0.95	0.9	0.3	Conglomerate	75.84755	42.70958	1266
1.3	1.08	0.55	Conglomerate	75.84755	42.70958	1266
1.05	0.6	0.4	Conglomerate	75.84755	42.70958	1266
1.3	1.1	0.9	Granite	75.84755	42.70958	1266
1.72	0.95	0.65	Conglomerate	75.84755	42.70958	1266
1.65	1.27	0.8	Conglomerate	75.84755	42.70958	1266

S6 MATLAB function to calculate discharge

The MATLAB function below calculates discharge using Manning's equation if the hydraulic radius of an irregular channel cross-section is unknown.

```
function [Q,h,err] = manningseq(V,S,n,d,z,plt)

% MANNINGSEQ Solve Mannings for discharge given an irregular cross section
%
% Syntax
%
%     [Q,h,err] = manningseq(V,S,n,d,z)
%     [Q,h,err] = manningseq(V,S,n,d,z,plt)
%
% Description
%
%     manningseq solves for discharge and maximum flow depth given flow
%     velocity V, channel bed gradient S, Manning's n, and an irregular
%     river cross-section defined by the vertices in the vector d=distance
%     and z=elevation. The function finds the zero of the function
%
%        Q = 1/n * (A/P)^(2/3) * S^(1/2) * A
%
%     where A is the channel cross-sectional area and P is the wetted
%     perimeter. A/P is the hydraulic radius R.
%
%     The function requires fminsearchbnd by John D'Errico available on the
%     File Exchange (http://www.mathworks.com/matlabcentral/fileexchange/8277)
%
% Input arguments
%
%     V         flow velocity [m/s]
%     S         slope [m/m]
%     n         Manning's n [s/m^(1/3)]
%     d         horizontal distance vector of channel profile [m]
%     z         elevation vector of channel profile [m]
%     plt       plot results (true or false, default = true)
%
% Output arguments
%
%     Q         discharge [m^3/s]
%     h         maximum depth
%     err       deviation between Q/A and V. Large errors indicate that
%               maximum flow depth may exceed the profile's maximum height
%
% Example
%
%     d = [0 10 20 30 40 50 60 70];
%     z =[20 10 5  3  4  8  10 20];
%     [Q,h,err] = manningseq(5,0.01,0.03,d(:),z(:));
%
%
% See also: fminsearchbnd
%
% Author: Wolfgang Schwanghart (w.schwanghart[at]geo.uni-potsdam.de)
% Date: 18. December, 2015

if nargin == 5;
    plt = true;
end

% force column vectors
d = d(:);
z = z(:);
z = z-min(z);

h0 = 10;
h = fminsearchbnd(@(h) mann(h),h0,1,min(z([1 end])));
```

```
% h = fminsearch(@(h) mann(h),h0);
[A,U] = getprof(d,z,h);

% check flow velocity
Vhat  = 1/n*(A/U)^(2/3)*S^.5;
err   = Vhat-V;

Q = A*V;

if plt
    plot(d,z,'k-*');
    [~,~,dnew,znew] = getprof(d,z,h);
    hold on
    p = patch(dnew,znew,zeros(size(dnew)));
    set(p,'FaceColor',[0.3 0.3 1])
    hold off
end

function dV = mann(h)

[A,U] = getprof(d,z,h);
R     = hydradius(A,U);
Vhat  = 1/n *R.^(2/3) * S.^(.5);
dV    = abs(Vhat-V);
end
end

function R = hydradius(A,U)

% R = A/U

R = A./U;
end

function [A,U,dnew,znew] = getprof(d,z,h)

[xint,yint,seg1] = wpolyxpoly(d,z,[min(d)-1 max(d)+1],[h h]);

dnew = [xint(1); [d((seg1(1)+1) : seg1(2))]; xint(2)];
znew = [yint(1); [z(seg1(1)+1 : seg1(2))]; yint(2)];

A = polyarea(dnew,znew);
U = max(getdistance(dnew,znew));
end



function varargout = wpolyxpoly(varargin)

% return intersections of two polylines
%
% [xint,yint] = wpolyxpoly(x1,y1,x2,y2)
% [xint,yint,seg1,seg2] = wpolyxpoly(x1,y1,x2,y2)
% [...] = wpolyxpoly(x1,y1,x2,y2,maxdist)
% [...] = wpolyxpoly(x1,y1,x2,y2,maxdist,tol)
%
% Wolfgang Schwanghart
% w.schwanghart@unibas.ch (28. January 2008)


%
% check number of input arguments
if nargin==4;
    [x1,y1,x2,y2] = varargin{:};
    flagmaxdist=0;
    tol = 1e-7;
elseif nargin==5;
    [x1,y1,x2,y2,maxdist] = varargin{:};
    flagmaxdist=1;
    tol = 1e-7;
    if ~isscalar(maxdist)
        error('maxdist must be a scalar')
    end
```

```
elseif nargin==6;
    [x1,y1,x2,y2,maxdist,tol] = varargin{:};
    flagmaxdist=1;
    if ~isscalar(maxdist)
        error('maxdist must be a scalar')
    end
    if ~isscalar(tol)
        error('tol must be a scalar')
    end
else
    error('wrong number of input arguments')
end

% check input arguments
if size(x1) ~= size(y1);
    error('x1 and y1 must have same size')
elseif size(x2) ~= size(y2);
    error('x2 and y2 must have same size')
end

% force column vectors
x1 = x1(:);
y1 = y1(:);
x2 = x2(:);
y2 = y2(:);

% number of segments in polyline 1 and 2
nrseg1 = length(x1)-1;
nrseg2 = length(x2)-1;

% start of each segment vector
stvecx1 = x1(1:end-1);
stvecy1 = y1(1:end-1);

stvecx2 = x2(1:end-1);
stvecy2 = y2(1:end-1);

% create b
srcx = bsxfun(@minus,stvecx2,stvecx1');
srcy = bsxfun(@minus,stvecy2,stvecy1');

srcx = srcx(:);
srcy = srcy(:);

% create Index for segments
IXseg1 = repmat(1:nrseg1,nrseg2,1);
IXseg1 = IXseg1(:);
IXseg2 = repmat((1:nrseg2)',1,nrseg1);
IXseg2 = IXseg2(:);

% exclude segments with starting points with a distance
% farther than maxdist
if flagmaxdist
    dis    = hypot(srcx,srcy);
    i      = logical(dis<maxdist);
    srcx   = srcx(i);
    srcy   = srcy(i);
    IXseg1 = IXseg1(i);
    IXseg2 = IXseg2(i);

    if isempty(srcx)
        varargout{1}=[];
        varargout{2}=[];
        varargout{3}=[];
        varargout{4}=[];
        return
    end
end

% list end of each segment vector
endvecx1 = x1(2:end)-stvecx1;
endvecy1 = y1(2:end)-stvecy1;
```

```
endvecx2 = x2(2:end)-stvecx2;
endvecy2 = y2(2:end)-stvecy2;

% create equation matrix
x1enh = repmat(endvecx1,1,nrseg2)';
x1enh = x1enh(:);
y1enh = repmat(endvecy1,1,nrseg2)';
y1enh = y1enh(:);

x2enh = repmat(endvecx2,nrseg1,1);
y2enh = repmat(endvecy2,nrseg1,1);

% remove values
if flagmaxdist
    x1enh = x1enh(i);
    y1enh = y1enh(i);
    x2enh = x2enh(i);
    y2enh = y2enh(i);
    clear i
end

% find parallel segments using cross products
% --> determination of the area of a parallelogram
c  = x1enh.*y2enh - y1enh.*x2enh;
i3 = abs(c)<tol;
clear c
if sum(i3) ~= 0;
    x1enh  = x1enh(~i3);
    y1enh  = y1enh(~i3);
    x2enh  = x2enh(~i3);
    y2enh  = y2enh(~i3);
    IXseg1 = IXseg1(~i3);
    IXseg2 = IXseg2(~i3);
    srcx   = srcx(~i3);
    srcy   = srcy(~i3);
    clear i3
else
    clear i3;
end

% create sparse block-diagonal matrix A

nrintmax=length(srcx);

b     = reshape([srcx srcy]',nrintmax*2,1);
col0  = reshape([x1enh y2enh]',nrintmax*2,1);
colm1 = reshape([y1enh zeros(nrintmax,1)]',nrintmax*2,1);
colp1 = reshape([zeros(nrintmax,1) x2enh ]',nrintmax*2,1);

clear x1enh y1enh x2enh y2enh

A = spdiags([colm1 col0 colp1],[-1 0 1],nrintmax*2,nrintmax*2);

% solve the set of equations Ax = b
x = A\b;
clear A b;

% reshape x
x = reshape(x,2,nrintmax)';

% find rows where alpha and beta are both between 0 and 1;
i2 = (x(:,1)>=0 & x(:,1)<1) & (x(:,2)<=0 & x(:,2)>-1);

% check last segments
% if any(x(end,:) == 1)
%     i2(end) = true;
% end

seg1=IXseg1(i2);
seg2=IXseg2(i2);

if isempty(seg1)
    varargout{1}=[];
```

```
    varargout{2}=[];
    varargout{3}=[];
    varargout{4}=[];
    varargout{5}=[];
else
    alpha = x(i2);
    int = [x1(seg1) y1(seg1)] + bsxfun(@times,[endvecx1(seg1) endvecy1(seg1)],alpha);

    varargout{1} = int(:,1);
    varargout{2} = int(:,2);
    varargout{3} = seg1;
    varargout{4} = seg2;
    varargout{5} = x(i2);
end
end
```

S7 Physical and chemical sample treatment (TCN)

Samples were crushed, sieved (125–500 μm) and magnetic minerals were removed using a Frantz magnetic separator. Quartz enrichment by at least three times diluted HF treatment and ICP measurement to exclude contaminations was accomplished at the University of Potsdam, subsequent sample treatment at the Helmholtz-Zentrum Dresden-Rossendorf (HZDR). Samples were cleaned from atmospheric ^{10}Be by three times 10% partial dissolution with HF (48%). We added one processing blank for seven samples, containing ~300 μg of the ^{9}Be carrier Phenakite DD ($3.025 \pm 0.009 \times 10^{-3}$ ^{9}Be g^{-1}) (Merchel et al., 2008); for the boulder samples we also added ~500 μg of the commercial ^{27}Al carrier ROTH (1000.5 ± 2.0 mg/L; δ = 1.011 g/cm^3) to separate Be and Al (Merchel and Herpers, 1999). BeO was mixed with Nb powder (4 × BeO mass) and Al_2O_3 with Ag powder (1 × Al_2O_3 mass) and pressed into Cu cathodes. We determined natural ^{27}Al in aliquots by ICP-AES at the University of Potsdam to calculate ^{26}Al from ^{26}Al/^{27}Al.

S8 Sample treatment (Luminescence)

We collected the samples in light-tight tubes horizontally, and immediately closed these tubes with light-tight caps and black tape after sampling. Samples were opened in the lab under red-light conditions. Sediment from the outer parts from the tubes was removed and used to determine dose rate-relevant elements using high-resolution gamma spectrometry (Preusser and Kasper, 2001). The remaining material was sieved, chemically pre-treated (HCl, H_2O_2, Na-oxalate), and the quartz and feldspar fraction was isolated using heavy liquids. Grains were mounted on stainless steel discs (2 mm aliquots). Measurements were done in a Freiberg Lexsyg Research devise (Richter et al., 2013), with modified versions of the Single Aliquot Regenerative Dose (SAR) protocol (Reimann and Tsukamoto, 2012) with an initial IRSL stimulation at 50°C for 150 s (IR-50) followed by a second stimulation at 150°C for 200 s (pIR), both using a 850 nm laser diode with 250 mW cm^{-3}. After a test dose measurement, a hot bleach at 200°C for 300 s was applied. Detection was by a ET-9235QB photomultiplier using a Schott BG39 (3 mm) and AHF BrightLine HV 414/46 interference (3.5 mm) filter. Preheating was

at 180°C (natural/regen doses) and 160°C (test dose) for 10 s each.

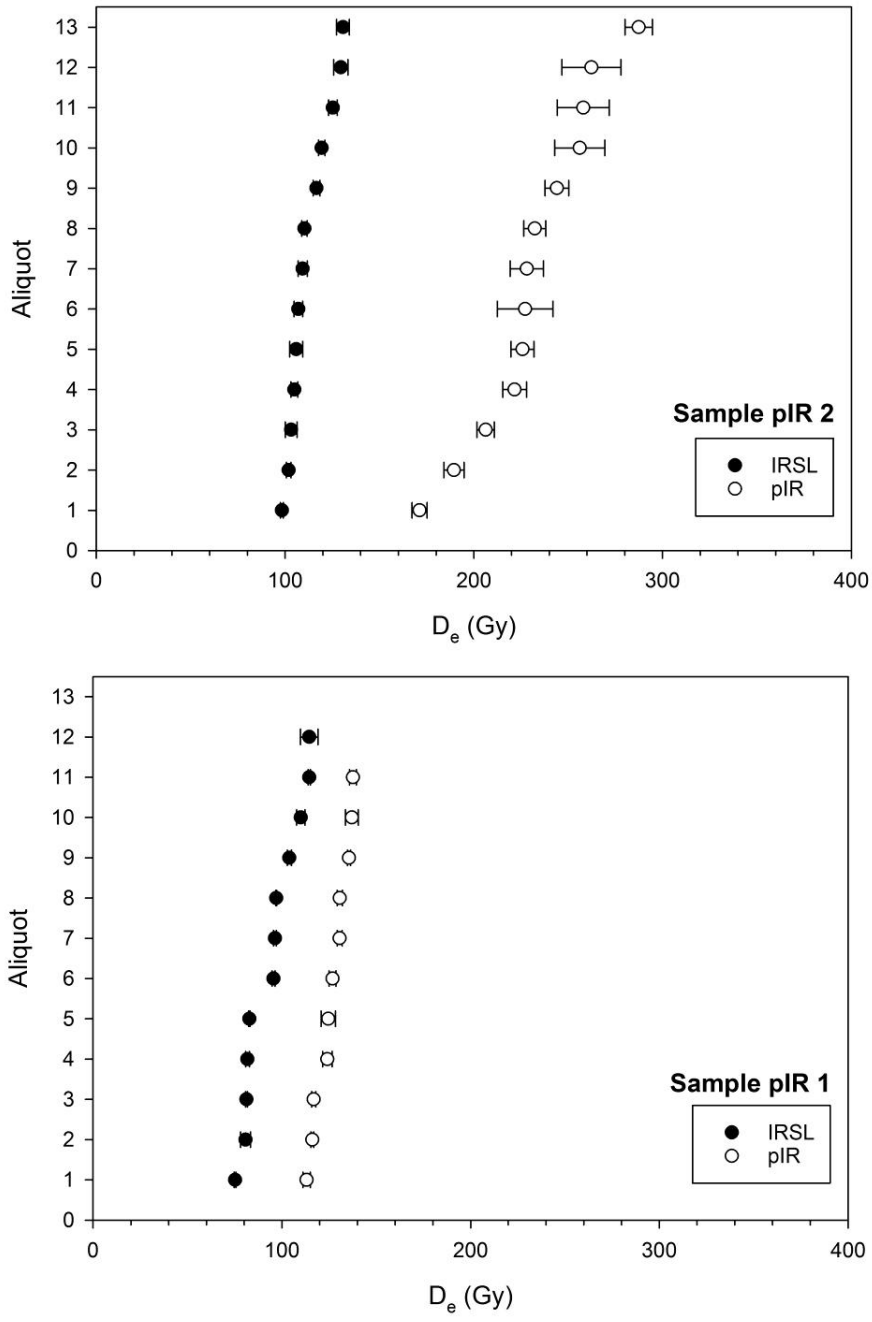

Figure S8: De distribution plots of the two luminescence samples. For sample pIR2 the pronounced spread in the De distribution of pIR implies the presence of differential leaching.

S9 Flow velocity and critical boulder transport velocity versus boulder diameter

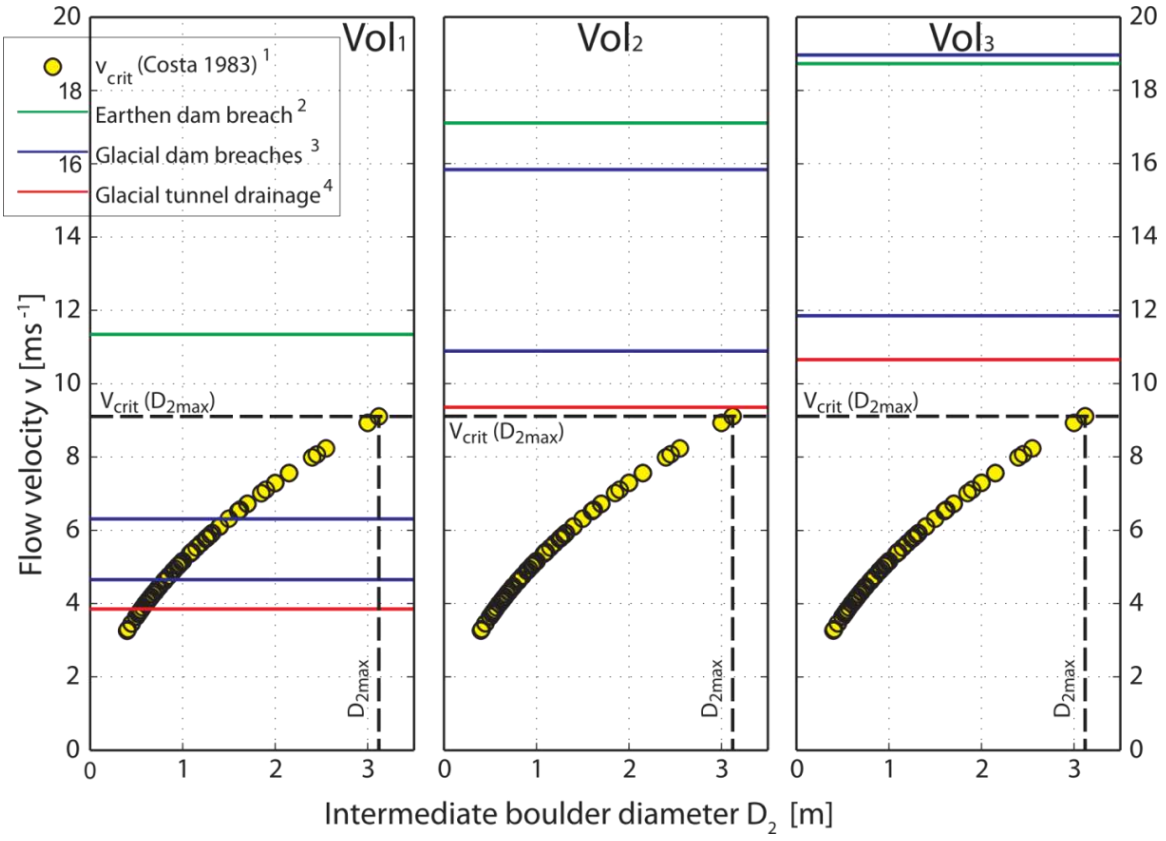

Figure S9. Exceeding the critical velocity for the biggest boulder implies that all boulders could have been transported by the flow from dam breach models by (1) Costa, 1983, (2) Walder and O'Connor, 1997, (3) Minimum for lowest and maximum velocities for highest peak discharges from glacial dam breaches by overtopping waters, and (4) Walder and Costa, 1996.

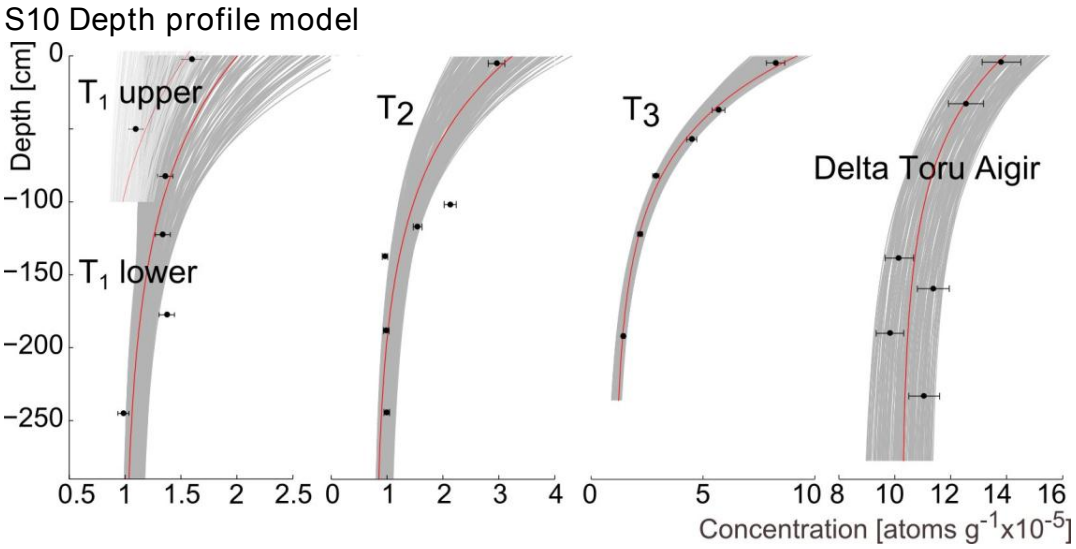

Figure S10. Depth profiles of Boam gorge outlet terraces T_{1-3}, and delta deposits at northern Issyk Kul shore (Toru Aigir) modelled with Matlab Input GUI (Hidy et al., 2010). The best fit (red) of 50,000 iterations (grey) is shown.

S11 Table of boulder exposure ages and depth profile parameters modelled with Matlab Input GUI (Hidy et al., 2010) with a ^{10}Be half-life of 1.387 ± 0.012 Ma (Chmeleff et al., 2010; Korschinek et al., 2010).

Location		10Be age [ka]	Inheritance [10^4 atoms g^{-1}]	Erosion rate [cm ka^{-1}]	26Al age [ka]	Inheritance [10^4 atoms g^{-1}]	Erosion rate [cm ka^{-1}]
Boulder TCN1	mean	19.3	0.00	0.23			
	median	19.0	0.00	0.23			
	mode	17.1	0.00	0.32			
	min chi^2	19.7	0.00	0.23			
	maximum	30.0	0.00	0.5			
	minimum	10.0	0.00	0			
	Bayesian most probable	19.5	0.00	0.39			
	Bayesian 2-sigma upper	23.2	0.00	0.48			
	Bayesian 2-sigma lower	15.7	0.00	0			
Boulder TCN2	mean	19.4	0.00	0.23	19.4	0.00	0.23
	median	19.2	0.00	0.23	19.2	0.00	0.23
	mode	13.1	0.00	0.12	10.3	0.00	0.09
	min chi^2	19.3	0.00	0.03	21.5	0.00	0.32
	maximum	30.0	0.00	0.5	30	0.00	0.50
	minimum	10.0	0.00	0.00	10	0.00	0.00
	Bayesian most probable	20.0	0.00	0.35	20	0.00	0.33
	Bayesian 2-sigma upper	26.1	0.00	0.48	29.3	0.00	0.48
	Bayesian 2-sigma lower	12.9	0.00	0	10	0.00	NaN
Boulder TCN3	mean	20.1	0.00	0.24	19.3	0.00	0.23
	median	20.0	0.00	0.23	19.0	0.00	0.23
	mode	18.8	0.00	0.25	12.1	0.00	0.01

	min chi^2	19.7	0.00	0.03	18.8	0.00	0.3
	maximum	27.3	0.00	0.5	30.0	0.00	0.5
	minimum	14.2	0.00	0	10.0	0.00	0
	Bayesian most probable	20.5	0.00	0.42	18.6	0.00	0.33
	Bayesian 2-sigma upper	22.1	0.00	0.46	27.2	0.00	0.48
	Bayesian 2-sigma lower	18.3	0.00	0	10.6	0.00	0
TCN 4 (T1 lower)	mean	8.6	8.87	0.05			
	median	7.5	9.04	0.03			
	mode	1.3	9.44	0.01			
	min chi^2	7.2	9.83	0.03			
	maximum	24.9	10	0.45			
	minimum	1	7.01	0			
	Bayesian most probable	11.4	10	0.05			
	Bayesian 2-sigma upper	11.3	9.99	0.05			
	Bayesian 2-sigma lower	1.4	8.92	NaN			
TCN 4 (T1 upper)	mean	3.4	8.47	0.1			
	median	2.9	8.44	0.07			
	mode	1.3	7.69	0.03			
	min chi^2	5.1	7.16	0.09			
	maximum	8.7	10	0.48			
	minimum	1	7	0			
	Bayesian most probable	6.2	7	0.11			
	Bayesian 2-sigma upper	6.1	9.42	0.14			
	Bayesian 2-sigma lower	NaN	NaN	NaN			
TCN 5 (T2)	mean	17.9	7.91	0.49			
	median	17.6	7.89	0.49			
	mode	17.2	7.49	0.63			
	min chi^2	17.4	7.74	0.01			
	maximum	31.3	10	1			
	minimum	10	6	0			
	Bayesian most probable	18.6	7.42	0.53			
	Bayesian 2-sigma upper	22.6	9.1	0.96			
	Bayesian 2-sigma lower	13.6	6.23	0.02			
TCN 6 (T3)	mean	63.6	8.28	0.44			
	median	63.1	8.2	0.44			
	mode	62.5	7.72	0.44			
	min chi^2	72.6	9.98	0.39			
	maximum	80	11	0.6			
	minimum	50	6	0.3			
	Bayesian most probable	66.3	8.39	0.47			
	Bayesian 2-sigma upper	77.1	10.7	0.58			
	Bayesian 2-sigma lower	53.9	6.14	0.3			
TCN 7 (Delta Toru Aigir)	mean	25	101.14	0.4			
	median	25	101.09	0.4			
	mode	25	102.6	0.25			
	min chi^2	22	103.38	0.22			
	maximum	30	115.27	0.6			
	minimum	20	86.52	0.2			
	Bayesian most probable	22.2	100.55	0.55			
	Bayesian 2-sigma upper	29.6	109.38	0.59			
	Bayesian 2-sigma lower	20.1	92.41	0.21			

S12 Table of yearly average and maximum discharge values for Chu and Chon Kemin rivers (water cadastre, 1987)

River	Time	Average yearly discharge [m^3s^{-1}]	Maximum discharge [m^3s^{-1}]	Minimum discharge [m^3s^{-1}]
River Chu- river mouth Chon-Kemin	1957-1985	27.3	155 (17.07.1958)	0.63 (14.02.1958)
River Chu-v.Kochkor	1931-1985	27.1	242 (19.06.1966)	9.20 (29.05.1985)
River Chon-Kemin (mouth)	1935-1985	21.8	189 (15.07.1958)	6.00 (15.01.1974)
River Chu-river mouth Kutemaldy	1910-1962	–	112 (1962)	0.00 (1962)

Bibliography

Abdrakhmatov, K. and A. Strom (2002): "Rockslides and rock avalanches of the central and northern Tien Shan," *In: Evans, S.G. and Martino, S. (eds.), NATO advanced research workshop, Celano (AQ), Italy, June 16-21, 2002: Massive rock slope failure: New models for hazard assessment*, 1–6.

Abdrakhmatov, K. E., K. D. Djanuzakov, and D. Delveaux (2002): "Active tectonics and seismic hazard of the Issyk-Kul basin in the Kyrgyz Tian-Shan," *In: Klerkx, J. and Imanackunov, B. (eds.), NATO Science Series, Lake Issyk-Kul : Its Natural Environment*, 147 – 160.

Aizen, V., E. Aizen, J. Melack, and T. Martma (1996): "Isotopic measurements of precipitation on central Asian glaciers (southeastern Tibet, northern Himalayas, central Tien Shan)," *Journal of Geophysical Research*, 101, 9185.

Aizen, V. B., E. M. Aizen, D. R. Joswiak, K. Fujita, N. Takeuchi, and S. A. Nikitin (2006): "Climatic and atmospheric circulation pattern variability from ice-core isotope/geochemistry records (Altai, Tien Shan and Tibet)," *Annals of Glaciology*, 43, 49–60.

Aizen, V. B., E. M. Aizen, and J. M. Melack (1995): "Climate, Snow Cover, Glaciers, and Runoff in the Tien Shan, Central Asia1," *JAWRA Journal of the American Water Resources Association*, 31, 1113–1129.

Aizen, V. B., E. M. Aizen, J. M. Melack, and J. Dozier (1997):

"Climatic and hydrologic changes in the Tien Shan, central Asia," *Journal of Climate*, 10, 1393–1404.

Aizen, V. B., V. A. Kuzmichenok, A. B. Surazakov, and E. M. Aizen (2007): "Glacier changes in the Tien Shan as determined from topographic and remotely sensed data," *Global and Planetary Change*, 56, 328–340.

Akhmadaliev, S., R. Heller, D. Hanf, G. Rugel, and S. Merchel (2013): "The new 6 MV AMS-facility DREAMS at Dresden," *Nuclear Instruments and Methods in Physics Research Section B: Beam Interactions with Materials and Atoms*, 294, 5–10.

Andres, N., D. Palacios, S. Brynjólfsson, and o. Sæmundsson (2015): "Time needed for first lichen colonization of terminal moraines in the Tröllaskagi peninsula (North Iceland)," *Geophysical Research Abstracts, EGU General Assembly 2015*, 17, EGU2015–9873–2.

Angillieri, M. (2010): "Application of frequency ratio and logistic regression to active rock glacier occurrence in the Andes of San Juan, Argentina," *Geomorphology*, 114, 396–405.

Archer, D., N. Forsythe, H. Fowler, and S. Shah (2010): "Sustainability of water resources management in the Indus Basin under changing climatic and socio economic conditions," *Hydrology and Earth System Sciences*, 14, 1669–1680.

Arenson, L. and M. Jakob (2010): "The significance of rock glaciers in the dry Andes - A discussion of Azócar and Brenning (2010) and Brenning and Azócar (2010)," *Permafrost and Periglacial Processes*, 21, 282—-285.

Armstrong, R. a. (1983): "Growth Curve of the Lichen Rhizocarpon geographicum," *New Phytologist*, 94, 619–622.

Armstrong, R. A. (2011): "The biology of the crustose lichen Rhizocarpon geographicum," *Symbiosis*, 55, 53–67.

Avouac, J.-P. and P. Tapponnier (1993): "Kinematic model of active deformation in Central Asia," *Geophysical Research Letters*, 20, 895–898.

Azócar, G. F. and A. Brenning (2010): "Hydrological and geomorphological significance of rock glaciers in the dry Andes, Chile (27°-33°S)," *Permafrost and Periglacial Processes*, 21, 42–53.

Baker, V. R. (1973): "Paleohydrology and sedimentology ok {Lake Missoula} flooding in eastern {Washington}," *Geological Society of America Special Paper*, 144.

Barsch, D. (1977): "Nature and importance of mass-wasting by rock glaciers in Alpine permafrost environments," *Earth Surface Processes*, 2, 231–245.

——— (1992): "Permafrost Creep and Rockglaciers," *Permafrost and Periglacial Processes*, 3, 175–188.

——— (1996): *Rockglaciers: Indicators for the Present and Former Geoecology in High Mountain Environments*, Springer Berlin Heidelberg.

Benedict, J. (1990a): "Experiments on lichen growth I. Seasonal patterns and environmental controls," *Arctic and Alpine Research*, 22, 244–254.

——— (1990b): "Winter frost injury to lichens: Colorado front range," *The Bryologist*, 93, 423–426.

——— (1991): "Experiments on lichen growth II. Effects of a seasonal snow cover," *Arctic and Alpine Research*, 23, 189–199.

Berg, L. (1904): "Lake Issyk-Kul (in Russian)," *Zemlevedeniye*, 1–85.

Berthling, I. (2011): "Beyond confusion: Rock glaciers as cryo-conditioned landforms," *Geomorphology*, 131, 98–106.

Beschel, R. E. (1973): "Lichens as a measure of the age of recent moraines," *Arctic, Antarctic, and Alpine Research*, 5, 303–309.

Bindi, D., S. Parolai, A. Gomez-Capera, M. Locati, Z. Kalmetyeva, and N. Mikhailova (2014): "Locations and magnitudes of earthquakes in Central Asia from seismic intensity data," *Journal of Seismology*, 18, 1–21.

Bodin, X., S. Jaillet, A. Rabatel, and E. Thibert (2016a): "Multitemporal mapping of rock glacier displacements: insights from SfM , ALS and TLS high-resolution datasets on the Laurichard rock glacier, French Alps," *In: Conference Paper, XI. International Conference on Permafrost*, Abstract of Contribution 1119.

Bodin, X., J. M. Krysiecki, P. Schoeneich, O. Le Roux, L. Lorier, T. Echelard, M. Peyron, and A. Walpersdorf (2016b): "The 2006 Collapse of the Bérard Rock Glacier (Southern French Alps)," *Permafrost and Periglacial Processes*, 28, 209–223.

Boeckli, L., a. Brenning, S. Gruber, and J. Noetzli (2012): "A statistical approach to modelling permafrost distribution in the European Alps or similar mountain ranges," *The Cryosphere*, 6, 125–140.

Bogdanovitch, K., I. Kark, B. Korolkov, and D. Musketov (1914): "Earthquake of the 4th January 1911 in the northern districts of the Tien Shan," *Tr. Geol. Com. Ser*, 89.

Bolch, T. (2007): "Climate change and glacier retreat in northern Tien Shan (Kazakhstan/Kyrgyzstan) using remote sensing data," *Global and Planetary Change*, 56, 1–12.

Bolch, T. and A. P. Gorbunov (2014): "Characteristics and origin of rock glaciers in the northern Tien Shan (Kazakhstan/ Kyrgyzstan)," *Permafrost and Periglacial Processes*, 25, 320–332.

Bolch, T., a. Kulkarni, a. Kaab, C. Huggel, F. Paul, J. G. Cogley, H. Frey, J. S. Kargel, K. Fujita, M. Scheel, S. Bajracharya, and M. Stoffel (2012): "The State and Fate of Himalayan Glaciers," *Science*, 336, 310–314.

Bolch, T. and S. Marchenko (2006): "Significance of glaciers, rock-glaciers, and ice-rich permafrost in the Northern Tien Shan as water towers under climate change conditions," *Proceedings of the workshop "Assessment of snow-glacier and water resources in Asia"*, 199–211.

Bollmann, E., A. Girstmair, S. Mitterer, and J. Stötter (2015): "A Rock Glacier Activity Index Based on Rock Glacier Thickness Changes and Displacement Rates Derived From Airborne Laser Scanning," *Permafrost and Periglacial Processes*, 26, 347–359.

Bondarev, L. and D. Sevastianov (1991): "Relief of shores and lake bottom," in *The history o f Sevan, Issyk Kul, Balkhash, Zaisan and Aral Lakes*, Nauka Leningrad, 78–86.

Bookhagen, B., R. C. Thiede, and M. R. Strecker (2005): "Late Quaternary intensified monsoon phases control landscape evolution in the northwest Himalaya," *Geology*, 33, 149–152.

Bowman, D., A. Korjenkov, and N. Porat (2004a): "Late-Pleistocene seismites from Lake Issyk-Kul, the Tien Shan range, Kyrghyzstan," *Sedimentary Geology*, 163, 211–228.

Bowman, D., A. Korjenkov, N. Porat, and B. Czassny (2004b): "Morphological response to Quaternary deformation at an intermontane basin piedmont, the northern Tien Shan, Kyrghyzstan," *Geomorphology*, 63, 1–24.

Bradwell, T. (2009): "Lichenometric dating: A commentary, in the light of some recent statistical studies," *Geografiska Annaler, Series A: Physical Geography*, 91, 61–69.

Bradwell, T. and R. A. Armstrong (2007): "Growth rates of Rhizocarpon geographicum lichens: a review with new data from Iceland," *Journal of Quaternary Science*, 22, 311–320.

Brenning, A. (2005): "Climatic and geomorphological controls of rock glaciers in the Andes of Central Chile: Combining statistical modelling and field mapping." 114.

——— (2009): "Benchmarking classifiers to optimally integrate terrain analysis and multispectral remote sensing in automatic rock glacier detection," *Remote Sensing of Environment*, 113, 239–247.

Brenning, A. and D. Trombotto Liaudat (2006): "Logistic regression modeling of rock glacier and glacier distribution: Topographic and climatic controls in the semi-arid Andes," *Geomorphology*, 81, 141–154.

Bull, W. B. (2014): "Using earthquakes to assess lichen growth rates," *Geografiska Annaler, Series A: Physical Geography*, 96, 117–133.

Bull, W. B., M. T. Brandon, and N. Haven (1998): "Lichen dating of earthquake-generated regional rock-fall events, Southern Alp, New Zealand," *Geological Society of America Bulletin*, 110, 60–84.

Burger, K., J. Degenhardt, and J. Giardino (1999): "Engineering geomorphology of rock glaciers," *Geomorphology*, 31, 93–132.

Burgette, R. J. (2008): "Uplift response to tectonic convergence: The Kyrgyz Tian Shan and cascadia subduction zone, PhD Thesis, University of Oregon," 242.

Burgette, R. J., R. J. Weldon, K. Y. Abdrakhmatov, C. Ormukov, L. A. Owen, and S. C. Thompson (2017): "Timing and process of river and lake terrace formation in the Kyrgyz Tien Shan," *Quaternary Science Reviews*, 159, 15–34.

Buslov, M., J. Klerkx, K. Abdrakhmatov, D. Delveaux, V. Y. Batalev, O. Kuchai, B. Dehandschutter, and A. Muraiev (2003): "Recent strike-slip deformation of the nortehrn Tien Shan," *Geological Society, London, Special Publications*, 210, 53–64.

Buslov, M. M. (2004): "Cenozoic tectonics of Central Asia: Basement control," *Himalayan Journal of Sciences*, 2, 104–105.

Buylaert, J.-P., M. Jain, A. S. Murray, K. J. Thomsen, C. Thiel, and R. Sohbati (2012): "A robust feldspar luminescence dating method for Middle and Late Pleistocene sediments," *Boreas*, 41, 435–451.

Calkin, P. E. and J. M. Ellis (1984): "Development and Application of a Lichenometric Dating Curve, Brooks Range, Alaska," *Developments in Palaeontology and Stratigraphy*, 7, 227–246.

Carling, P., A. Kirkbride, S. Parnachov, P. Borodavko, and G. Berger (2002): "Late Quaternary catastrophic flooding in th Altai Mountains of south-central Siberia: a synoptic overview and an introduction to flood deposit sedimentology," in *Special Publication Number 32 of the International Association of Sedimentologists: Flood and Megaflood processes and deposits: Recent and ancient examples*, ed. by I. P. Martini, V. R. Baker, and G. Garzón, Blackwell Publishing Ltd., Oxford, UK, 17–35.

Chmeleff, J., F. von Blanckenburg, K. Kossert, and D. Jakob (2010): "Determination of the 10Be half-life by multicollector ICP-MS and liquid scintillation counting," *Nuclear Instruments and Methods in Physics Research, Section B: Beam Interactions with Materials and Atoms*, 268, 192–199.

Clague, J. J. and S. G. Evans (1994): "Formation and failure of natural dams in the Canadian Cordillera," *Geological Society of America Bulletin*, 100, 1054 – 1068.

climate-zone.com (2017): "climate-zone.com," .

Cooley, D., P. Naveau, V. Jomelli, A. Rabatel, and D. Grancher (2006): "A Bayesian hierarchical extreme value model for lichenometry," *Environmetrics*, 17, 555–574.

Costa, J. (1983): "Paleohydraulic reconstruction of flash-flood peaks from boulder deposits in the Colorado Front Range," *Geological Society of America Bulletin*, 94, 986–1004.

Costa, J. E. and R. L. Schuster (1988): "Formation and Failure of Natural Dams." *Bulletin of the Geological Society of America*, 100, 1054–1068.

Cremonese, E., S. Gruber, M. Phillips, P. Pogliotti, L. Boeckli, J. Noetzli, C. Suter, X. Bodin, A. Crepaz, A. Kellerer-Pirklbauer, K. Lang, S. Letey, V. Mair, U. Morra Di Cella, L. Ravanel, C. Scapozza, R. Seppi, and A. Zischg (2011): "Brief communication: "An inventory of permafrost evidence for the European Alps"," *Cryosphere*, 5, 651–657.

Cross, W., E. Howe, and F. Ransome (1905): "Silverton Folio Colorado," *USGS*, Folio No. 120.

Das, I., A. Stein, N. Kerle, and V. K. Dadhwal (2012): "Landslide susceptibility mapping along road corridors in the Indian Himalayas using Bayesian logistic regression models," *Geomorphology*, 179, 116–125.

Davis, W. (1882): "On the classification of lake basins," *Boston Society of Natural History Proceedings*, 21, 315–381.

De Batist, M., Y. Imbo, P. Vermeesch, J. Klerkx, S. Giralt, D. Delvaux, V. Lignier, C. Beck, I. Kalugin, and K. Abdrakhmatov (2002): "Bathymetry and sedimentary environments of Lake Issyk-Kul, Kyrgyz Republic (Central Asia): A large, high-altitude, tectonic lake," 23.

Decaulne, A. (2016): "Lichenometry in Iceland, results and application," *Géomorphologie*, 22, 77–91.

Delaloye, R., C. Lambiel, and I. Gärtner-Roer (2010): "Overview of rock glacier kinematics research in the Swiss Alps: seasonal rhythm, inter-

annual variations and trends over several decades," *Geographica Helvetica*, 65, 135–145.

Delaney, K. B. and S. G. Evans (2011): *Natural and Artificial Rockslide Dams*, vol. 133.

Etzelmüller, B., E. S. Flo Heggem, N. Sharkhuu, R. Frauenfelder, A. Kääb, and C. Goulden (2006): "Mountain permafrost distribution modelling using a multi-criteria approach in the Hövsgöl area, Northern Mongolia," *Permafrost and Periglacial Processes*, 17, 91–104.

Falaschi, D., T. Tadono, and M. Masiokas (2015): "Rock Glaciers in the Patagonian Andes: An Inventory for the Monte San Lorenzo (Cerro Cochrane) Massif, 47° S," *Geografiska Annaler, Series A: Physical Geography*, 97, 769–777.

Fick, S. and R. Hijmans (2017): "WorldClim 2: new 1-km spatial resolution climate surfaces for global land areas," *International Journal of Climatology*, 37.

Foulds, S. a., H. M. Griffiths, M. G. Macklin, and P. a. Brewer (2014): "Geomorphological records of extreme floods and their relationship to decadal-scale climate change," *Geomorphology*, 216, 193–207.

Frauenfelder, R. and A. Kääb (2000): "Towards a palaeoclimatic model of rock-glacier formation in the Swiss Alps," *Annals of Glaciology*, 31, 281–286.

Fread, D. (1992): "Flood routing models and the Manning n," in *International Conference for Centennial of Manning's Formula and Kuichling's Rational Formula*, ed. by B. C. Yen, Water Resources Publications, 421–436.

García-Castellanos, D. (2006): "Long-term evolution of tectonic lakes: Climatic controls on the development of internally drained basins," *Geological Society of America Special Papers*, 398, 283–294.

Garcin, Y., A. Junginger, D. Melnick, D. O. Olago, M. R. Strecker, and M. H. Trauth (2009): "Late Pleistocene-Holocene rise and collapse of Lake Suguta, northern Kenya Rift," *Quaternary Science Reviews*, 28, 911–925.

Garibotti, I. A. and R. Villalba (2017): "Colonization of mid- and late-Holocene moraines by lichens and trees in the Magellanic sub-Antarctic province," *Polar Biology*, 40, 1739–1753.

Gärtner-Roer, I. (2012): "Sediment transfer rates of two active rock-glaciers in the Swiss Alps," *Geomorphology*, 167-168, 45–50.

Gerasimov, I. (1953): "Paleogeographical puzzle of Lake Issyk-Kul (in Russian)," in *Geographical investigations in Central Tien Shan*, Izd. Acad. Nauk, Moscow, 69–83.

Getker, M. I. E. (1988): "Meteorological Recommendations for Calculations of Snow Cover Characteristics in the Middle Asia Mountains, Tashkent." *Hydrometeo Publishing, Leningrad, USSR*, 145 pp. (in Russian).

Giardino, J., R. Netra, and J. Vitek (2011): "Rock Glaciers," *Encyclopedia of Earth Sciences Series*, 943–948.

Giardino, J. R. and J. D. Vitek (1988): "The significance of rock glaciers in the glacial-periglacial landscape continuum," *Journal of Quaternary Science*, 3, 97–103.

Giese, E. and I. Mossig (2004): "Klimawandel in Zentralasien," *Discussion Paper/Zentrum für Internationale Entwicklungs- und Umweltforschung, Justus-Liebig-Universität Gießen*, 70.

Giralt, S., R. Julià, J. Klerkx, S. Riera, S. Leroy, T. Buchaca, J. Catalan, M. D. Batist, C. Beck, V. Bobrov, V. Gavshin, I. Kalugin, F. Sukhorukov, M. Brennwald, R. Kipfer,

F. Peeters, S. Lombardi, V. Matychenkov, Vladimir Romanovsky, V. Podsetchine, and N. Voltattorni (2003): "1 000-year environmental history of Lake Issyk-Kul," 30.

Golledge, N. R., J. D. Everest, T. Bradwell, and J. S. Johnson (2010): "Lichenometry on Adelaide Island, Antarctic Peninsula: Size-frequency studies, growth rates and snowpatches," *Geografiska Annaler, Series A: Physical Geography*, 92, 111–124.

Gorbunov, A. (1983): "Rock glaciers in the mountains of Middle Asia," in *Proceedings of the 4th International Conference on Permafrost*, Washington DC, 359–362.

——— (1996): "Monitoring the evolution of permafrost in the Tien Shan," *Permafrost and Periglacial Processes*, 7, 297–298.

Gorbunov, A. P., S. N. Titkov, and V. G. Polyakov (1992): "Dynamics of rock glaciers of the northern Tien Shan and the Djungar Ala Tau, Kazakhstan," *Permafrost and Periglacial Processes*, 3, 29–39.

Grosswald, M., M. Kuhle, and J. Fastook (1994): "Würm Glaciation of Lake Issyk-Kul Area, Tien Shan Mts.: A Case Study in Glacial History of Central Asia," *GeoJournal*, 33.2, 273–310.

Gruber, S., R. Fleiner, E. Guegan, P. Panday, M.-O. Schmid, D. Stumm, P. Wester, Y. Zhang, and L. Zhao (2017): "Review article: Inferring permafrost and permafrost thaw in the mountains of the Hindu Kush Himalaya region," *The Cryosphere*, 11, 81–99.

Haeberli, W. (1985): "Creep of mountain permafrost: Internal structure and flow of alpine rock glaciers," in *Mitteilungen der Versuchsanstalt für Wasserbau, Hydrologie und Glaziologie*, ed. by D. Vischer, Eidgenössische Technische Hochschule Zürich, 77.

Haeberli, W., B. Hallet, L. Arenson, R. Elconin, O. Humlum, and A. Kääb (2006): "Permafrost creep and rock glacier dynamics," *Permafrost and Periglacial Processes*, 17, 189–214.

Haeberli, W., M. Hoelzle, A. Kääb, F. Keller, D. Vonder Müll, and S. Wagner (1998): "Ten years after drilling through the permafrost of the active rock glacier Murtèl, Eastern Swiss Alps: Answered questions and new perspectives," *PERMAFROST - Seventh International Conference*, 403–410.

Haeberli, W. and D. Vonder Mühll (1996): "On the characteristics and possible origins of ice in rock glacier permafrost," *Zeitschrift fur Geomorphologie*, Supplementband 104, 43–57.

Hales, T. C. and J. J. Roering (2007): "Climatic controls on frost cracking and implications for the evolution of bedrock landscapes," *Journal of Geophysical Research: Earth Surface*, 112, 14.

Harris, S., G. Cheng, X. Zhao, and D. Yongqin (1998): "Nature and Dynamics of an Active Block Stream, Kunlun Pass, Qinghai Province, People's Republic of China," *Geografiska Annaler, Series A: Physical Geography*, 80A, 123–133.

Havenith, H. B., A. Strom, F. Calvetti, and D. Jongmans (2003): "Seismic triggering of landslides. Part B: Simulation of dynamic failure processes," *Natural Hazards and Earth System Science*, 3, 663–682.

Hayat, T., I. Khan, H. Shah, M. U. Qureshi, S. Karamat, and I. Towhata (2010): "Attabad landslide - dam disaster in Pakistan 2010," *ISSMGE Bulletin*, 4, 20–31.

Heindel, R. C., L. E. Culler, and R. A. Virginia (2017): "Rates and processes of aeolian soil erosion in West Greenland," *The Holocene*, 27, 1281–1290.

Herget, J. (2005): "Reconstruction of Pleistocene ice-dammed lake outburst floods in the Altai mountains, Siberia," *The Geological Society of America*, Special Paper, 118.

Hermanns, R., S. Niedermann, S. Ivy-Ochs, and P. Kubik (2004): "Rock avalanching into a landslide-dammed lake causing multiple dam

failure in Las Conchas valley (NW Argentina) — evidence from surface exposure dating and stratigraphic analyses," *Landslides*, 1, 113–122.

Hermanns, R. and M. Strecker (1999): "Structural and lithological controls on large Quarternary rock svalanches (sturzstroms) in arid northwestern Argentina," *Geological Society of America Bulletin*, 111, 934–948.

Hewitt, K. (2014): "Rock glaciers and related phenomena," in *Glaciers of the Karakoram Himalaya: Glacial environments, processes, hazards and resources, Advances in Asian Human-Environmental Research*, Dordrecht: Springer Science+Business Media, 267–289.

Hewitt, K., J. J. Clague, and J. F. Orwin (2008): "Legacies of catastrophic rock slope failures in mountain landscapes," *Earth-Science Reviews*, 87, 1–38.

Hidy, A. J., J. C. Gosse, J. L. Pederson, J. P. Mattern, and R. C. Finkel (2010): "A geologically constrained Monte Carlo approach to modeling exposure ages from profiles of cosmogenic nuclides: An example from Lees Ferry, Arizona," *Geochemistry, Geophysics, Geosystems*, 11, 18.

Higuchi, K., H. Fushimi, T. Ohata, S. Iwata, K. Yokoyama, H. Higuchi, A. Nagoshi, and T. Iozawa (1978): "Preliminary report on glacier inventory in the Dudh Kosi Region," *Journal of the Japanese Society of Snow and Ice*, 40, 78–79.

Hubbard, A., T. Bradwell, N. Golledge, A. Hall, H. Patton, D. Sug-den, R. Cooper, and M. Stoker (2009): "Dynamic cycles, ice streams and their impact on the extent, chronology and deglaciation of the British-Irish ice sheet," *Quaternary Science Reviews*, 28, 759–777.

Humlum, O. (1998): "The Climatic Significance of Rock Glaciers," *Permafrost and Periglacial Processes*, 9, 375—395.

Huss, A., B. Bookhagen, C. Higgel, D. Jacobsen, R. Bradley, J. Clague, M. Vuille, W. Buytaert, D. Cayan, G. Greenwood,

B. Mark, A. Milner, R. Weingartner, and M. Winder (2017): "Toward mountains without permanent snow and ice," *Earth's Future*, 5, 418—-435.

Ikeda, A. and N. Matsuoka (2002): "Degradation of talus-derived rock glaciers in the upper engadin, Swiss alps," *Permafrost and Periglacial Processes*, 13, 145–161.

Immerzeel, W., L. van Beek, and M. Bierkens (2010): "Climate change will affect the Asian water towers," *Science*, 328, 1382–1385.

Innes, J. L. (1983): "Size frequeny distribution as a lichenometric tecnique: an assessment," *Arctic and Alpine Research*, 15, 285–294.

——— (1985): "Lichenometry," *Progress in Physical Geography*, 9, 187–254.

Iribarren Anacona, P., A. Mackintosh, and K. P. Norton (2015): "Hazardous processes and events from glacier and permafrost areas: Lessons from the Chilean and Argentinean Andes," *Earth Surface Processes and Landforms*, 40, 2–21.

Ischuk, A. R. (2011): "Usoi Rockslide Dam and Lake Sarez, Pamir Mountains, Tajikistan," in *Natural and Artificial Rockslide Dams*, ed. by S. G. Evans, R. L. Hermanns, A. Strom, and G. Scarascia-Mugnozza, Springer Berlin Heidelberg, vol. 133 of *Lecture Notes in Earth Sciences*, 423–440.

Jacobson, R., J. O'Connor, and T. Oguchi (2003): "Surficial geologic tools in fluvial geomorphology," in *Tools in fluvial geomorphology*, ed. by G. Kondolf and H. Piégay, John Wiley & Sons, 25–57.

Janke, J. R. (2005): "Modeling past and future alpine permafrost distribution in the Colorado Front Range," *Earth Surface Processes and Landforms*, 30, 1495–1508.

——— (2013): "Using airborne LiDAR and USGS DEM data for assessing rock glaciers and glaciers," *Geomorphology*, 195, 118–130.

Janke, J. R., A. C. Bellisario, and F. A. Ferrando (2015): "Classification of debris-covered glaciers and rock glaciers in the Andes of central Chile," *Geomorphology*, 241, 98–121.

Janský, B., M. Šobr, and Z. Engel (2010): "Outburst flood hazard: Case studies from the Tien-Shan Mountains, Kyrgyzstan," *Limnologica*, 40, 358–364.

Janský, B., M. Sobr, and S. Yerokhin (2006): "Typology of high mountain lakes of Kyrgyzstan with regard to the risk of their rupture," *Limnol. Rev.*, 6, 135–140.

Johnsen, T. and T. Brennand (2004): "Late-glacial lakes in the Thompson Basin, British Columbia: paleogeography and evolution," *Canadian Journal of Earth Science*, 41, 1367–1383.

Jomelli, V., D. Grancher, P. Naveau, D. Cooley, and D. Brunstein (2007): "Assessment study of lichenometric methods for dating surfaces," *Geomorphology*, 86, 131–143.

Jones, D., S. Harrison, K. Anderson, H. Selley, J. Wood, and R. Betts (2018): "The distribution and hydrological significance of rock glaciers in the Nepalese Himalaya," *Global and Planetary Change*, 160, 123—-142.

Kalmetieva, Z., A. Mikolaichuk, B. Moldobekov, A. Meleshko, M. Jantaev, and A. Zubovich (2009): "Atlas of Earthquakes in Kyrgyzstan," *Central-Asian Institute for Applied Geosciences and United Nations International Strategy for Disaster Reduction Secretariat Office in Central Asia, Bishkek*, 176.

Kellerer-Pirklbauer, A., B. Wangensteen, H. Farbrot, and B. Etzelmüller (2008): "Relative surface age-dating of rock glacier systems near Hólar in Hjaltadalur, northern Iceland," *Journal of Quaternary Science*, 23, 137–151.

Kipfer, R. (2011): "personal communication," .

Kirkbride, M. and A. Dugmore (2001): "Can Lichenometry be Used to Date the "Little Ice Age" Glacial Maximum in Iceland?" *Climatic Change*, 48, 151–167.

Konrad, S. K. and D. H. Clark (1998): "Evidence for an Early Neoglacial Glacier Advance from Rock Glaciers and Lake Sediments in the Sierra Nevada, California, U.S.A." *Arctic and Alpine Research*, 30, 272–284.

Koppes, M., A. R. Gillespie, R. M. Burke, S. C. Thompson, and J. Stone (2008): "Late Quaternary glaciation in the Kyrgyz Tien Shan," *Quaternary Science Reviews*, 27, 846–866.

Korjenkov, A. (2011): "personal communication," .

Korjenkov, A. M., I. E. Povolotskaya, and E. Mamyrov (2007): "Morphologic expression of Quaternary deformation in the northwestern foothills of the Ysyk-Kol basin, Tien Shan," *Geotectonics*, 41, 130–148.

Korschinek, G., U. Bergmaier, A. Faestermann, T. Gerstmann, K. Knie, G. Rugel, A. Wallner, I. Dillmann, G. Dollinger, K. von Gostomski, C.L. Kossert, M. Maiti, M. Poutivtsev, and A. Remmert (2010): "A new value for the half-life of 10Be by heavy ion elastic recoil detection and liquid scintillation counting," *Nucl. Instrum. Methods Phys. Res. Sect. B Beam Interact. Mater. Atoms*, 268.

Korup, O. (2005): "Geomorphic hazard assessment of landslide dams in South Westland, New Zealand: Fundamental problems and approaches," *Geomorphology*, 66, 167–188.

Korup, O., J. J. Clague, R. L. Hermanns, K. Hewitt, A. L. Strom, and J. T. Weidinger (2007): "Giant landslides, topography, and erosion," *Earth and Planetary Science Letters*, 261, 578–589.

Koshoev, M. (1986): "Assessment of dangerous nival and glacial events in the Issyk-Kul/Chu territorial complex," *Moscow State University, Doctoral Thesis (unpublished)*.

Kruschke, J. K. (2012): "Bayesian Estimation Supersedes the t Test." *Journal of Experimental Psychology: General*, 142, 573–603.

Larsen, I. J. and M. P. Lamb (2016): "Progressive incision of the Channeled Scablands by outburst floods," *Nature*, 538, 229–232.

Lehmkuhl, F., M. Klinge, H. Rother, and D. Hülle (2016): "Distribution and timing of Holocene and late Pleistocene glacier fluctuations in western Mongolia," *Annals of Glaciology*, 57, 1–10.

Lehmkuhl, F., G. Stauch, and O. Batkhishig (2003): "Rock glacier and periglacial processes in the Mongolian Altai," *Proceedings of the Eighth International Conference of Permafrost, Zürich, Switzerland.*, 639–644.

Lilleøren, K. and B. Etzelmüller (2011): "Aregional inventory of rock glaciers and ice-cored moraines in Norway," *Geografiska Annaler: Series A, Physical Geography*, 93, 175–191.

Loso, M. G. and D. F. Doak (2006): "The biology behind lichenometric dating curves." *Oecologia*, 147, 223–229.

Lowick, S., M. Trauerstein, and F. Preusser (2012): "Testing the application of post IR-IRSL dating to fine grain waterlain sediments," *Quaternary Geochronology*, 8, 33–40.

Lukashov, N. and C. Lukashov (2012): "Antique and medieval cities at Issyk Kul," in *Underwater research: Archeology, history, diving*, 31–46.

Maizels, J. (1997): "Jokulhlaup deposits in proglacial areas," *Quaternary Science Reviews*, 16, 793–819.

Maksimov, E. (1985): "Mistery of Lake Issyk-Kul (in Russian)," *LGU, Leningrad.*

Malone, E. (2010): "Changing glaciers and hydrology in Asia - addressing vulnerabilities to glacier melt impacts," *Technical Report USAID*, 133.

Mangerud, J., M. Jakobsson, H. Alexanderson, V. Astakhov, G. K. C. Clarke, M. Henriksen, C. Hjort, G. Krinner, J. P. Lunkka, P. M??ller, A. Murray, O. Nikolskaya, M. Saarnisto, and J. I. Svendsen (2004): "Ice-dammed lakes and rerouting of the drainage of northern Eurasia during the Last Glaciation," *Quaternary Science Reviews*, 23, 1313–1332.

Manning, R. (1904): *Transactions of the Institutions of Civil Engeneers of Ireland*, vol. 20, Dublin: Institution of Civil Engeneers of Ireland.

Marchenko, S. S. and A. P. Gorbunov (1997): "Permafrost Changes in the Northern Tien Shan During the Holocene," *Permafrost and Periglacial Processes*, 8, 427–435.

Markov, K. (1971): "Sequence of the latest deposits of the Issyk Kul basin," *Moscow University Publishing House [in Russian]*, 164 pp.

Matthews, J. A. and H. E. Trenbirth (2011): "Growth Rate Of A Very Large Crustose Lichen (Rhizocarpon Subgenus) And Its Implications For Lichenometry," *Geografiska Annaler, Series A: Physical Geography*, 93, 27–39.

McCarthy, D. (1999): "A biological basis for lichenometry?" *Journal of Biogeography*, 26, 379–386.

McCarthy, D. P. and K. Zaniewski (2001): "Digital Analysis of Lichen Cover: A Technique for Use in Lichenometry and Lichenology," *Arctic, Antarctic, and Alpine Research*, 33, 107.

Merchel, S., M. Arnold, G. Aumaître, L. Benedetti, D. Bourlès, R. Braucher, V. Alfimov, S. Freeman, P. Steier, and A. Wallner (2008): "Towards more precise 10Be and 36Cl data from measurements at the 10–14 level: Influence of sample preparation," *Nuclear Instruments and Methods in Physics Research Section B: Beam Interactions with Materials and Atoms*, 266, 4921–4926.

Merchel, S. and W. Bremser (2004): "First international 26Al interlaboratory comparison - Part I," *Nucl. Instr. and Meth. in Phys. Res. B (Proceedings of AMS-9)*, 223-224, 393–400.

Merchel, S. and U. Herpers (1999): "An Update on Radiochemical Separation Techniques for the Determination of Long-Lived Radionuclides via Accelerator Mass Spectrometry," *Radiochim. Acta*, 84, 215–219.

Millar, C. I. and R. D. Westfall (2008): "Rock glaciers and related periglacial landforms in the Sierra Nevada, CA, USA; inventory, distribution and climatic relationships," *Quaternary International*, 188, 90–104.

Miller, G. and J. T. Andrews (1972): "Quaternary History of Northern Cumberland Peninsula, Easr Baffin Island, N.W.T., Canada Part VI: Priliminary Lichen Growth Curve for Rhizocarpon geographicum," 83, 1133–1138.

Molnar, P. and P. Tapponnier (1975): "Cenozoic tectonics of Asia: Effects of a continental collision," *Science*, 189, 419–426.

Monnier, S. and C. Kinnard (2015): "Internal Structure and Composition of a Rock Glacier in the Dry Andes, Inferred from Ground-penetrating Radar Data and its Artefacts," *Permafrost and Periglacial Processes*, 26, 335–346.

Mushketov, I. V. (1891): "Materials for investigation of earthquakes in Russia.,," *Annex to the 27th volume of tidings of the Imperial Russian Geographical Society.*

Narama, C., A. Kääb, M. Duishonakonov, and K. Abdrakhmatov (2009): "Remote-sensing based analysis of glacier change and glacier lake hazards in the outer ranges of the Tien Shan mountains," *Assembly*, 11, 6588–6588.

Nelson, D. (2012): *Gormorphic and stratigraphic development of Lake Bonneville's intermediate paleoshorelines during the Late Pleistocene*, Dissertation, Department of Geology and Geophysics, University of Utah.

Nikonov, A. A. and T. Y. Shebalina (1979): "Lichenometry and earthquake age determination in Central Asia," *Nature*, 280, 675–677.

Nishiizumi, K., M. Imamura, M. Caffee, J. Southon, R. Finkel, and J. McAninch (2007): "Absolute calibration of 10Be AMS standards," *Nuclear Instruments and Methods in Physics Research Section B: Beam Interactions with Materials and Atoms*, 258, 403–413.

O'Connor, J. and R. Beebee (2009): "Floods from natural rock-material dams," in *Megaflooding on Earth and Mars*, ed. by D. Burr, P. Carling, and V. Baker, Cambridge University Press, 128–171.

O'Connor, J. and J. Costa (2004): "The world's largest floods, past and present - Their causes and magnitudes," *USGS Circular*, 1254, 13.

Orwin, J. F., K. M. Mckinzey, M. a. Stephens, and A. J. Dugmore (2008): "Identifying moraine surfaces with similar histories using lichen size distributions and the U2 statistic, Southeast Iceland," *Geografiska Annaler, Series A: Physical Geography*, 90 A, 151–164.

Osborn, G., D. McCarthy, A. LaBrie, and R. Burke (2015): "Corrigendum to "Lichenometric dating: Science or pseudo-science?",Quaternary Research 83 (2015), 1–12," *Quaternary Research*, 83, 394.

Oviatt, C. G., D. R. Currey, and D. Sack (1992): "Radiocarbon chronology of Lake Bonneville, Eastern Great Basin, USA," *Palaeogeography, Palaeoclimatology, Palaeoecology*, 99, 225–241.

Owen, L. A. and J. England (1998): "Observations on rock glaciers in the Himalayas and Karakoram Mountains of northern Pakistan and India," *Geomorphology*, 26, 199–213.

Panagiotopoulos, F., M. Shahgedanova, A. Hannachi, and D. B. Stephenson (2005): "Observed trends and teleconnections of the Siberian high: A recently declining center of action," *Journal of Climate*, 18, 1411–1422.

Pelli, F. (2005): "Water management improvement project, Review of dam safety issues, Juli–August 2005," Tech. rep., Department of Water Resources Kyrgyz Republic.

Pigati, J. S., J. Quade, T. M. Shahanan, and C. V. Haynes (2004): "Radiocarbon dating of minute gastropods and new constraints on the timing of late Quaternary spring-discharge deposits in southern Arizona, USA," *Palaeogeography, Palaeoclimatology, Palaeoecology*, 204, 33–45.

Pomortsev, O. (1980): "The glaciers of the southern slope of Kungey Alatau range (in russian)," *Leningrad University, Doctoral Thesis*, 172.

Potter, N. (1972): "Ice-Cored Rock Glacier, Galena Creek, Northern Absaroka Mountains, Wyoming," *Geological Society of America Bulletin*, 83, 3025–3058.

Preusser, F. and H. U. Kasper (2001): "Comparison of dose rate determination using high-resolution gamma spectrometry and inductively coupled plasma - mass spectrometry," *Ancient TL*, 19 No. 1, 19–23.

Preusser, F., K. Ramseyer, and C. Schlüchter (2006): "Characterisation of low OSL intensity quartz from the New Zealand Alps," *Radiation Measurements*, 41, 871–877.

Pritchard, H. D. (2017): "Asia's glaciers are a regionally important buffer against drought," *Nature*, 545, 169–174.

Reimann, T. and S. Tsukamoto (2012): "Dating the recent past (<500 years) by post-IR IRSL feldspar - Examples from the North Sea and Bal-tic Sea coast," *Quaternary Geochronology*, 10, 180–187.

Reimer, P. J., E. Bard, A. Bayliss, J. W. Beck, P. G. Blackwell, and C. B. Ramsey (2013): "IntCal13 and Marine13 Radiocarbon Age Calibration Curves 0–50,000 Years cal BP," *Radiocarbon*, 55, 1869–1887.

Richter, D., A. Richter, and K. Dornich (2013): "Lexsyg — A new system for luminescence research," *Geochronometria*, 40, 220–228.

Ricketts, R. D., T. C. Johnson, E. T. Brown, K. a. Rasmussen, and V. V. Romanovsky (2001): "The Holocene paleolimnology of Lake Issyk-Kul, Kyrgyzstan: Trace element and stable isotope composition of ostracodes," *Palaeogeography, Palaeoclimatology, Palaeoecology*, 176, 207–227.

Roer, I. and M. Nyenhuis (2007): "Rockglacier activity studies on a regional scale : comparison of geomorphological mapping and photogrammetric monitoring," *Earth Surface Processes and Landforms*, 32, 1747–1758.

Romanovsky, V. (2002): "Water level variations and water balance of lake Issyk-Kul," in *Lake Issyk-Kul : Its Natural Environment*, ed. by J. Klerkx and B. Imanackunov, 45–57.

Roof, S. and A. Werner (2011): "Indirect growth curves remain the best choice for lichenometry: Evidence from directly measured growth rates from Svalbard," *Arctic, Antarctic, and Alpine Research*, 43, 621–631.

Rugel, G., S. Pavetich, S. Akhmadaliev, S. M. Enamorado Baez, A. Scharf, R. Ziegenrücker, and S. Merchel (2016): "The first four years of the AMS-facility DREAMS: Status and developments for more accurate radionuclide data," *Nucl. Instr. and Meth. in Phys. Res.*, B 370, 94–100.

Sancho, L. G., R. de la Torre Noetzel, and A. Pintado (2008): "Lichens, new and promising material from experiments in astrobiology," *Fungal Biology Reviews*, 122, 103–109.

Sancho, L. G., D. Palacios, T. G. A. Green, M. Vivas, and A. Pintado (2011): "Extreme high lichen growth rates detected in recently deglaciated areas in Tierra del Fuego," *Polar Biology*, 34, 813–822.

Sanhueza-Pino, K., O. Korup, R. Hetzel, H. Munack, J. T. Weidinger, S. Dunning, C. Ormukov, and P. W. Kubik (2011): "Glacial

advances constrained by 10Be exposure dating of bedrock landslides, Kyrgyz Tien Shan," *Quaternary Research*, 76, 295–304.

Savoskul, O. and O. Solomina (1996): "Late Holocene glacier variations in the frontal and inner range of the Tien Shan, Central Asia," *The Holocene*, 6, 25–35.

Schildgen, T. F., W. M. Phillips, and R. S. Purves (2005): "Simulation of snow shielding corrections for cosmogenic nuclide surface exposure studies," *Geomorphology*, 64, 67–85.

Schmid, M. O., P. Baral, S. Gruber, S. Shahi, T. Shrestha, D. Stumm, and P. Wester (2015): "Assessment of permafrost distribution maps in the Hindu Kush Himalayan region using rock glaciers mapped in Google Earth," *Cryosphere*, 9, 2089–2099.

Schrott, L. (1996): "Some geomorphological-hydrological aspects of rock glaciers in the Andes (San Juan, Argentina)," *Zeitschrift fur Geomorphologie, Supplementband*, 104, 161–173.

Schwanghart, W. and D. Scherler (2014): "Short Communication: TopoToolbox 2 – MATLAB-based software for topographic analysis and modeling in Earth surface sciences," *Earth Surface Dynamics*, 2, 1–7.

Scotti, R., F. Brardinoni, S. Alberti, P. Frattini, and G. B. Crosta (2013): "A regional inventory of rock glaciers and protalus ramparts in the central Italian Alps," *Geomorphology*, 186, 136–149.

Scotti, R., G. Crosta, and A. Villa (2017): "Destabilisation of creeping permafrost: The Plator rock glacier case study (Central Italian Alps)," *Permafrost and Periglacial Processes*, 28, 224—-236.

Selander, J., M. Oskin, C. Ormukov, and K. Abdrakhmatov (2007): "The role of inherited strike-slip faults in the growth of the Northern Tian Shan," *American Geophysical Union, Fall Meeting 2007, abstract T23D-1634*.

——— (2012): "Inherited strike-slip faults as an origin for basement-cored uplifts: Example of the Kungey and Zailiskey ranges, northern Tian Shan," *Tectonics*, 31, 1–22.

Sevastianov, D., A. Shnitnikov, and E. Al. (1980): "Tian Shan lakes and their history (in Russian)," *Nauka, Leningrad*.

Shahgedanova, M., G. Nosenko, T. Khromova, and A. Muraveyev (2010): "Glacier shrinkage and climatic change in the Russian Altai from the mid-20th century: An assessment using remote sensing and PRECIS regional climate model," *Journal of Geophysical Research Atmospheres*, 115, 1–12.

Sharkhuu, N. (2003): "Recent Changes in the Permafrost of Mongolia," *Proceedings of the Eighth International Conference on Permafrost*, 2, 1029–1034.

Smirnova, T. and A. Nikonov (1990): "A revised lichenometric method and its application dating great past earthquakes," *Arctic and Alpine Research*, 22, 375–388.

Solomina, O. (1987): "The Holocene moraines studied by bioindication methods," *Institue of Geography, Russian Academy of Sciences, Doctoral Thesis*.

Solomina, O., O. Savoskul, and a.E. Cherkinsky (1994): "Glacier variations, mudflow activity and landscape development in the Aksay Valley (Tian Shan) during the late Holocene," *The Holocene*, 4, 25–31.

Solomina, O. N., R. S. Bradley, V. Jomelli, A. Geirsdottir, D. S. Kaufman, J. Koch, N. P. McKay, M. Masiokas, G. Miller, A. Nesje, K. Nicolussi, L. A. Owen, A. E. Putnam, H. Wanner, G. Wiles, and B. Yang (2016): "Glacier fluctuations during the past 2000 years," *Quaternary Science Reviews*, 149, 61–90.

Sorg, A., T. Bolch, M. Stoffel, O. Solomina, and M. Beniston (2012): "Climate change impacts on glaciers and runoff in Tien Shan (Central Asia)," *Nature Climate Change*, 2, 725–731.

Sorg, A., A. Kääb, A. Roesch, C. Bigler, and M. Stoffel (2015): "Contrasting responses of Central Asian rock glaciers to global warming," *Scientific Reports*, 5, 8228.

Stone, J. (2000): "Air pressure and cosmogenic isotope production," *Journal of Geophysical Research*, 105, 753–759.

Strom, A. (2010): "Landslide dams in Central Asia region," *Journal of the Japan Landslide Society*, 47, 309–324.

Strom, A. L. and O. Korup (2006): "Extremely large rockslides and rock avalanches in the Tien Shan Mountains, Kyrgyzstan," *Landslides*, 3, 125–136.

Sundriyal, Y., A. Shukla, N. Rana, R. Jayangondaperumal, P. Srivastava, L. Chamyal, S. Sati, and N. Juyal (2015): "Terrain response to the extreme rainfall event of June 2013 : Evidence from the Alaknanda and Mandakini River Valleys , Garhwal Himalaya, India," *IUGS*, 38, 179–188.

Takeuchi, N., K. Fujita, V. B. Aizen, C. Narama, Y. Yokoyama, S. Okamoto, K. Naoki, and J. Kubota (2014): "The disappearance of glaciers in the Tien Shan Mountains in Central Asia at the end of Pleistocene," *Quaternary Science Reviews*, 103, 26–33.

Tapponnier, P. and P. Molnar (1979): "Active faulting and cenozoic tectonics of the Tien Shan, Mongolia, and Baykal Regions," *Journal of Geophysical Research*, 84, 3425–3459.

Thies, H., U. Nickus, M. Tolotti, R. Tessadri, and K. Krainer (2013): "Evidence of rock glacier melt impacts on water chemistry and diatoms in high mountain streams," *Cold Regions Science and Technology*, 96, 77–85.

Trenbirth, H. E. and J. a. Matthews (2010): "Lichen growth rates on glacier forelands in southern Norway: Preliminary results from a 25-year monitoring programme," *Geografiska Annaler, Series A: Physical Geography*, 92, 19–39.

Trofimov, A. (1978): "The history of Issuk-Kul Lake during Holocene," *Bull. Komis. po izuchen. chervert perioda*, 48, 79–86.

Unger-Shayesteh, K., S. Vorogushyn, D. Farinotti, A. Gafurov, D. Duethmann, A. Mandychev, and B. Merz (2013): "What do we know about past changes in the water cycle of Central Asian headwaters? A review," *Global and Planetary Change*, 110, 4–25.

Wahrhaftig, C. and A. Cox (1959): "Rock glaciers in the Alaska Range," *The Geological Society of America Bulletin*, 70, 383–436.

Wake, C. (1989): "Glaciochemical investigation as a tool for Determining the spatial and seasonal variation of snow accumulation in the central Karakoram, northern Pakistan," *Annals of Glaciology*, 13, 279–284.

Walder, J. S. and J. E. O'Connor (1997): "Methods for predicting peak discharge of floods caused by failure of natural and constructed earthen dams," *Water Resources Research*, 33, 2337.

water cadastre, S. (1987): "Annual data on the mode and resources of a surface water of land," in *Part 1. Rivers and Channels. Part 2. Lakes and Reservoirs*, Kyrgyz SSR, Obninsk.

Watson, G. S. (1961): "Goodness-of-fit Tests on a Circle," *Biometrica*, 48, 109–114.

Whalley, W. B. and A. Azizi (2003): "Rock glaciers and protalus landforms: Analogous forms and ice sources on Earth and Mars," *Journal of Geophysical Research*, 108, 8032.

Winchester, V. and S. Harrison (1994): "A development of the lichenometric method applied to the dating of glacially influenced debris flows in southern chile," *Earth Surface Processes and Landforms*, 19, 137–151.

Wobus, C., K. Whipple, E. Kirby, N. Snyder, N. Johnson, K. Spyropolou, B. Crosby, and D. Sheehan (2006): "Tectonics from topography: procedures, promise, and pit- falls," in *Tectonics, Climate, and Landscape Evolution*, ed. by S. Willett, N. Hovius, M. Brandon, and D. Fisher, Geological Society of America Special Paper, 55–74.

Yerokhin, S. (2002): "Tipy gornykh ozer a kratkaya ikh kharakteristika (Typology of High-mountain Lakes and their Characteristic)," *State Institute of Geology, Bishkek*.

Zubovich, A. V., X.-Q. Wang, Y. G. Scherba, G. G. Schelochkov, R. Reilinger, C. Reigber, O. I. Mosienko, P. Molnar, W. Michajljow, V. I. Makarov, J. Li, S. I. Kuzikov, T. A. Herring, M. W. Hamburger, B. H. Hager, Y.-m. Dang, V. D. Bragin, and R. T. Beisenbaev (2010): "GPS velocity field for the Tien Shan and surrounding regions," *Tectonics*, 29, 23 pp.